

**POLY(ARYLENE SULPHIDE)/THERMOTROPIC LIQUID
CRYSTALLINE POLYMER BLENDS**

**A THESIS
SUBMITTED TO THE
UNIVERSITY OF POONA
FOR THE DEGREE OF
DOCTOR OF PHILOSOPHY
(IN CHEMISTRY)**

**BY
T.G. GOPAKUMAR**

**POLYMER SCIENCE AND ENGINEERING GROUP
CHEMICAL ENGINEERING DIVISION
NATIONAL CHEMICAL LABORATORY
PUNE, MAHARASHTRA
INDIA - 411 008**

SEPTEMBER 1997

Dedicated to my Parents and Teachers

TH 1126

CERTIFICATE

Certified that the work incorporated in this thesis “**Poly(arylene sulphide)/Thermotropic Liquid Crystalline Polymer Blends**” submitted by **Mr. T.G. Gopakumar** was carried out by the candidate under my supervision. Such material as has been obtained from other sources has been duly acknowledged in the thesis.



Dr. S. Ponrathnam

(Research Guide)

ACKNOWLEDGEMENTS

I wish to express my sincere gratitude to my research guide Dr. S. Ponrathnam, Scientist, National Chemical Laboratory, Pune, for his invaluable guidance and help rendered throughout the course of my doctoral research work without which I could not have completed this investigation successfully. He taught, criticised, encouraged and advised - all of which has helped me during my doctoral research and preparation of this thesis. As an outstanding scientist and teacher, he has given me the benefit of his excellent training in abundant measure. I am very much personally obliged to Dr. C.R. Rajan, Scientist, National Chemical Laboratory, Pune, for inspiring discussions, constant encouragement and valuable advice in crucial times of my research work. I am grateful to both of them much more than what words can express.

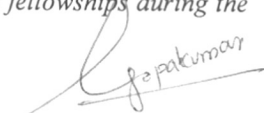
I am deeply indebted to Dr. Ramesh C. Ghadage, Research Associate, Chemical Engineering Division for constant professional help during my course of research work.

I sincerely thank Dr. A. Lele, Dr. J.P. Jog, Chemical Engineering Division and Dr. Sainkar, Special Instruments Laboratory for extending their co-operation in carrying out some part of my research work.

I am grateful to Prof. V.N. Rajasekharan Pillai, Vice-Chancellor, Mahatma Gandhi University, Kottayam, Dr. Sabu Thomas, Reader, School of Chemical Sciences, Mahatma Gandhi University, Kottayam and Dr. C. Pavithran, Scientist, Regional Research Laboratory, Thiruvananthapuram, for their inspiration during initial period my research career.

I would like to thank my colleagues Ms. Smita, Dr. Sunny, Dr. Milind, Suresh, Raju, Yemul, Sunita, Dr. Anjali, Dr. Arika, Rethi, Varsha for their co-operation rendered throughout my research work. I thank Mr. S.N. Sathe for his timely assistance during my research work. I would be failing in my duty if I do not thank my friends Vinod, Radhakrishnan, Jayaprakash, Santhosh, Rajeev, Nandan, Mahesh, Pradeep Pallan, Sivasankaran, Harish and other friends and well wishers of mine who helped me and encouraged me during my stay in Pune.

I thank Dr. P. Paul Ratnasamy, Director, NCL, Pune, for permitting me to submit this work in the form of a thesis. I also would like to thank Indo-French centre for the Promotion of Advanced Research (IFCPAR), New Delhi and Council for Scientific and Industrial Research (CSIR), New Delhi for providing me research fellowships during the tenure of this work.


T.G. Gopakumar

		CONTENTS	
CHAPTER – 1	GENERAL INTRODUCTION		PAGE
			2
1.1	POLYMER BLENDS, ALLOYS AND COMPOSITES		2
1.1.1	Methods of blending		4
1.1.2	Types of blends and composites: <i>Terminology</i>		4
1.2	MISCIBILITY IN BLENDS AND COMPOSITES		5
1.2.1	Miscibility and compatibilisation		5
1.2.2	Definition of compatibility		7
1.3	METHODS OF COMPATIBILISATION		8
1.3.1	Thermodynamic miscibility		8
1.3.2	Addition of block and graft copolymers		9
1.3.3	Addition of functional polymers		11
1.3.4	Reactive compatibilisation		11
1.4	CHARACTERISATION OF POLYMER BLENDS AND COMPOSITES		12
1.4.1	Mechanical properties		13
1.4.2	Thermal properties of polymers		14
1.4.3	Melting and crystallization behaviour of blends		16
1.4.4	Phase morphology		17
1.4.5	Rheological behaviour		18
1.5	<i>IN SITU</i> FIBRE COMPOSITES FROM POLYMER BLENDS		20
1.5.1	Macro composites		21
1.5.2	Microfibrillar composites		21
1.5.3	In situ molecular composites		22
1.6	LIQUID CRYSTALLINE POLYMERS (LCPs)		23
1.6.1	Lyotropic liquid crystalline polymers		23
1.6.2	Thermotropic liquid crystalline polymers (TLCPs)		24
1.6.3	Properties, processing and applications of TLCPs		28

1.7	POLYMER BLENDS CONTAINING TLCPs	32
1.7.1	TLCPs as reinforcement	34
1.7.2	TLCPs as Processing aid	34
1.8	POLY (PHENYLENE SULPHIDE) (PPS)	35
1.8.1	Structure, properties and applications	36
1.8.2	Modification of properties PPS composites and blends	39
1.9	PPS/TLCP BLENDS: A REVIEW	40
1.9.1	Phase behaviour and morphology	41
1.9.2	Thermal and crystallization behaviour	41
1.9.3	Mechanical properties	44
1.9.4	Rheological properties	46
1.10	SCOPE AND OBJECTIVES OF THE PRESENT WORK	47
1.11	REFERENCES	48
<u>CHAPTER 2</u>	THERMAL PROPERTIES, PHASE BEHAVIOUR AND	56
	MORPHOLOGY OF PPS/PET -OB BLENDS	
2.1	INTRODUCTION	55
2.2	EXPERIMENTAL	57
2.2.1	Materials	57
2.2.2	Preparation of blends	58
2.2.3	Thermal analysis	58
2.2.4	Polarised light optical microscopy	59
2.2.5	Scanning electron microscopy	59
2.3	RESULTS AND DISCUSSION	60
2.3.1	Melting and crystallization behaviour	60
2.3.2	Phase behaviour	68
2.3.3	Morphology	71

2.3.3.1	Polarised light optical microscopy	71
2.3.3.2	Scanning electron microscopy	75
2.4	COMPARATIVE STUDY OF BLENDS	77
2.4.1	Thermal properties	77
2.4.2	Crystallisation behaviour	80
2.4.3	Degree of crystallinity	82
2.4.4	Morphology	84
2.4.4.1	Polarised light optical microscopy	84
2.4.4.2	Scanning electron microscopy	86
2.5	CONCLUSION	89
2.6	REFERENCES AND NOTES	91
CHAPTER -3	CRYSTALLISATION KINETICS OF PPS AND PPS/PET -OB BLENDS	94
3.1	INTRODUCTION	95
3.2	EXPERIMENTAL	97
3.2.1	Materials	97
3.2.2	Effect of annealing on the thermal behaviour of PPS	97
3.2.3	Isothermal crystallization kinetics of PPS	98
3.2.4	Preparation of blends	98
3.2.5	Non-isothermal crystallization kinetics of PPS and PPS/PET-OB blends	98
3.3	RESULTS AND DISCUSSION	99
3.3.1	Effect of annealing	99
3.3.2	Isothermal crystallization kinetics	103
3.3.3	Non-isothermal crystallization kinetics of PPS and PPS/PET-OB blends	109
3.4	CONCLUSION	121
3.5	REFERENCES AND NOTES	123

<u>CHAPTER -4</u>	SYNTHESIS OF COMPATIBILISER AND	126
	COMPATIBILISATION OF PPS/PET -OB BLENDS	
4.1	INTRODUCTION	127
4.2	EXPERIMENTAL	128
4.2.1	Materials	128
4.2.2	Measurements	130
4.2.3	Preparation of blends	131
4.2.4	Polarised light optical microscopy	131
4.2.5	Scanning electron microscopy	131
4.3	RESULTS AND DISCUSSION	131
4.3.1	Effect of oxybenzoate (OB) content	133
4.3.2	dependence of DCTPPS: PET/OB composition	139
4.3.3	Effect of reaction time	143
4.3.4	Uncompatibilised and compatibilised PPS/PET-OB Blends	146
4.3.4.1	Thermal behaviour	146
4.3.4.2	Melting behaviour	146
4.3.4.3	Crystallisation behaviour	149
4.3.4.4	Degree of crystallinity	151
4.3.4.5	Morphology	152
4.3.4.5.1	Polarised light optical microscopy	152
4.3.4.5.2	Scanning electron microscopy	154
4.4	CONCLUSION	156
4.5	REFERENCES AND NOTES	157

<u>CHAPTER – 5</u>	REACTIVE COMPATIBILISATION OF PPS/VECTRA	159
	A950 BLENDS	
5.1	INTRODUCTION	160
5.2	EXPERIMENTAL	161
5.2.1	Materials	161
5.2.2	Methods	161
5.2.3	Reactive blending	161
5.2.4	Processing	163
5.2.5	Testing and analysis	163
5.2.5.1	Thermal properties	163
5.2.5.2	Tensile properties	164
5.2.5.3	Impact properties	164
5.2.5.4	Scanning electron microscopy	164
5.2.5.5	Rheology	165
5.2.5.6	Polarised light optical microscopy	165
5.3	RESULTS AND DISCUSSION	165
5.3.1	<i>In situ</i> reactive compatibilisation	165
5.3.2	Thermal properties	168
5.3.3	Mechanical properties	175
5.3.4	Rheology	178
5.3.5	Polarised light optical microscopy	180
5.3.6	Scanning electron microscopy	180
5.4	CONCLUSION	186
5.5	REFERENCES AND NOTES	187
<u>CHAPTER 6</u>	SCOPE FOR FUTURE WORK	190

LIST OF FIGURES

FIGURE No.	CAPTION	PAGE
<u>CHAPTER 1</u>		
1.1	Influence of interfacial behaviour in Polymer Blends	7
1.2	Schematic diagrams for binary blends showing LCST and UCST behaviour	9
1.3	Schematic diagram showing location of block and graft copolymers at phase interfaces	10
1.4	Schematic representation of molten two-phase dispersed polymer blend flowing through a capillary. (a) fibre-like domain; (b) droplet-like domains	19
1.5	Variables affecting physical and mechanical properties of polymer blends	20
1.6	Anisotropic units giving rise to liquid crystal phases	24
1.7	Comparison of three liquid crystal phases (a, b and c) with isotropic state (d)	25
1.8	Types of liquid crystal polymers	26
1.9	Commercially available TLCPs	27
CHAPTER 2		
2.1	DSC thermograms of PPS/PET-OB blends at the heating rate of 20% C/min.	61
2.2	Typical DSC thermograms obtained after isothermal Crystallisation at various temperatures for one hour: (a) PPS and (b) PPS (70) PET-OB (30) blend.	63
2.3	Hoffman-Weeks plots for pure PPS and PPS/PET-OB Blends.	65

2.4	DSC crystallisation exotherms of PPS/PET-OB blends at The cooling rate of 20°C/min.	67
2.5	Phase diagram of the PPS/PET-OB blend system, showing the equilibrium melting transition ($T^{\circ}m$) of PPS and the crystallisation temperatures (T_c) of both PPS and PET - OB, crystal \leftrightarrow nematic transition as well as single glass Transition temperature (T_g) of PET-OB.	70
2.6	Optical micrographs (same magnification =100X) showing phase behaviour of 70/30/% wt./wt. PPS/PET-OB blend in molten state (at 320°C).	72
2.7	Optical micrographs (same magnification, bar 100X) of the spherulite morphology of PPS in blends with PET-OB at various compositions; (a) pure PPS after 20 min. at 238 °C; (b) 90/10; (c) 80/20 and (d) 70/30 PPS/PET-OB blends	74
2.8	SEM micrographs showing morphology of PPS in blends with PET-OB at various compositions. (a) pure PPS (b) 90/10 and (c) 50/50 (wt./wt.) PPS/PET-OB blends.	76
2.9	DSC thermograms (second heating scan) of melt-mixed and co-precipitated PPS/PET-OB blends at the heating rate 20°C/min.	78
2.10	DSC crystallisation exotherms (second cooling scan) of melt-mixed and co-precipitated PPS/PET-OB blends at the cooling rate 20°C/min.	81
2.11	Effect of PET-OB content on the degree of crystallinity (α) of PPS phase in both melt-mixed and co-precipitated blends.	83

2.1.2	Optical micrographs (same magnification, 100X) of the phase behaviour and morphology of melt-mixed and co-precipitated PPS/PET-OB blends at various compositions at 320°C. Pure PPS: (a)., melt-mixed: (b) 70/30 and (d) 50/50 % (wt./wt.), and co-precipitated: (c) 70/30 and (e) 50/50 % (wt./wt.) blends.	85
2.13	SEM micrographs showing morphology of freeze-fractured samples of melt-mixed [(a). 90/10, (c). 70/30 & (e).50/50 % (wt./wt.) and co-precipitated [(b). 90/10, (d). 70/30, & (f). 50./50 % (wt./wt/)] PPS/PET-OB blends. (PET-OB was termed as LCP in micrographs of melt-mixed blends and as PET-OB in micrographs of co-precipitated blends).	87

CHAPTER 3

3.1	Superimposed plot of six heating cycles showing effect of Annealing on T _m in PPS (sample annealed for 5 min. at 320°C)	100
3.2	Superimposed plot of six heating cycles showing effect of annealing on T _m in PPS (sample annealed for 10 min. at 320°C)	101
3.3	Superimposed plot of six heating cycles showing effect of annealing on T _m in PPS (sample annealed for 20 min. at 320°C)	102
3.4	A typical isothermal crystallisation peak at 267°C.	105
3.5	Crystallisation isotherm of PPS at temperature 267°C.	106
3.6	Avrami plot of PPS at temperature 267°C.	107
3.7	The extent of crystallisation vs.time at 267°C.	108
3.8	D.S.C cooling traces of PPS/PET-OB blends, recorded at 10°C/min.	111
3.9	Fraction of crystallised PPSvs. Crystallisation time.	113

3.10	Fraction of crystallised PPS phase in PPS (905)/PET-OB (10%) vs. crystallisation time.	114
3.11	Ozawa plot of non-isothermal crystallisation for neat PPS.	115
3.12	Ozawa plots of non-isothermal crystallisation for neat PPS/PET-OB blends.	116
3.13	Plot cooling crystallisation function vs. of PPS/PET-OB blends.	118
3.14	Plot of Avrami exponent [n] vs. temperature of PPS/PET-OB blends.	119

CHAPTER 4

4.1	Laboratory scale reaction set-up for the synthesis of PPS-PET/OB block copolymer	129
4.2	A typical optical micrograph of 50/50 (wt./wt. %) PPE - PET/OB (containing 45 mol % OB) block copolymer.	135
4.3	DSC thermograms (second heating) showing the effect of oxybenzoate content (with respect to the PET content) on the thermal behaviour of block copolymer. (a) Heating scans. (b) Cooling Scans.	136
4.4	X-ray diffraction profiles of 50/50 wt./wt. % PPS-PET/OB Block copolymer.	138
4.5	DSC thermograms (second heating) showing the effect of TLCP content on the thermal behaviour of 50/50 wt./wt. % PPS-PET/OB block copolymer. (a) Heating scans. (b) Cooling scans.	140
4.6	DSC thermograms (second heating) showing the effect Reaction time contend on the thermal behaviour of 50/50 Wt./wt.% PPS-PET/OB block copolymer. (a) Heating scans. (b) Cooling scans.	144
4.7	DSC thermograms (second heating scan) of uncompatibilised and compatibilised PPS/TLCP blends at the heating rate 20°C/min.	147

4.8	DSC crystallisation exotherms (second cooling scan) of uncompatibilised and compatibilised PPS/TLCP blends at the cooling rate 20°C/min.	150
4.9	Optical micrographs (same magnification, 100X) of the phase behaviour and morphology of uncompatibilised and compatibilised PPS/PET-OB blends at various compositions at 320°C. Pure PPS : (a)., uncompatibilised : (b) 70/30 and (d) 50/50 %(wt./wt.) and compatibilised: (c) 70/30 and (e) 50/50 % wt./wt.) blends.	153
4.10	SEM micrographs showing morphology of freeze-fractured samples of uncompatibilised [(a). 90/10, (c) 70/30 & (e). 50/50 % (wt./wt.) and compatibilised [(b). 90/10, (d). 70/30, & (f). 50/50 % (wt./wt.)] PPS/PET-OB blends	155

CHAPTER 5

5.1	Torque vs. Time graph for Vectra A 950, DCTPPS and (50/50 %w/w) DCTPPS/ Vectra A950 blend.	166
5.2	IR spectra of pure Vectra A 950, DCTPPS and (50/50 % w/w)DCTPPS/TLCP blend.	167
5.3	DSC curves corresponding to second heating scan of <i>in situ</i> compatilised PPS/ Vectra A950/DCTPPS.	170
5.4	DSC curves corresponding to second cooling scan of <i>in situ</i> compatilised PPS/Vectra A950/DCTPPS.	172
5.5	Plot of apparent viscosity vs. shear rate showing rheological properties of uncompatibilised and compatibilised PPS/Vectra A950 blends.	179
5.6	Polarised light optical microscope photograph showing molten morphology of uncompatibilised and	181

compatibilised PPS/Vectra A950 blends.

- 5.7 SEM micrograph showing skin morphology of uncompatibilised PPS/Vectra A950 blend: (a) Perpendicular to injection flow direction, skin region; (b) core region of the same specimen; (c) Parallel to injection moulded direction, skin region; (d) Core region of the same specimen. 182

LIST OF TABLES

<u>TABLE No,</u> <u>CHAPTER 1</u>		PAGE
1.1	Processing-Structure-Property Relations in Polymers and Polymer blends	13
1.2	Commercially available thermotropic liquid crystalline polymer and their physical properties.	29
1.3	A comparison of properties of thermoplastics and Thermotropic liquid crystalline polymer	30
1.4	Commercial Applications of LCPs	31
1.5	Applications of thermoplastics/liquid crystalline polymer blends	34
1.6	Important published papers on PPS/TLCP polymer blends	43
1.7	Some Important Patents on PPS/TLCP blends	45
 <u>CHAPTER 2</u>		
2.1	Thermal data of PPS and PPS phase in of PPS/PET-OB Blends	62
2.2	Hoffman-Weeks Analysis	66
2.3	Comparison of thermal data of PPS phase in melt-mixed and co-precipitated PPS/PET-OB Blends	80
 <u>CHAPTER 3</u>		
3.1	Effect of PET-OB on the crystallization temperature (T_c), degree of crystallinity (α), half-width of crystallisation peak (ΔT) and Avrami exponent (n) of PPS in PPS/PET-OB blends.	117

CHAPTER 4

		PAGE
4.1	Effect of oxybenzoate content on the thermal behaviour of PPS blocks in copolymer	137
4.2	Effect of PET-OB content on the thermal behaviour of PPS blocks in copolymer	141
4.3	Effect of reaction time on the thermal behaviour of copolyester	145
4.4	Comparison of thermal data of PPS phase in Uncompatibilised and compatibilised PPS/ Effect of PET - OB content on the thermal behaviour of PPS block in copolymer blends	148

CHAPTER 5

5.1	Cylinder temperature (°C) of the Extruder	162
5.2	Processing Conditions	163
5.3	Thermal Properties of uncompatibilised and compatibilised PPS/Vectra A950 Blends	169
5.4	Thermal Properties of uncompatibilised and compatibilised PPS/Vectra A 950 Blends	176
5.5	Impact Properties of uncompatibilised and compatibilised PPS/Vectra A 950 Blends	177

SYMBOLS AND ABBREVIATIONS

PPS	:	Poly(phenylene sulphide)
OB	:	Oxybenzoate
PET-OB	:	Poly(ethylene terephthalate-co-oxybenzoate)
TLCP	:	Thermotropic liquid crystalline polymer
Vectra A950	:	Copolyester of hydroxy naphthoic acid and hydroxyl benzoic acid
VectraB950	:	Copolyester of hydroxy naphthoic acid, terephthalic acid and aminophenol
ΔH_m	:	Heat of fusion
ΔH_c	:	Heat of Crystallisation
η	:	Crystal lamellar thickness
n	:	Avrami exponent
χ	:	Cooling crystallisation function
α	:	Degree of crystallinity

CHAPTER 1

GENERAL
INTRODUCTION

TH 1126

CHAPTER 1

1.0 GENERAL INTRODUCTION

The field of polymer science and technology has undergone an enormous expansion over the last few decades primarily through chemical diversity.¹⁻⁵ First, there was the development of new polymers from a seemingly endless variety of monomers. Next, random copolymerisation was used as an effective technique for tailoring or modifying polymers. Later, more controlled block and graft copolymerisation was introduced. The list of new concepts in polymer synthesis has not been exhausted. However, it has become clear that new chemical structures or organisation are not always needed to meet new needs or to solve old problems.

1.1 Polymer blends, alloys and composites

Mixing two or more polymers together to produce a blend (or 'alloy') is one well established strategy for achieving a specified portfolio of physical properties, without the need to synthesise specialised polymer systems.²⁻⁷ The subject is vast and has been the focus of much work, both theoretical and experimental.

More recently, an extraordinary research effort in polymer blends and alloys, in both academia and industry, has led to a mushrooming growth of the patent and scientific literature. A number of books, reviews and congress proceedings covering all aspects of the preparation, phase behaviour and applications of the different types of blends have been published.¹⁻¹⁴ The earlier development in polymeric materials involved synthesis of new homopolymers and copolymers for tailoring properties. The realisation that new molecules are not always required to attain desired properties

and that blending can be employed more readily has led to the commercial as well as scientific interest in blend technology. Polymer blends are mixtures of chemically different polymers and/or copolymers. They are mainly multiphase systems with the structure dependent on composition and processing conditions. 'Blends' are a direct result of the blending action and 'alloys' are the final blends of well-defined morphology and set of properties. Polymer alloys are a class of polyblends in which a large interpenetration of domains is secured by either chemical or physical means. As raw material cost contributes from 35 to 80 percent of the finished article, the future of polyblends lies in their attractive cost/performance ratio. The primary advantages in employing polymer blends or alloys are as follows: (a) higher performance at a reasonable price; (b) modification of performance as a market develops; (c) extending the performance of expensive resins; (d) reuse of plastic scrap; (e) generation of a unique materials with respect to processability and/or performance. Blends/alloys can be developed at a much faster rate than new polymers allowing manufacturers to respond rapidly to changing market requirements, since their properties are a function of composition. For these reasons the growth rate of polymer blends/alloys is about 40 % per year compared to the 10 % growth rate of the entire polymer industry. There is an increasing number of patents filed in the area and about 295 blends/alloys are commercially available.² The development of polymer blends/alloys requires a sound scientific basis and offers opportunities for interesting fundamental work. The interest amongst scientists in this area is evidenced by the large number of research papers, books and symposia held in this fast growing area.

1.1.1 Methods of blending

The manner in which two polymers are mixed together is of vital importance in controlling the properties of blends and to the ensuing properties of blends.^{4,5}

Preparation of polymer blends can be accomplished by: (i) melt mixing; (ii) solvent casting; (iii) co-precipitation; (iv) latex blending; (v) interpenetrating polymer networks (IPN) technology.

(i) **melt mixing** involves mixing of two polymers in the molten state under shear is usually achieved with the help of either a Brabender Plasticorder batch mixer or an extruder (single or double screw). For economic reasons mechanical blending predominates.

(ii) **solvent casting** involves dissolving the polymers in common solvent and the subsequent evaporation of solvent.

(iii) **co-precipitation** involves dissolving the polymers in a common solvent and the subsequent removal of solvent by precipitation using nonsolvent.

(iv) **latex blending** involves mixing the lattices of two polymers and spraying the mixture followed by drying.

(v) **interpenetrating polymer networks (IPN) technology** involves the polymerisation of a monomer in the presence of another polymer.

1.1.2 Types of blends and composites: *Terminology*

Polymer blend: A mixture of at least two polymers or copolymers.

Homogeneous blend: A mixture of two homologous polymers, usually narrow molecular weight distribution fractions of the same polymer.

Miscible polymer blend: Polymer blend homogenous down to the molecular level, associated with the negative value of free energy of mixing; $\Delta G = \Delta H \leq 0$.

Immiscible polymer blend: Any polymer blend whose $\Delta G = \Delta H \geq 0$.

Compatible polymer blend: A term indicating a commercially attractive polymer mixture with enhanced physical properties over the constituent polymers.

Polymer alloy: An immiscible polymer blend having a modified interface and/or morphology.

Compatibilisation: A process of modifying interfacial properties of an immiscible polymer blend, leading to the creation of a polymer alloy.

Composites: Composites consist of a thermoplastic matrix and reinforcing fibres as dispersed phase.

Macrocomposites: Inorganic materials like glass fibres or carbon fibres are used as reinforcement.

Microfibrillar Composites (MFCs): Upon drawing and annealing, the components of the immiscible blend are oriented and microfibrils are formed. Bundles of highly oriented microfibrils act as reinforcing elements in MFCs.

Molecular composites: Rigid rod molecules (eg. liquid crystalline polymer) are used as reinforcement dispersed phase within flexible coil matrix (eg. thermoplastic matrix).

1.2 Miscibility in blends and composites

Polymer blends can be characterised by their phase behaviour as being either miscible or immiscible. Immiscible blends show multiple amorphous phases with each phase consisting of essentially pure components whereas the phases of partially immiscible blends may contain some of each component. Blends can also be

completely miscible and have only one amorphous phase. The mechanical, thermal, rheological and other properties of a polymer blend depends strongly on its state of miscibility.¹⁻⁵

Only a few polymer blends are truly miscible on a molecular scale, poly(phenylene oxide)/polystyrene (PPO/PS) and poly(vinyl chloride)/polycaprolactam (PVC/PCL) are examples of such systems. Miscible systems exhibit a single glass transition temperature (T_g) located between the T_g values of the two components and are expected to behave like single component polymers. They are generally transparent and can be moulded without streaking. The heat distortion temperatures (HDT) of miscible blends vary smoothly with composition and thus are easy to predict and to control.

Most polymer mixtures are immiscible and form multiphase systems. The interface between two adjacent phases is not clear-cut. There are composition gradients whose levels depend on the intensity of mixing and on solubility parameter values (δ) of the polymers. These sometimes require compatibilisation in order to decrease the degree of immiscibility or to improve compatibility by mechanical or chemical means. Compatibilisers are generally graft or block copolymers of a mutually 'compatible' polymer or plasticiser and lead to the formation of alloys where interpenetration of domains is achieved to a greater extent.

1.2.1 Compatibilisation

Compatibilisation of blend components is a major consideration while designing blends and is often the primary criterion for commercial success. The major future challenges and developments for compatibilisation technology lie in

three main areas: engineering polymer blends, superior commodity polymers and polymer recycling. The influence of interfacial behaviour in polymer blends is schematically represented as in *Figure 1*.

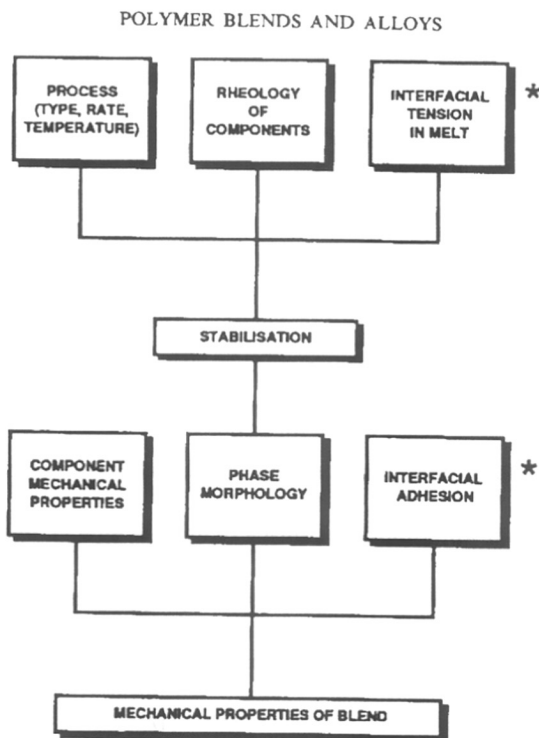


Figure 1.1 Influence of interfacial behaviour in Polymer Blends

1.2.2 Definition of compatibility

Blends are considered as compatible when they possess a desirable set of properties. Compatibilisation can interact in complex ways to influence final blend properties¹³: (i) reduce the interfacial tension in the melt, causing an emulsifying

effect and leading to an extremely fine dispersion of one phase in another; (ii) increase the adhesion at phase boundaries giving improved stress transfer; (iii) stabilise the dispersed phase against growth during annealing, which would modify the phase boundary interface.

1.3 Methods of compatibilisation

A number different approaches have been established for compatibilisation:^{4,5}

(1) Achievement of thermodynamic miscibility; (2) Addition of block or graft copolymers; (3) Addition of functional/reactive polymers; (4) *In situ* grafting/polymerisation (reactive blending)

1.3.1 Thermodynamic miscibility

It is recognised that the miscibility between polymers is determined by a balance of enthalpic and entropic contributions to the free energy of mixing. While for small molecules the entropy is high enough to ensure miscibility, for polymers the entropy is almost zero, causing enthalpy to be decisive in determining miscibility. The change in free energy on mixing (ΔG) is written as:

$$\Delta G = \Delta H - T\Delta S$$

where H is enthalpy, S is entropy and T is temperature. For spontaneous mixing, ΔG must be negative, and so

$$\Delta H - T\Delta S < 0$$

This implies that exothermic mixtures ($\Delta H < 0$) will mix spontaneously, whereas for endothermic mixtures miscibility will occur only high temperatures. For two-component blends it is possible to construct a phase diagram which may exhibit lower or upper critical solution temperature (LCST or UCST). In practice, LCST

behaviour is more commonly seen, with phase separation occurring as temperature increases, because the intermolecular attractive forces responsible for the miscible behaviour tend to disappear as the internal energy of the molecules becomes high enough to overcome them as depicted in *Figure 1.2*.

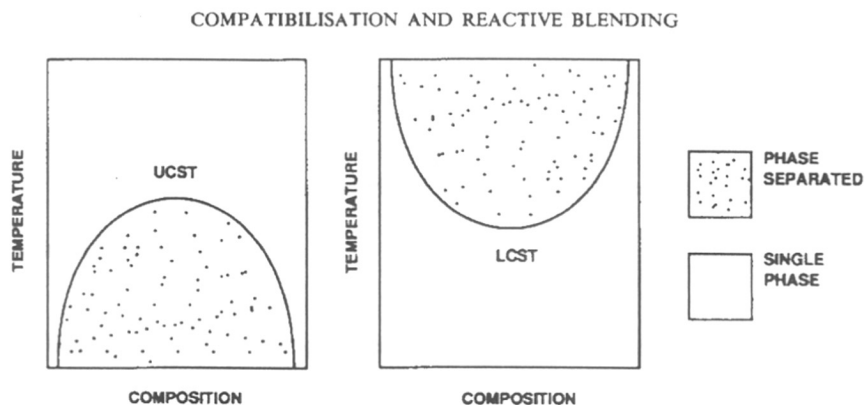


Figure 1.2 Schematic diagrams of binary blends showing LCST and UCST behaviour

1.3.2 Addition of block and graft copolymers

The addition of block or graft copolymers represents the most extensively researched approach to compatibilisation of blends. The block and graft copolymers containing segments chemically identical to the blend components are obvious choice as compatibilisers. The copolymer should meet certain structural and molecular weight requirements in order to locate it preferentially at the interface as shown in *Figure 1.3*.

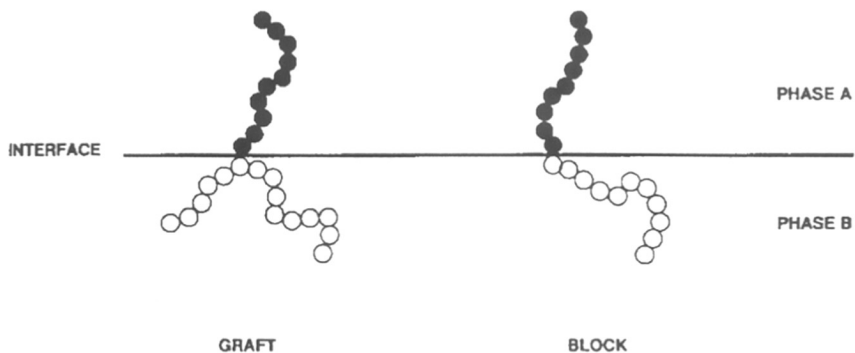


Figure 1.3 Schematic diagram showing location of block and graft copolymers at phase interfaces

Copolymer structure and molecular weight have important influence on their effectiveness as compatibilisers. The effect of different copolymer types on the compatibility of PE/PS blends has been studied extensively by Fayt et. al.¹⁵ Using ultimate tensile strength of the blends as a measure for effectiveness of compatibiliser, they concluded that:

- (a) Block copolymers are effective than graft copolymers.
- (b) Diblock copolymers are more effective than triblock or star-shaped copolymers.
- (c) ‘Tapered’ diblock copolymers are more effective than pure diblock copolymers.

Paul¹⁶ suggests that solubilisation of a discretely dispersed homopolymer into its corresponding domain of a block copolymer compatibiliser occurs only when the molecular weight of homopolymer is equal to or less than that of the corresponding block. Gaylord¹⁷ offers the pragmatic view that a balanced molecular weight is needed for copolymer compatibilisers i.e., the segment needs to be long enough to

anchor to the homopolymer (i.e. to solubilise) but short enough to minimise the amount of compatibiliser needed, and hence be cost-effective.

The requirement that the copolymer should locate preferentially at the blend interfaces also has implications for the molecular weight of the compatibiliser.¹⁸ Both the thermodynamic 'driving force' to the interface and the kinetic 'resistive force' to diffusion increase with molecular weight, suggesting that high molecular weight copolymers may be used if sufficiently long times are available during the process, but that lower molecular weights must be used if the available diffusion times are short.

1.3.3 Addition of functional polymers

The addition of functional polymers as compatibilisers has been described by many workers. A polymer chemically identical to one of the blend components is modified to contain functional (or reactive) units, which have some affinity for the second blend component. This affinity is usually the ability to chemically react with the second blend component, but other types of interaction (e.g: ionic) are possible. The functional modification may be achieved in a reactor or via an extrusion-modification process. Thus, on grafting maleic anhydride or similar compounds to polyolefins, the resulting pentent carboxyl groups acquire the ability to form a chemical linkage with polyamides via their terminal amino groups.

1.3.4 Reactive compatibilisation

A comparatively new method of producing compatible thermoplastic blends is via reactive blending, which relies on the *in situ* formation of copolymers or interacting polymers at the interface of the blends during melt blending.^{4,19-21}

Compared to batch-type melt mixers, continuous processing equipments such as single- or twin-screw extruders are often preferred for reactive blending. Continuous processing equipments have several advantages like excellent temperature control, continuous production as well as the provision for the removal of unwanted reaction products by devolatilisation.

A number of reactive blending mechanisms may be exploited:

(i) Formation of *in situ* graft or block copolymer by chemical bonding reactions between reactive groups on component polymers (also possible by the addition of free radical initiators);

(ii) Formation of a block copolymer by an interchange reaction in the backbone of the components (this is common in condensation polymers); (iii) Mechanical scission and recombination of component polymers to form graft or block copolymers; (iv) Promotion of reaction by catalysis. The area of reactive blending is one in which there is currently a great deal of developmental activity, and much proprietary knowledge.

1.4 CHARACTERISATION OF POLYMER BLENDS AND COMPOSITES

This section describes the important polymer blend properties and methods to characterise them. The main interests of those developing new polymer blends are to investigate and to measure the degree of miscibility and the interaction of phases, as they can significantly influence the properties and behaviour of the blend.²⁻⁵ Table I shows the structure-property relation in polymer and polymer blends.

1.4.1 Mechanical properties

Since plastics are primarily used for structural applications, the mechanical properties of these materials are of great importance. Important parameters affecting polymer properties are time, temperature and humidity.

Modulus of elasticity: The stiffness of material is usually expressed by modulus of elasticity.

Table 1.1: Processing - Structure - Property Relations in Polymers and Polymer blends

Molecular architecture	:	<ul style="list-style-type: none"> * Molecular weight/ * Molecular weight distribution * Linearity/rigidity * Molecular interactions * Packing ability
Inherent polymer properties	:	<ul style="list-style-type: none"> * Glass transition temperature * Crystallising ability * Melting/softening temperature * Melt viscosity * Elasticity
Processing conditions	:	<ul style="list-style-type: none"> * Pressure/temperature/quench rate * Shear or extension * Heat deflection temperature (HDT)
Structure	:	<ul style="list-style-type: none"> * Degree of crystallinity * Orientation (crystalline/amorphous) * Crystalline morphology * Crystalline size distribution * Fibre orientation
Product properties	:	<ul style="list-style-type: none"> * Tensile strength * Impact strength * Flexural modulus

Tensile properties: These are related to the basic property describing the atomic bond strength. The properties of polymers are dominated by the strength of the covalent carbon-carbon bond. Properties determined under flexural loading most closely duplicate stresses experienced under practical applications. The specimen is extended at a predetermined, constant rate and the resulting stress (load acting at the upper jaw) is determined.

Flexural properties: Flexural property is the material response to a combination of tensile and compressive forces.

Impact strength: Impact strength is nothing but the total ability of the material to absorb impact energy. The Impact strength of blend depends upon its interfacial behaviour.

1.4.2 Thermal properties of polymers

Thermal analysis techniques are very useful in the characterisation of polymeric materials. Several structural transitions can occur in polymers during heating. These transitions are melting and crystallisation, glass transition, crystal transformations, decompositions and other chemical reactions, volatilisation and annealing effects.^{6,7} Other thermal properties of interest are heat distortion temperature and linear coefficient of thermal expansion. For characterisation of polymer blends the most important transitions are the glass transition temperature and the melting point.

Structural changes are usually associated with changes in heat absorption or emission and are measured using differential scanning calorimetry (DSC). DSC can

measure changes at constant heating or cooling rates. The differences in heat loss or gain between the sample and the reference cells are measured in a differential scanning calorimeter. The heat input needed to maintain both cells at the same temperature is measured. DSC can be used to measure melting transition temperature (T_m), crystallisation temperature (T_c) and glass transition temperature (T_g).

Glass transition temperature: The glass transition temperature (T_g) is neither a thermodynamic transition such as the melting transition nor a sharp temperature point. T_g is a characteristic material constant. It is the transition associated with the change in the specific heat capacity and thus is related to the freedom of molecular motions. T_g is influenced by degree of crystallinity and molecular weight. The sudden change in heat capacity at T_g is manifested as a step on the temperature versus differential heat absorbed curve. The material has different mechanical and other properties on either sides of this transition. In physical blends of two polymers each polymer retains its own transition temperature. The presence of single glass transition temperature for a blend is an indication of homogeneity on a molecular level and thus mechanical integrity.³⁻⁵ The measurement of glass transition temperature can therefore assist in the determination of compatibility of amorphous polymer blends.

Heat deflection temperature: Heat deflection temperature (HDT) is the point at which the 10.2 cm long test bar deflects by 0.025 cm.

Linear thermal expansion coefficient: Thermal shrinkage is a material property of the solidifying polymer. To obtain the correct dimensions of precision (dimensional stability) moulded parts, the mould shrinkage must be taken into account. Polymer with low coefficient of thermal expansion can easily be moulded into discrete shapes. The highly oriented thermotropic liquid crystalline polymers have lower coefficient of

thermal expansion than thermoplastics. Thermomechanical analyser (TMA) is used for measuring linear thermal expansion coefficient.

1.4.3 Melting and crystallisation behaviour of blends:

Blends with crystallisable components have received increasing attention both for fundamental and practical reasons.²² The two components may influence each other giving rise to very interesting effects such as: (i) depression of the equilibrium melting temperature; (ii) decrease or increase of the crystallinity and of the rate of crystallisation; (iii) drastic change in morphological features such as lamellar thickness; (iv) change in the size and shape of the spherulites.

The following morphologies may be encountered in alloys with one crystallisable component: (a) the spherulites of the crystallisable components grow in a matrix consisting mainly of the non-crystallising polymer; (b) the non-crystallisable component may be incorporated in the interlamellar regions of the spherulites of crystallisable polymer and the spherulites fill all the available volume; (c) the noncrystallisable component may be included within the spherulites of the crystallisable polymer forming domains having dimensions larger than the interlamellar spacing.

For blends having both crystallisable components the most probable morphologies are: (i) crystals of the two components are dispersed in an amorphous matrix; (ii) one component crystallises according to a spherulite structure while other crystallises in a simpler structure; (iii) both components exhibit separate spherulitic structures; (iv) the two components crystallise giving rise to the formation of mixed spherulites containing lamellae of both polymers.

The crystallisation kinetics of a polymer crystallising from a mixture containing another polymeric component may be strongly influenced by composition, particularly when the two polymers have a certain degree of compatibility in the melt. The dispersed phase may influence the shape, size and growth rate of the spherulite texture.

A substantial depression in the melting temperature of crystalline component has been often observed in crystallisable blends. This effect is particularly relevant in blends where the two components are compatible in the amorphous state. A melting point depression has been observed also in systems which are not compatible in the molten state. In such cases the melting point depression must be attributed to kinetic and morphological effects of the noncrystallisable polymer producing a reduction in crystal size, lamellae thickness or crystal perfection.

TH 1126

1.4.4 Phase morphology

The morphological studies are very important in order to establish how the processing condition may govern the morphological features and hence the end-use properties of these blends.²³ The basic modes of dispersion are: (i) ribbons and lamellae (stratified morphology), (ii) rods and fibrils and (iii) droplets. The overall morphology, i.e, the modes and the state of dispersion of different phases in mixture of incompatible molten polymers depends on the blend compositions, starting particle size, molecular weight distribution of individual components, and blending method adopted.

Scanning electron microscopy (SEM): SEM can give information on surface topography of the materials. It can reveal the level of interfacial adhesion of different

phases in polymer blends. The shape, size and degree of mixing of dispersed phase can be investigated by SEM.

Transmission electron microscopy (TEM): TEM provides information on the fine structure of materials down to atomic or molecular levels.

Polarised light optical microscopy (PLOM): The morphology of blends in the molten state, the size and shape of spherulites of matrix polymer in the presence of another polymer can be studied using PLOM.

Light scattering, Neutron scattering, X-ray scattering and Spectroscopy can give quantitative informations about interaction between the phases.

1.4.5 Rheological behaviour

In two phase blends, the component forming the discrete phase (droplets or long ribbon) is dispersed in the continuous phase. The dispersed phase is usually not uniform in size and shape and the average size depends on blending conditions such as mixing equipments, time of mixing etc.²⁴

The rheological behaviour of polymer blends is closely related to the deformation of the droplets in the continuous phase. Much of the work carried out on the rheology of heterophase systems deals with the deformation of Newtonian droplets suspended in a Newtonian fluid.²⁵ A schematic representation of two-phased molten polymer blend flowing through a capillary is shown in *Figure 1.4*.

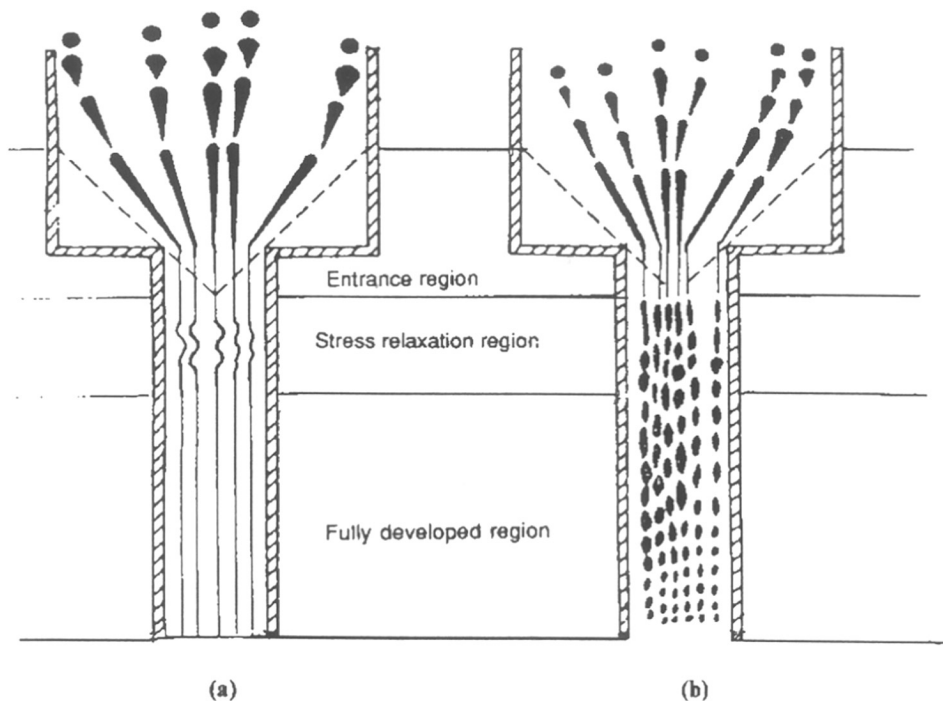


Figure 1.4 Schematic representation of molten two-phase dispersed polymer blend flowing through a capillary. (a) fibre-like domain; (b) droplet-like domains

Moreover, the behaviour of droplets in non-uniform shear flow depends on the location of the droplets in the plane of shear. The deformation and the orientation angle of the droplets are expressed as a function of the viscosity ratio of the droplet and the suspending medium, the droplet radius, the interfacial tension and the rate of deformation. A study on droplet deformation performed by Chin and Han²⁶ showed that increased droplet deformations occur on increasing the medium viscosity, the initial droplet size or the elongational rate and on decreasing the interfacial tension.

Figure 1.5 illustrates a schematic representation of different variables affecting physical and mechanical properties of polymer blends.

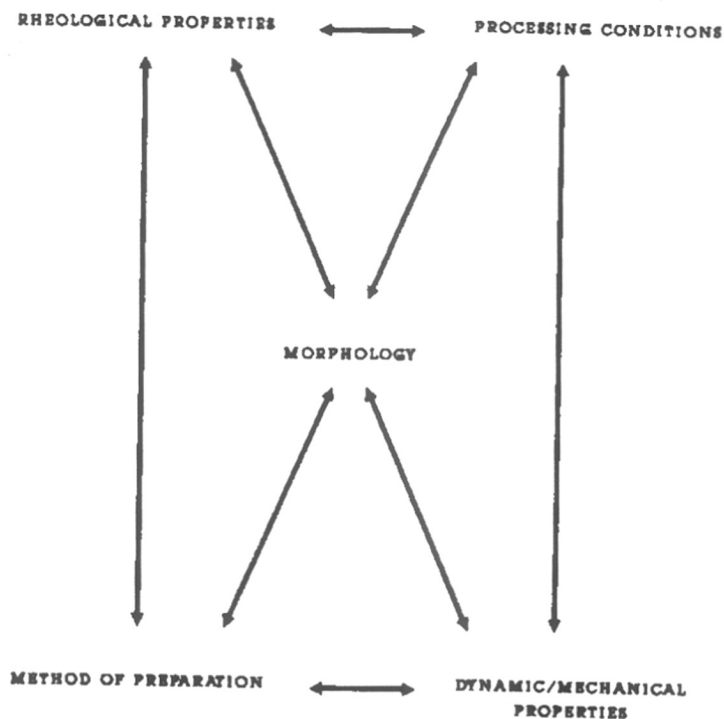


Figure 1.5 Variables affecting physical and mechanical properties of polymer blends

1.5 *IN SITU* FIBRE COMPOSITES FROM POLYMER BLENDS

Fibre-reinforcement has been used for many years to increase the engineering performance of thermoplastics. There are three different types of composites:

1.5.1 Macro-composites

In macro-composites, inorganic fibres and fillers like glass fibres, carbon fibres are used as reinforcements. However, the use of solid fibres in thermoplastics causes a substantial increase in melt-viscosity and lowers the ease of processing. The *in situ* generation of reinforcing species offers advantages over the addition of solid fibres and fillers.

1.5.2 Microfibrillar reinforced composites (MFCs)

A new type of polymer composite called microfibrillar reinforced composite (MFC)²⁷⁻²⁹ has been developed recently. With respect to the size of the reinforcing elements, MFCs take an intermediate position between the two extreme groups of polymer composites, macrocomposites and molecular composites. Unlike classic composites, MFCs are formed from two immiscible (eg: polyamides/polycondensates system), crystallisable homopolymers by drawing the polymer blend and then annealing. Upon drawing, the components of the blend are oriented and microfibrils are formed. The structural perfection develops during subsequent annealing. The temperature and duration of annealing have been shown to significantly affect the structure and properties of the blend. If the annealing temperature is set in between the melting temperatures (T_m) of the two components, the low melting component melts to form an isotropic matrix while the microfibrillar regions involving the component with higher T_m preserve their orientational and morphological characteristics. The resulting material is referred to as a microfibrillar-reinforced composite (MFC). Bundles of highly oriented microfibrils act as reinforcing elements in MFC.

1.5.3 *In situ* molecular composites

The rigid-rod polymeric materials fabricated from the liquid crystalline state far exceed the strength and modulus properties of structural metals used currently in advanced aircraft and aerospace systems.^{4,30-40} It is very easy to produce fibres and films from these rigid materials. It is however difficult to laminate liquid crystalline polymeric materials to obtain large bulk specimen due to its anisotropic nature as well as the close proximity of glass transition temperature (T_g) to its decomposition temperature.

One of the solutions is to blend these materials with flexible coil polymers. Thus a molecular composite is defined as rigid-rod molecules molecularly dispersed in a matrix of flexible coil polymer such that the rods act as the reinforcing elements. Compared to conventional fibre composites, these molecular composites show excellent dimensional stability as well as very good fracture and impact toughness. The high modulus strength of rigid-rod LCPs is transferred to the flexible thermoplastic matrix to form a virtually ideal *in situ* molecular composite.

Thus, molecular composites based on thermoplastic as matrix and liquid crystalline polymers as reinforcement offer exciting engineering technologies in the field of structural materials.

The ensuing section deals with the structure, properties, processing and applications of liquid crystalline polymers and their blends with thermoplastics.

1.6 LIQUID CRYSTALLINE POLYMERS

Liquid crystalline polymers (LCPs) are a new class of engineering plastics which have attracted significant interest in the last two decades.^{4,30-44} De Gennes,³⁰ Onsager³¹ and Flory^{32,33} predicted some 40 years ago that the incorporation of liquid crystallinity would result in very interesting and exiting performances in plastics and fibres. A liquid crystal is quite simply a state of matter between the liquid and crystalline states.

A liquid crystal is an ordered fluid. Structural elements which act as rigid rods are essential in the polymer chain to form liquid crystal phases. Rods, discs, planks and helices as depicted in *Figure 1.6* are well documented examples.

1.6.1 Lyotropic liquid crystalline polymers

Polymers in which liquid crystalline properties are induced in the presence of a solvent are called *lyotropic* (Example: KEVLAR). In these, the liquid crystallinity is observable within definite range of concentration in solution. These are the first generation liquid crystalline polymers. Lyotropic liquid crystal polymers can be processed from solutions in highly polar solvents by wet spinning methodologies.

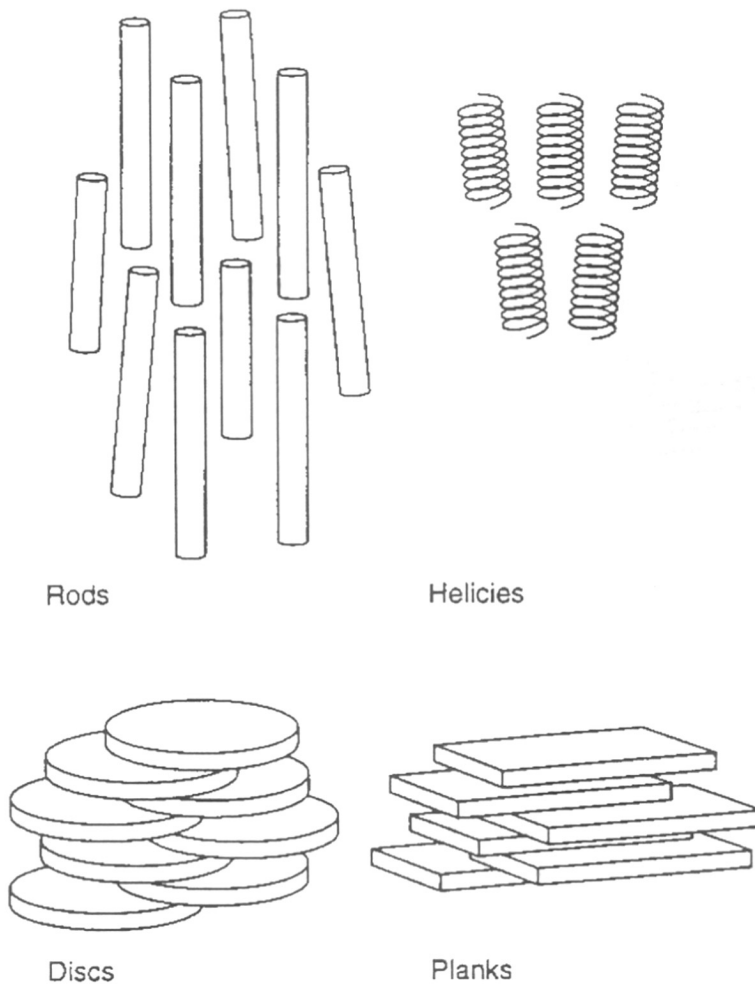


Figure 1.6 Anisotropic units giving rise to liquid crystal phases

1.6.2 Thermotropic liquid crystalline polymers

These are the second generation high performance polymeric systems. In these, the ordered liquid crystalline molten state is observed over a temperature range above the crystalline solid state and below the formation of a normal molten state with

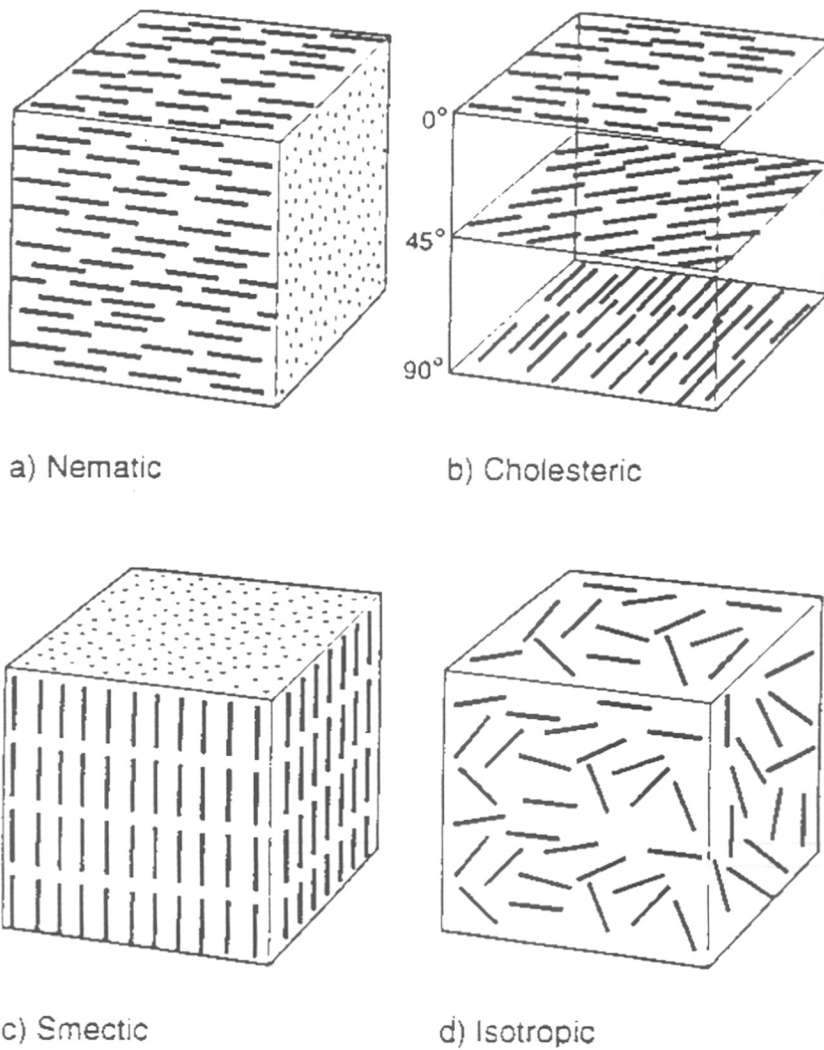
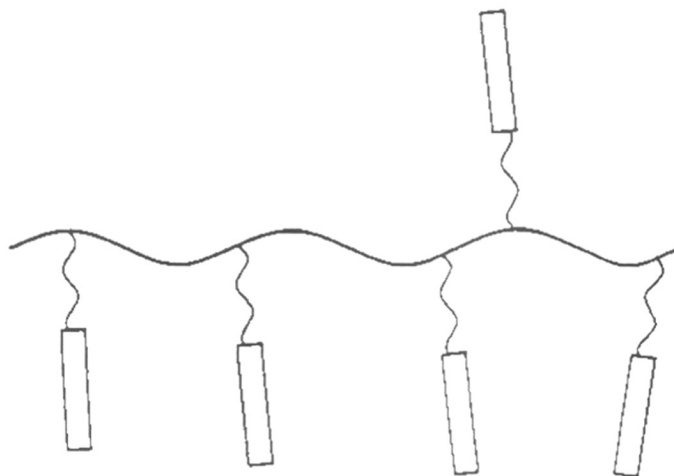


Figure 1.7 Comparison of three liquid crystal phases (a, b and c) with isotropic state (d)



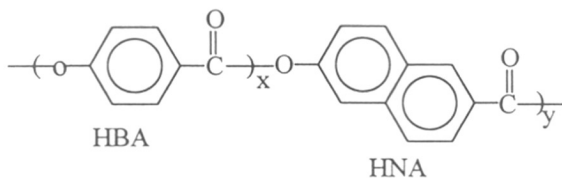
a) Side chain liquid crystal polymer



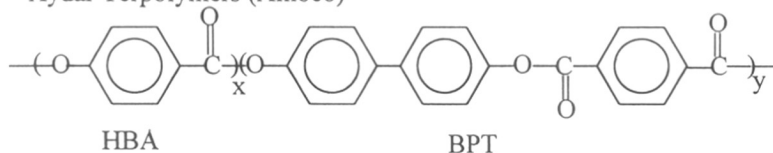
b) Main chain liquid crystal polymer

Figure 1.8 Types of liquid crystal polymers

Vectra Copolyesters (Hoechst Celanese)



Xydar Terpolymers (Amoco)



X-7G (Kodak, Tennessee Eastman)

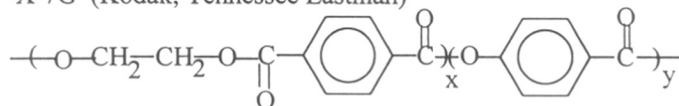


Figure 1.9 Commercially available TLCPs

a random arrangement of chains. Thermotropic liquid crystalline polymers need to be processed from the ordered molten state to have the inherent high performances frozen in the solid state.

Thermotropic liquid crystals can be classified into 3 types according to the arrangements of their molecules. They are: (i) smectic, (ii) nematic and (iii) cholesteric phases as illustrated in *Figure 1.7*.

Cholesteric phase is induced by the presence of an optically active centre in the liquid crystal or by the addition of an optically active compound to a nematic liquid crystalline (LC) polymer. Cholesteric LC polymers show reflection of colours.

Thermotropic liquid crystalline polymers (TLCPs) would exhibit one of the above liquid crystalline structures. There are two main ways by which anisotropic LC building block can be transferred into a polymer: by joining end to end to form a main chain TLCP or by dangling from the side of a normal polymer chain to form a side chain TLCP, as shown in *Figure 1.8*. “Main-chain” LCPs have already met commercial applications as high modulus materials, whereas “side-chain” LCPs are currently very actively investigated in view of their potential applications in optoelectronics.

The most important TLCPs for blending with bulk polymers are thermotropic main chain TLCPs that exhibit a liquid crystal phase within the processing window of the bulk polymer but which then solidifies on cooling to room temperature. As with any polymer, a LCP can either crystallise on cooling or go through a glass transition temperature. Hence, at room temperature, the structure of the TLCP is that of an ordered glass or a semi-crystalline polymer. The chemistry of commercial TLCPs has been dominated by aromatic polyamides (e.g. Du Pont’s Kevlar) and aromatic polyesters (e.g. Hoechst Celanese’s Vectra or Amoco’s Xydar). Other commercial types have been synthesised (e.g. liquid crystal polycarbonates, liquid crystal polyphosphazenes and liquid crystal siloxanes). The structures of commercially available TLCPs are shown in *Figure 1.9*.

1.6.3 Properties, processing and applications of TLCPs

Thermotropic LCP materials have very good thermal, physical, dielectric, optical and mechanical properties as well as good chemical resistance, low flammability, very good dimensional stability. They also show excellent

processability and high melt strength. The thermal properties of commercial TLCPs are tabulated in *Table 1.2*.

Table 1.2: Commercially available thermotropic liquid crystalline polymers and their physical properties.

LCP name	Manufacturer	Formulation	Melting point T _m (°C)	Glass transition temperature T _g (°C)	Processing temperature (°C)
VECTRA A	Hoechst Celanese	HNA(27%),HBA (73%)	283	105	320-340
VECTRA B	Hoechst Celanese	HNA(58%), TPA(21%), 4AP(21%)	280	110	300-330
X7	Eastman Kodak	PET/HBA (HBA 40, 60 or 80%)	250-300	70, 143	270-350
RODRUN	Unitika	PET/HBA	250	70, 143	270-350
LX-series	Du Pont	TA, HQ, PHQ	310	195	270-350
ULTRAX KR	BASF	?	-	-	340-360
XYDAR	AMOCO	BP, HBA, TA	412	-	>420
VITREX SRP	ICI	HBA, HQ, IA	280	-	300-350
KU-9211	Bayer	HBA, TA, HQ, IA, BP	-	198	330-360

HNA: 2-hydroxy-6-naphthoic acid
4AP: 4-aminophenol
TA: terephthalic acid
PHQ: phenyl hydroquinone
IA: isophthalic acid

HBA: 4-hydroxy benzoic acid
PET: poly(ethylene terephthalate)
HQ: hydroquinone
BP: 4,4'-dihydroxybiphenyl

Thermotropic materials are processed by injection moulding, extrusion, thermoforming, blow moulding etc. Nematic liquid crystals possess a relatively low viscosity and can be deformed by small external forces. Some property profiles of thermoplastics and TLCPs are compared in *Table 1.3*.

Table 1.3: A comparison of properties of thermoplastics and thermotropic liquid crystalline polymers

TLCPs	Thermoplastics
Anisotropic	Isotropic
Low linear thermal expansion coefficient	High linear thermal expansion coefficient
Low melt viscosity	High melt viscosity
Low mould shrinkage	Comparatively high mould shrinkage
Very good melt strength	Poor melt strength
Easy processability	Poor processability
Very good mechanical properties	Poor mechanical properties
Excellent barrier properties	Poor barrier properties

Liquid crystalline polymers offer many advantages over conventional thermoplastics in injection moulding such as low mould shrinkage, minimum warpage and distortion, fast cycle time, low moisture etc.

Table 1.4: Commercial applications of LCPs

Area	Property	Applications
Electrical/Electronics	Low dielectric constant, high dielectric strength, arc resistance, resistance to vapour phase and wave soldering.	Connectors, capacitor housing, potentiometers, switches, Printed circuit boards.
Fibre optics	Excellent mechanical properties, inherent flame retardance, good moisture resistance and low coefficient of thermal expansion	Connectors, strength membranes and couplers
Aircraft/Aerospace	High strength to weight ratio high temperature performance, low coefficient of thermal expansion and excellent dimensional stability	Parts of space vehicles, Aircraft engines, Helicopters, Missiles
Industrial	Excellent mechanical strength, very good dimensional stability and heat resistance	Motor components, lamp housing, conveyer belt components, gears
Automotive	Resistance to automobile fluids, solvents, very good dimensional stability and flame retardance	Fuel-system components, electrical/electronics systems
Medical	Toughness, low permeability, non-toxicity, compatibility with sterilisation techniques.	Various medical components
Chemical process	Chemical resistance, heat resistance, dimensional stability	Chemical tower packings and in oil well logging devices.
Cookware	Toughness, heat resistance, resistance to staining and odour retention	Microwave equipment and turntables
Fibre applications	LCP fibres with excellent tensile properties, low density, thermal resistance, low creep, weatherability	Protective fabrics, gloves, clothing, ropes, sewing threads, rubber reinforcement in radial tyres, belts, cement reinforcements etc.
Other	Dimensional stability, mechanical properties and good moisture resistance	Watch components, safety equipments etc.

Thermotropic LCP rods are manufactured by extrusion under conditions which produce a strong molecular orientation in the flow direction. The orientation is preserved by rapid cooling. These LCP rods are useful in optical keyboard applications. LCP rods have low weight, considerable flexibility, low thermal expansion coefficient and excellent tensile properties.

Oriented LCP sheets and films are produced either by pressing the fibres at melt temperature or by extruding the solution of LCP. LCP films have very good mechanical properties and low coefficients of diffusion and are used as high performance packaging materials. Sheets of mineral filled LCP materials have been used for thermoforming and electroplating of printed circuit boards. Typical applications of LCPs are listed in *Table 1.4*.

LCP/carbon - fibre composites have been developed and are used in aerospace industry. LCP matrices offer low viscosity for the impregnation of fibres and excellent chemical resistance. Impregnation is achieved in a cross-head die, after which the panels are prepared by compression moulding the stacked prepreg sheets.

The liquid crystalline polymer market will grow to USD 10 billion by 2000, from USD 3.4 billion in 1996, according to a study that covers three broad classes - lyotropic aromatic polyamides used for fibres, thermotropic aromatic polyesters for structural parts and functional LCPs with nonlinear optical properties.

1.7 POLYMER BLENDS CONTAINING TLCPs

The concept of molecular composites first originated from the work of Flory³³ on the polymer rigid rods. He studied ternary blends of rigid rods (PBX type, aramids, and copolyesters) with conventional polymers in solvents. A molecular composite is

defined as rigid-rod molecules molecularly dispersed in a matrix of flexible coil polymer such that the rods act as the reinforcing elements. Reinforcement through the addition of TLCPs to thermoplastics has been investigated over the last few years with some encouraging results.^{4,32-40} The principal goal is to achieve improvements in mechanical properties by using the TLCP component to reinforce the flexible thermoplastics through the formation of fibres. Blending is also considered as a possible route to overcome the highly anisotropic physical properties of TLCP that

Table 1.5: Applications of thermoplastics/liquid crystalline polymer blends

Area	Properties	Application
Electronic	Excellent mouldability, dielectric property and good thermal stability	Moulded interconnected devices, multi layer circuit boards
Automotive	Excellent processability, high use temperature	Engine parts and in under-the-hood parts
Aircraft	High use temperature, good fatigue resistance, high modulus and excellent processability	Primary/secondary structural components in aircraft
Medical	Excellent barrier properties, High use temperature and non-toxicity	Thin films with high strength finds applications in various medical equipments
Packaging	Selective permeability, excellent processability	Thin films are used for packaging applications

can be problematic in many applications. The challenge is to produce organic TLCP fibres *in situ* that give the required level of reinforcement at a realistic cost. The use of TLCPs in polymer blends looks attractive from a number of view points: (a) The high para-linked aromatic content gives polymers with good moduli; (b) TLCPs have very low melt viscosities allowing good flow properties and ease of processing; (c) TLCPs form fibrous structures; (d) TLCPs show excellent chemical resistance and low mould shrinkages.

1.7.1 TLCPs as reinforcement

The ability of LCPs to form fibrillar morphology within a thermoplastic matrix during melt processing makes it possible to develop *in situ* fibril reinforced molecular composites from thermoplastics/liquid crystalline polymer blends. The control of LCP's morphology, its interfacial adhesion with blend matrix, thermoplastics to LCP composition ratio are important for the achievement of maximum desirable properties. Thermoplastics/LCP blends have started to compete effectively with carbon or glass fibre reinforced composites. Techniques with high extensional flow such as spinning, extrusion and injection moulding ideally facilitate the high performance properties of the thermoplastics/LCP blends.

1.7.2 TLCPs as processing aid

The melt viscosity of LCPs are lower than that of thermoplastics. Therefore, on blending with thermoplastics, the blend viscosity drops dramatically. LCPs can act as processing aid for thermoplastics thereby reducing energy consumption. Also,

other advantages such as less degradation of polymers and easy filling of complex moulds have been demonstrated.

Engineering plastics so far used as matrix for LCP blends are polycarbonate (PC),⁴⁵⁻⁵¹ poly(ethylene terephthalate) (PET),⁵¹⁻⁵⁶ poly(butylene terephthalate) (PBT),^{57,58} polyamides (PA),⁵⁷⁻⁵⁹ Poly(ether sulfone) (PES),^{58,60} polyether imide (PEI),^{58,61} poly(ethyl ether ketone) (PEEK),^{58,60} polypropylene (PP),⁶² polyethylene,⁶³ polyvinyl chloride (PVC),⁶⁴ poly(phenylene oxide) (PPO),⁶⁵ polystyrene (PS)^{59,60,65} etc. The application potentials of TP/TLCP blends in different fields are presented in *Table 1.5*.

One of the important thermoplastics selected as matrix for *in situ* composite is poly(phenylene sulphide). The following section deals with the structure, properties, modification of properties and applications of poly(phenylene sulphide).

1.8 POLY(PHENYLENE SULPHIDE) (PPS)

Poly(phenylene sulphide) (PPS) is a high performance engineering plastic, based on aromatic monomer units. The polymer was first reported in 1897.⁶⁶ The first commercial plant was put up in 1972 by Phillips Petroleum Company in USA. The polymer has been marketed under the trade name Ryton. There are 72 different grades of PPS marketed by various companies using the base resin produced by Phillips Petroleum Company.

Friedel and Crafts⁶⁷ in 1888 and Genvresse⁶⁶ in 1897 tried to synthesise PPS by the reaction of benzene with sulphur in the presence of aluminium chloride. But the products were oligomeric. Other synthetic route involved the self condensation of

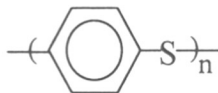
cuprous p-bromo thiophenoxide reported by Lenz in 1962.⁶⁸ Although the reaction gave a linear PPS, removal of the by-product, cuprous bromide, from the polymer was difficult.

The commercial process for the production of PPS was discovered by Edmonds and Hill.⁶⁹ This involves the production of PPS from relatively inexpensive starting materials, p-dichloro benzene and sodium sulphide in a polar solvent under high temperature and pressure. The polymer produced by this method is linear, containing 150-200 repeat units, and has molecular weight in the range 15,000-20,000.

Polymer obtained from this process is referred to as "virgin" polymer. We can produce moulding resins from virgin polymer by a process known as solid state polymerisation below the melt temperature of the resin.

1.8.1 Structure, properties and applications of PPS

Structurally, the polymer backbone of PPS consists of p-substituted aromatic rings inter-connected by sulphur linkages. Linear PPS has one sulphur atom between the p-phenylene units. The chemical structure of the PPS can be represented as,



Poly (phenylene sulphide)

PPS is a unique resin in a number of ways. It combines the properties of both thermoplastic and thermosetting class of materials. Under normal conditions, PPS behaves as a true thermoplastic. The polymer can be repeatedly melted and solidified with minor changes in its mechanical properties. It can behave as a thermoset

polymer when it is subjected to a process called "curing", even though the reactions involved are many times slower than that in typical thermosets.

PPS is a crystallisable polymer with crystalline melting point, T_m of 285 °C and a glass transition temperature, T_g of 85 °C. The repeating p-phenylene units impart rigidity to the polymer chain and the symmetry due to p-phenylene linkages imparts a high degree of crystallinity. PPS exhibits good thermal stability, chemical resistance, inherent flame retardance, good mechanical strength and processability. The polymer is insoluble in most organic solvents. It is soluble to a limited extent in some aromatic solvents at elevated temperatures. 1-chloro naphthalene at around 206 °C is a typical solvent for PPS. PPS is an inherently conducting polymer. Doping with arsenic pentafluoride increases the conducting properties of PPS and yet retains its melt-processable characteristics.⁷⁰

"Curing" is the thermal treatment by which we can improve the mechanical properties of PPS⁶⁷. There are two types of curing processes - melt curing and solid state curing. The cure reaction of PPS consists of chain scission, extension and some degrees of crosslinking. When the polymer is cured at different temperatures (all below T_m), an increase in the curing temperature results in increases in both cure rate and amount of cure. Either air or oxygen is used as curing atmosphere. Curing rate is higher in oxygen atmosphere. The process is known as solid state polymerisation and is carried out below the melt temperature of the virgin resin. The solid-state cure behaviour of PPS is also affected by the particle size. As the particle size increases, the rate of cure decreases.

During the curing process of PPS, changes in its properties such as an increase in molecular weight, loss of solubility, increase in melt viscosity, a change in colour

from off-white to dark-brown and a decrease in ultimate crystallinity all occur. The resultant cured polymer is much tougher, stronger and easier to process by injection or compression moulding than the virgin polymer. The magnitude of these changes depends on the degree of cure. The degree of cure is controlled by the time and temperature employed in the curing process.

Due to the inherent excellent chemical resistance of PPS resin, the elucidation of the cure mechanism by chemical method is difficult. The various reactions that are believed to be involved in curing process⁷¹⁻⁷³ are: (1) Disproportionation to produce a higher molecular weight moiety and diphenyl sulfide; (2) Heating in presence of air results in the formation of aryl-ether crosslinks between adjacent polymer chains; (3) Thermal crosslinking in the absence of air produces bridges in which connecting species are aryl or sulphur.

When an alkali metal carboxylate is used as polymerisation modifier, higher molecular weight PPS can be obtained. By the incorporation of a small amount of trichloro aromatic compound, we can prepare even higher molecular weight, soluble polymer. Compared to cured resin, a high molecular weight polymer provides higher tensile strength, elongation, flexural strength and impact strength.

Because of its unique combination of properties and wide range of melt viscosities, PPS finds applications in many areas, including electrical, electronic, mechanical, automotive and coating applications. Most end products are fabricated by injection moulding. For applications involving injection moulding, PPS is compounded with glass fibres and fillers. Small amount of PPS is used in sintering and compression mouldings. Typical applications include bearings, roller elements and seals, rods, tubes, electrical components, valves, pistons, rings, lighting reflectors,

thermostat housings, street light design etc. Exhaust gas emission valve on Toyota automobiles is a specific application of PPS. The polymer can be made conductive by doping and possible applications in the fabrication of printed circuit boards are obvious.

1.8.2 Modification of properties of PPS: PPS Composites and Blends

The applications of neat PPS have been somewhat limited owing to its demerits such as relatively low T_g compared to its high T_m and inclination to brittleness. Reinforcement of PPS with long fibre produces thermoplastic composites exhibiting increased strength and toughness.⁷⁴⁻⁷⁸ The PPS thermoplastic composites based on long glass fibres are characterised by high impact strength and flexural moduli. When long carbon fibres are used as reinforcing agent in the PPS composites, an even higher level of mechanical properties can be obtained.

Composites have been investigated so as to provide an effective means to achieve property balances, processing characteristics, and often to reduce costs. In particular, PPS has been used as a thermoplastic matrix for advanced thermoplastic composites. Blends of PPS with other polymers, glass and carbon fibres have been examined. The other polymers blended with PPS have been poly(ethylene terephthalate),^{74,75} polyethylene,⁷⁶ polyether sulphone (PS)⁷⁷ and polyamides.⁷⁸ It will be interesting to examine blends of PPS with thermotropic liquid crystalline polymers. The crystallisation kinetics of such blends of PPS will be enhanced by the thermotropic liquid crystalline polymers which tend to crystallise rapidly.⁷⁵ This would also alter the morphological characteristics of PPS. In these the morphological features, of extreme importance, are dictated by the processing conditions and fibre

characteristics. However, the use of inorganic fibres and fillers in PPS leads to an increase in melt viscosity and lowers the ease of processing.

The crystallisation behaviour and morphology of PPS are found to improve on blending with other thermoplastic polymers.⁷⁴⁻⁷⁸ Blending of liquid crystalline polymers (TLCP) with engineering thermoplastics like PPS improves properties such as impact resistance, stiffness, heat distortion temperature, chemical resistance, thermal stability etc.⁷⁰ The LCP phase in these blends has lower viscosity than PPS and results in the formation of molecular composites. In the crystallisation of PPS, LCP will act as a nucleating agent.

1.9 PPS/TLCP blends: A Review

Several studies have been published on the phase morphology, thermal and crystallisation behaviour, mechanical and rheological properties of the blends of PPS and various commercially available TLCPs such as VECTRA A950, VECTRA B950, HX 4000.

Baird and coworkers⁷⁹ made a preliminary investigation of the morphology, rheology and mechanical properties of PPS blends with three different LCPs, with the main objective of defining the conditions for the *in-situ* formation of LCP reinforcing fibrils in the PPS matrix. Stupp and Wu⁸⁰ made a NMR investigation on a thermotropic LCP containing 5 and 20% PPS, and found that the LCP induced an orientational order in the PPS dispersed phase.

The properties of the blends are affected by the size, shape and distribution of the LCPs in the matrix polymer, which in turn are related to the processing conditions such as the blend composition, the extrusion and drawing conditions, the viscosity

ratio of the component polymers and the type and grade of the LCPs and matrix polymers.⁸¹

1.9.1 Phase behaviour and morphology

The TLCPs are normally immiscible with thermoplastics such as PPS and thus the blends consists of two separate phases. The resultant morphology of the blend largely depends on the interfacial tension, ratio of viscosities of the components and shear rate. The TLCP phase appeared in the matrix in the form of small spheres or fibres depending on the TLCP content and the orientation during processing.⁷⁹⁻⁸² There are conflicting reports on the morphology and phase behaviour of PPS/Vectra A950. Subramaniam and coworkers⁸² and Minkova and coworkers⁸⁸ reported that this TLCP reacted with PPS during extrusion. The blends exhibited a foam structure, and no elongation of the LCP phase was found. They attributed the lack of fibrillation in the PPS/Vectra A950 system to possible chemical reaction between the two components under the prevailing processing conditions. Seppala and coworkers^{83,84} have observed a skin-core morphology for PPS/Vectra A950 blend. They concluded that the properties improved as a result of fibrous blend morphology and there were no reactions between PPS and TLCP during extrusion.

Gabellini et al⁹² studied the morphology of PPS/HX 4000 (copolyester of terephthalic acid, phenyl hydroquinone and hydroquinone) blend and concluded that the blends were partially miscible.

1.9.2 Thermal and crystallisation behaviour

The mechanical properties of crystalline PPS are highly dependent on the processing conditions which govern the crystallisation processes. Much efforts has been made to describe the thermal and crystallisation behaviour of PPS containing

TLCP.⁸⁸⁻⁹² In general, crystallisation proceeds through homogeneous and/or heterogeneous nucleation, followed by growth of the nucleated spherulites. Nucleating agents tested include inorganic additives such as talc, chalk, glass and silica, organic compounds such as polycarboxylic acids and their salts, and polymers such as high density polyethylene (HDPE) and LCPs. The crystallisation behaviour of neat PPS,⁹³ of PPS with solid fillers⁹⁴⁻⁹⁶ and of PPS blended with thermoplastic polymers⁶⁵⁻⁶⁹ have already been studied extensively by isothermal methods. Lopez and Wilkes⁹³ reported non-isothermal study of linear and branched PPS samples. They found that the Avrami exponent, as determined by the Ozawa equation from non-isothermal measurements, were in good agreement with those estimated by isothermal methods. These studies demonstrated that the Ozawa equation holds good not only for PPS but for the blends and composites as well. The presence of a nucleating polymer has a profound influence on the crystallisation kinetics of crystalline PPS. Some imported published literatures on PPS/TLCP blends are tabulated in *Table 1.6* and related patents are listed in *Figure 1.7*.

In previous reports⁸⁷ the isothermal crystallisation behaviour of blends of PPS and Vectra A950, Vectra B950 and HX4000 were described. The isothermal crystallisation of PPS was found to be strongly accelerated by the presence of Vectra B950, as a result of increased nucleation density, whereas no reduction of the degree of crystallinity could be noticed.

Minkova and coworkers^{88,89} found that blending PPS with Vectra B950, a wholly aromatic commercial LCP, leads to an increase in the non-isothermal crystallisation temperature without any reduction in the degree of crystallinity. The

Table 1.6: Important published papers on PPS/TLCP polymer blends

SL. No.	Blend components	Studied properties	References No.
1	PPS/PET-OB	NMR studies	80
2	PPS/(HNA-HBA)	mechanical properties, morphology, and thermal properties	79
3	PPS/(HNA-HBA)	DSC, mechanical properties	87
4	PPS/(HNA-TA-AP)	DSC, crystallisation behaviour	90
5	PPS/(HNA-TA-AP)	DSC, crystallisation behaviour	88
6	PPS/(HNA-TA-AP)	DSC, crystallisation behaviour	89
7	PPS/(HNA-HBA)	DSC, morphology	86
8	PPS/(HNA-TA-AP)	DSC, morphology, mechanical properties	85
9	PPS/(HNA-HBA)	DSC, morphology	91
10	PPS/(HNA-HBA)	rheology, mechanical properties, morphology	83
11	PPS/(PHQ-TPA-HQ)	DSC, morphology	92

PPS crystallisation rate coefficient (CRC) was found to increase three times upon addition of 2-50% Vectra B950. The values of the Avrami exponent n were close to 3 as found previously from isothermal analysis and did not vary appreciably on addition of Vectra B950. These findings show that the type of nucleation and the geometry of crystal growth do not change n in the presence of Vectra B950. Hong et.

al⁸⁷ studied isothermal and non-isothermal crystallisation kinetics of PPS/Vectra B950 blends. As the LCP content was increased, the supercooling required for PPS crystallisation, both half time for crystallisation and size of spherulites decreased. The PPS containing LCP exhibited a higher nucleation density than pure PPS, for which three dimensional growth and constant radial growth rate of spherulites are assumed. This study revealed a notable reduction in the Avrami exponent, which indicates that the nucleated process leads to rod shaped growth with thermal nucleation. Gebiliani et. al⁹² analysed the isothermal and non-isothermal crystallisation behaviour of PPS/HX4000 blend and observed that rate of crystallisation increased in presence of HX4000.

The heat deflection temperature (HDT) and coefficient of linear thermal expansion of PPS improved on blending with TLCPs.^{83,84} Thermal stability of PPS was found to increase in presence of TLCP.

1.9.3 Mechanical properties

As the polymers are not miscible, the poor adhesion between the two separate phases affects the properties of the blend. Seppala et. al^{83,84} reported that the tensile and impact properties of PPS is enhanced on blending with Vectra A950. Similar results of improvement in the mechanical properties has been reported by several authors.^{83,84,89,90} Shonaik et. al^{89,90} investigated the effect of TLCP distribution on the mechanical properties. They observed an increase in bending modulus with increasing TLCP content and attributed this to the reinforcing nature of the TLCP fibrils in the skin layer.

Table 1.7: Some Important Patents on PPS/TLCP blends

SL.No.	Composition of blend	Advantages/Applications	Reference
1	PPS/(HNA-HBA)	Coating Applications	97
2	PPS/(HBA-TPA-IPA-DODP)	Moulding composition with improved properties	98
3	PPS/LC Polyester	Fibre reinforced composites	99
4	PPS/TLCP	Moulding composition with improved properties	100
5	PPS/(HNA-HBA)	Coating applications	101
6	PPS/TLCP	Moulding composition with improved mechanical, thermal properties	102
7	PPS/TLCP	Moulding composition with improved mechanical, thermal properties	103
8	PPS/TLCP	Moulding composition with improved mechanical properties	104
9	PPS/TLCP	Moulding composition with improved mechanical, thermal properties	105
10	PPS/TLCP	Coating applications, Moulding composition with improved mechanical, thermal properties. Electronic applications	106
11	PPS/(HNA-HBA)	Moulding composition with improved mechanical, thermal properties	107
12	PPS/TLCP	<i>In-situ</i> composites, Electronic connectors	108
13	PPS/LC Polyester	Moulding composition with improved mechanical, thermal properties	109
14	PPS/LC Polyester	Coating applications, Moulding composition with improved mechanical, thermal properties	110
15	PPS/LC Polyester	Fibre reinforcement	111

1.9.4 Rheological properties

The rheology of LCP blends is a complex but exciting new field of academic interest where many significant questions remain to be answered. There are many reports of reduction in melt viscosity of PPS on addition of TLCP.⁸²⁻⁸⁴ Viscosity drops with TLCP amount, indicating that TLCP plays the role of a processing aid for the PPS phase.

1.10 SCOPE AND OBJECTIVES OF THE PRESENT WORK

The present work envisages a concerted, interdisciplinary research involving polymer synthesis, physico-chemical characterisation, processing, property evaluation to examine some critical issues relating to PPS/TLCP blends such as :

- i. To blend poly(phenylene sulphide) with aliphatic-aromatic and wholly aromatic thermotropic liquid crystalline polymers;
- ii. To study the effect of blending techniques and blending conditions on the thermal behaviour, phase behaviour and morphology poly(phenylene sulphide)/semi-aromatic thermotropic liquid crystalline polymer (PPS/TLCP) blends;
- iii. To study the thermal and crystallisation behaviour of poly(phenylene sulphide)-semi-aromatic thermotropic liquid crystalline polymer blends;
- iv. To synthesise and characterise block copolymers from poly(phenylene sulphide) and ethylene terephthalate-oxybenzoate blocks of varying lengths.
- v. Evaluation of the block copolymers as compatibilising agents for the Poly(phenylene sulphide)-semi aromatic thermotropic liquid crystalline polymer blends.
- vi. To develop an ideal *in situ* compatibilised molecular composites based on PPS and TLCP with unique properties by reactive extrusion in presence of dicarboxyl terminated poly(phenylene sulphide).
- vii. To study the effect of *in situ* compatibilisation of PPS/wholly aromatic thermotropic liquid crystalline polymer (TLCP) blends on thermal properties, morphology, mechanical properties and rheological properties.

1.11 REFERENCES

- 1 D.R. Paul and S. Newman, *Polymer Blends, Vol.1 & 2*, Academic Press, London (1978).
- 2 L.A. Utracki, *Polymer Alloys and Blends: Thermodynamics and Rheology*, Hanser Publications, New York (1990).
- 3 O. Obalasi, L.M. Robeson and M.T. Shaw, *Polymer-Polymer miscibility*, Academic Press, New York (1976).
- 4 N.A.J. Platzer, *Copolymers, Polyblends and Composites*, Amer Chem. Soc., Washington DC (1975).
- 5 M.J. Folkes and P.S. Hope, *Polymer Blends and Alloys*, Chapman & Hall, London, (1993).
- 6 J.A. Manson and L.H. Sperling, *Polymer Blends and Composites*, Plenum Press, New York, (1976).
- 7 D.J. Walsh, J.S. Higgins and A. Maconnachie, Eds., *Polymer Blends and Mixtures*, Martinus Nijhoff Publishers, Dordrecht (1985).
- 8 D.R. Paul and J.W. Barlow, *Polymer Compatibility and Incompatibility: Principles and Practice*, in K. Solc, Ed., MMI Symposium series, vol. 3, Howard Academic, New York, 1981.
- 9 D. Klemptner and K.L. Frisch, Eds., *Polymer Alloys: Blends, Blocks, Grafts and Interpenetrating Network*, Plenum, New York (1977).
- 10 E. Martuscelli and G.B. Demma, in E. Martuscelli, R. Palumbo, M. Kryszewski, Eds., "*Polymer Blends: Processing, Morphology and Properties*"; Plenum Press: New York, 1980.
- 11 H.F. Giles, "*Alloys and Blends*" in *Modern Plastic Encyclopedia*, 105, 1986.
- 12 L.A. Utracki and R.A. Weiss, *Multiphase Polymers: Blends and Ionomers*, American Chemical Society, Washington DC (1989).
- 13 J.G. Bonner and P.S. Hope, "*Compatibilisation and reactive Blending*", in M.J. Folkes and P.S. Hope, Eds., *Polymer Blends and Alloys*", Chapman & Hall, London, (1993).
- 14 W.M. Barentsen, D. Heikens and P. Piet, *Polymer*, **15**, 1974, 119.

- 15 R. Fayt, R. Jerome and Ph. Teyssie, *J. Polym. Sci., Polym. Lett. Edn.* **24**, 1974, 25.
- 16 D.R. Paul, "Interfacial agents (Compatibilisers) for polymer Blends" in *Polymer Blends*, Vol. 2, D.R. Paul and S. Newman, Eds., Academic Press, London (1978).
- 17 N.G. Gaylord, in N.A.J. Platzer, Ed., *Copolymers, Polyblends and Composites*, Amer Chem. Soc., Washington DC (1975).
- 18 R. Fayt, R. Jerome and Ph. Teyssie, *J. Polym. Sci., B. Polym. Phys.* **27**, 1989, 775.
- 19 L.M. Robenson, *J. Appl. Polym. Sci.*, **30**, 1985, 4081.
- 20 S.D. Sjoerdsma, *Polymer Communications*, **30**, 1989, 106.
- 21 S.B. Brown, in "Reactive Extrusion: A survey of Chemical reactions of monomers and polymers during extrusion processing" in M. Xanthos, Ed., *Reactive Extrusion: Principles and Practices*, Chapter 8, Hanser Publishers, New York, (1992).
- 22 E. Martuscelli, M. Pracella, M. Avella, R. Greco, G. Ragosta and A. Felice, in E. Martuscelli, R. Palumbo M. Kryszevski, Eds., *Polymer Blends: Processing, Morphology and Properties*, Plenum Press, New York, (1979).
- 23 H. VanOne, *J. Colloid and Interface Sci*, **40**, 1972, 448.
- 24 D. Acierno, M.R. Nobile, L. Nicolais and L. Incarnato, "Rheology of Blends of thermotropic Liquid Crystal and Thermoplastic Polymers" in A.A. Collyer and L.A. Utraki, Eds., *Polymer Rheology and Processing*, Elsevier Science Publishers Ltd, London (1990).
- 25 E. Martuscelli, C. Silvertre, R. Greco and G. Ragosta, in E. Martuscelli, R. Palumbo and M. Kryszevski, Eds., *Polymer Blends: Processing, Morphology and Properties*, Plenum Press, New York, (1979).
- 26 H.B. Chin and C.D. Han, *Journal Rheol.*, **23**, 1979, 557.
- 27 T. Serhatkulu, B. Ermon, I. Bahar, S. Fakirov, M. Evstatiev and D. Sapundjieva, *Polymer*, **36**, 1995, 2371.
- 28 S. Fakirov, M. Evstatiev and S. Petrovich, *Macromolecules*, **26**, 1993, 5219.
- 29 M. Evstatiev, and S. Fakirov, *Polymer*, **33**, 1991, 877.
- 30 P.G. De Gennes, *The physics of Liquid crystals*, Clarendon Press, Oxford (1971).
- 31 L. Onsagar, *The Effect of Shapes on the interaction of Colloidal Particles*, Ann. N.Y. Acad. Sci., **51**, 627, (1949).

- 32 P.J. Flory, *Macromolecules*, **11**, 1978, 1138.
- 33 P.J. Flory, *Phase Equilibrium in Solutions of Rodlike Particles*, Proc. R. Soc., A234: **73**, (1956).
- 34 A. Blumstein, Ed., *Liquid Crystalline Order in Polymers*, Academic Press, New York (1978).
- 35 H. Zeng, G. He and G. Yang, *Angew. Makromol. Chem.*, **143**, 1986, 25.
- 36 C.S. Brown and P.T. Alder, "Blends containing liquid crystal polymers" in M.J. Folkes and P.S. Hope, Eds., *Polymer Blends and Alloys*, Chapman & Hall, London, (1993).
- 37 S.C. Steadman, "Fibre forming blends and in situ fibre composites", in M.J. Folkes and P.S. Hope, Eds., *Polymer Blends and Alloys*, Chapman & Hall, London, (1993).
- 38 F.P. La Mantia, Ed., *Thermotropic liquid crystal Polymer Blends*, Technomic Publishing Co., New York (1993).
- 39 D. Acierno and F.P. La Mantia, Eds., *Processing and Properties of Liquid Crystalline Polymers and LCP Based Blends*, Chem Tech Publishing, Ontario (1993).
- 40 D.G. Baird, *Thermotropic-liquid crystal polymer blends; Advanced Composites Bulletin*, **6**, 1989.
- 41 P. Magagnini, "Molecular Design of Thermotropic", in F.P. La Mantia, Ed., *Main-Chain Liquid Crystalline Polymers; Thermotropic liquid crystal Polymer Blends*, Technomic Publishing Co., New York (1993).
- 42 A.A. Collyer, Ed., *Liquid crystalline Polymers: From Structure to Applications*, Elsevier Science Publications Ltd., London (1992).
- 43 C. Careagna, Ed., *Liquid Crystalline Polymers*, Elsevier Science Publications Ltd., London (1993).
- 44 L.L. Chapoy, Ed., *Recent Advances in Liquid Crystalline Polymers*, Elsevier Science Publications Ltd., London, 1985.
- 45 A. Blumstein, Ed., *Polymeric Liquid Crystals*, Plenum Press, New York (1983).
- 46 R.A. Weiss, N. Chung and A. Kohli, *Polym. Eng. Sci.*, **29**, 1989, 573.
- 47 K.G. Blizard and D.G. Baird, *Polym. News*, 1986, **12**, 44, 1986.

- 48 K. Min, J.L. White and J.F. Fellers, *Polym. Eng. Sci.*, **24**, 1984, 1327.
- 49 G. Kiss, *Polym. Eng. Sci.*, **27**, 1987, 410.
- 50 A.I. Isayev and M. Modic, *Polym. Compos.*, **8**, 1987, 158.
- 51 K.G. Blizard, C. Federici, O. Federco and L. Chapoy, *Polym. Eng. Sci.*, **30**, 1989, 1442.
- 52 E.G. Joseph, G.L. Wilkes and D.G. Baird, *Polym. Prepr.*, **25**, 1988, 94.
- 53 M. Amano and K. Nakagawa, *Polymer*, **28**, 1987, 263.
- 54 W. Brostow, T.S. Dziemianowicz, H. Romanski and W. Werber, *Polym. Eng. Sci.*, **28**, 1988, 785.
- 55 P. Zhuang, T. Kyu and J.L. White, *Polym. Eng. Sci.*, **28**, 1988, 1095.
- 56 A.M. Sukhadia, D. Done and D.G. Baird, *Polym. Eng. Sci.*, **27**, 1987, 684.
- 57 M. Kimura and R.S. Porter, *J. Polym. Sci., Polym. Phys. Ed.*, **22**, 1984, 1697.
- 58 K.G. Blizard and D.G. Baird, *SPE ANTEC*, **44**, 1986, 311.
- 59 R. Ramanathan, K.G. Blizard and D.G. Baird, *SPE ANTEC*, **45**, 1987, 1399.
- 60 F.N. Cogswell, B.P. Griffin and J.B. Rose, *Eur. Pat. 30 417*, App. 1980-11-07, Acc. 1981-06-17.
- 61 M.R. Nobile, D. Acierno, L. Incarnato, E. Amendola, L. Nicolais and C. Carfagna, *J. Appl. Polym. Sci.*, **41**, 1990, 2723.
- 62 B.-L. Lee, *Polym. Eng. Sci.*, **28**, 1988, 1107.
- 63 K. Yamaoka, T. Harada, K. Tomari, S. Tonogai and S. Nagai, *The Fifth Annual Meeting, PPS*, April 11-14. Kyoto, Japan, 1989.
- 64 A.I. Isayev and R. Viswanathan, *Polymer*, **36**, 1995, 1585.
- 65 R. Viswanathan and A.I. Isayev, *J. Appl. Polym. Sci.*, **55**, 1995, 1117.
- 66 P. Grenvesse, *Bull. Soc. Chem. Fr.*, **17**, 1897, 599.
- 67 C. Friedel and J.M. Crafts, *Ann. Chem Phys.*, **14**, 1888, 433.
- 68 R.W. Lenz and W.K. Carrington, *J. Polym. Sci.* **41**, 1959, 333.

- 69 J. T. Edmonds Jr., H. Hill and Wayne Jr., *U.S. Patent: 3,354,835.*, Phillips Petroleum Company, 1967.
- 70 Anon, *Chem. Eng. News.*, 36, 1980.
- 71 R.T. Hawkins, *Macromolecules*, **9**, 1976, 189.
- 72 H. Hill, and Jr. Wayne, "The history of poly(phenylene sulphide)" in R.S. Seymour and G.S. Krishenbaumin, Eds., *High Performance Polymer*, p135 (1986).
- 73 S. Akhter and J.L. White., *J. Appl. Polym. Sci.*, **31**, 1991, 84.
- 74 K. Ravindranath and J.P. Jog, *J. Appl. Polym. Sci.*, **49**, 1993, 1395.
- 75 J.P. Jog, V.L. Shingankuli and V.M. Nadkarni, *Polymer*, **34**, 1993, 1966.
- 76 V.M. Nadkarni, V.L. Shingankuli and J.P. Jog, *Intern. Polym. Proc.*, **2**, 1987, 55.
- 77 S. Radhakrishnan and S.G. Joshi, *Eur. Polym. J.*, **23**, 1987, 819.
- 78 V. M. Nadkarni and J.P. Jog, *J. Appl. Polym. Sci.*, **32**, 1986, 5817.
- 79 D.G. Baird, T.Sun, D.S. Done and R. Ramanathan, *Polym. Prepr.*, **30**, 1989, 546.
- 80 S.I. Stup and J. Wu, *ACS Polym. Mate. Sci. Eng.*, **58**, 1988, 714.
- 81 R. Ramanathan, K. Blizard and D.G. Baird, *SPE ANTEC*, **46**, 1988, 1123.
- 82 P.R. Subramaniam and A.I. Isayev, *Polymer*, **32**, 1991, 1961.
- 83 J. Seppala, M. Heino and C. Kapanen, *J. Appl. Polym. Sci.*, **44**, 1992, 1051.
- 84 J. Seppala, M. Heino and C. Kapanen, *J. Appl. Polym. Sci.*, **44**, 1992, 2185.
- 85 G.O.Shonaïke, H. Hamada, S.Yamaguchi, M. Nakamichi and Z. Makawa, *J. Appl. polym. Sci.*, **54**, 1994, 881.
- 86 G.O. Shonaïke, S.Yamaguchi, M. Ohta, H. Hamada, M. Nakamichi and Z. Makeawa, *Eur. Polym. J.*, **30**, 1994, 413.
- 87 S.M. Hong, B.C. Kim, K.U. Kim and I.J. Chung., *Polym. J.*, **24**, 1992, 727.
- 88 L.I. Minkova, M. Paci, M. Pracella and P. Magagnini, *Polym. Eng. Sci.*, **32**, 1992, 57.
- 89 L.I. Minkova and P. Magagnini, *Polymer*, **36**, 1995, 2059.

- 90 G.O.Shonaike, S.Yamaguchi, M. Ohta, H. Hamada, Z. Maekawa, M. Nakamichi, Z. Makawa, W.Kosaka and K. Toi, *Polym. Eng. Sci.*, **35**, 1995, 240.
- 91 B.C. Kim, S.M. Hong, S.S. Hwang and K.U. Kim, *Polym. Eng. Sci.*, **36**, 1996, 574.
- 92 G. Gabellini, M.B. de Moraes and R.E.S. Bretas, *J. Appl. Polym. Sci.*, **60**, 1996, 21.
- 93 L.C. Lopez and G.L.Wilkes, *Polymer*, **29**, 1988, 106.
- 94 G.P. Desio and L. Rebenfeld, *J. Appl. Polym. Sci.*, **39**, 1990, 39.
- 95 S.S. Song, J.L. White and M. Cakmak, *Polym. Eng. Sci.*, **30**, 1990, 994.
- 96 J.P. Jog and V.M. Nadkarni, *J. Appl. Polym. Sci.*, **30**, 1985, 997.
- 97 Japanese Patent, JP 01 74 265, assigned to Japan/Sekisui Chemical Co. Ltd. 1989.
- 98 European Patent, EP 321 236, assigned to European/Tosoh Corp., 1989.
- 99 Patent, DE 3, 813, 919, assigned Germany/Sieman, 1988.
- 100 Japanese Patent, JP 01, 292, 058, assigned to Toray Industries Inc., 1989.
- 101 Japanese Patent, JP 0321, 639, assigned to Toray Industries Inc., 1991.
- 102 Japanese Patent, JP 02, 206, 644, assigned to Toray Industries Inc., 1990.
- 103 Japanese Patent, JP 0395, 261, assigned to Toray Industries Inc., 1991.
- 104 Japanese Patent, JP 03 47, 861, assigned to Toray Industries Inc., 1991.
- 105 Japanese Patent, JP 03, 179, 051, assigned to Toray Industries Inc., 1991.
- 106 Japanese Patent, JP 92, 225, 054, assigned to Toray Industries Inc., 1992.
- 107 Japanese Patent, US 5, 182, 334, assigned to Heochst Celenesce, 1991.
- 108 Japanese Patent, JP 05, 112, 716, assigned to Tosoh Corp., 1993.
- 109 Japanese Patent, JP 05, 86, 266, assigned to Toray Industries Inc., 1993.
- 110 Japanese Patent, JP 04, 311, 758, assigned to Toray Industries Inc., 1992.
- 111 Japanese Patent, JP 05, 194, 847, Korea Institute Science and Technology, 1993.

CHAPTER 2

THERMAL PROPERTIES, PHASE
BEHAVIOUR AND MORPHOLOGY
OF PPS/PET-OB BLENDS¹⁻³

ABSTRACT

Thermal behaviour, phase behaviour and morphology of blends of poly(phenylene sulphide) (PPS) and poly(ethylene terephthalate-co-oxybenzoate) (PET-OB), an aliphatic-aromatic thermotropic liquid crystalline polymer (TLCP), were investigated. The DSC analysis showed that the crystallisation temperature (T_c) of PPS increases whereas the degree of super cooling reduced with the addition of PET-OB as a result of heterogeneous nucleation and phase inversion. The SEM studies shows that the blend exists as phase separated because of poor interfacial adhesion between the blend components. The equilibrium melting temperature and the crystal lamellar thickness of PPS phase decreases with an increase in PET-OB concentration. This phenomenon can be ascribable to the nucleating effect of PET-OB on the spherulite growth of PPS phase. Phase diagram shows that the PPS/PET-OB blend crystallises in well separated temperature regimes and that the PPS component will always be solidified before the crystallisation of PET-OB begins. The PPS/PET-OB blends exist as phase separated in the molten state. The reduction in the spherulite size of PPS phase, as revealed by PLOM, indicated that the spherulitic growth rate as well as the overall crystallisation rate of PPS is influenced by the presence of PET-OB. Melting transitions and phase behaviour of the blends were dependent on the preparation method. The melt-mixed blends show macrophase-separated-morphology indicating poor phase mixing whereas the co-precipitated blends of the same composition exhibit a disperse type morphology, as observed by PLOM. In comparison with melt-mixed blends, co-precipitated blends were seen to be uniform and continuous.

2.1 INTRODUCTION

Fibre-reinforcement has been used for many years to increase the engineering performance of thermoplastics.⁴ Such composite materials have found applications in the aircraft, aerospace vehicles, automotive, marine and electronic industries. The reinforcing materials are traditionally inorganic such as graphite, boron and glass. The use of inorganic fibres and fillers in thermoplastics leads to an increase in melt viscosity and lowers the ease of processing. Reinforcement through the addition of TLCPs to thermoplastics has been investigated over the last few years with encouraging results.²⁻¹³ The principal goal is to achieve improvements in mechanical properties by using TLCP to reinforce flexible thermoplastics through the *in situ* formation of fibres. Blending is also considered as a possible route to overcome the highly anisotropic physical properties of TLCPs that can be problematic in many applications. The low melt viscosity of the TLCPs can reduce the overall melt viscosity of the blend and thus act as a good processing aid. Moreover, the TLCP phase has been shown to influence the crystallisability of the thermoplastic matrix.

Poly(phenylene sulphide) (PPS) and thermotropic liquid crystalline polymers (TLCP) are high strength/high temperature speciality polymers that find applications in the aerospace, automotive, marine, electrical and electronic industries.⁴ Several studies⁴⁻⁷ have been published on the blends of PPS with wholly aromatic TLCPs such as Vectra A950 (copolyester of 25 mole % 2-hydroxy-6-naphthoic acid (HNA) and 75 mole % 4-hydroxy benzoic acid (HBA)) and Vectra B950 (copolyester of 60 mole % 2-hydroxy-6-

naphthoic acid, 20 mole % terephthalic acid and 20 mole % 4-amino phenol). Subramanian and Isayev⁴ found that for effective reinforcement and betterment of mechanical properties, the viscosity of TLCP must be lower than that of the PPS at the processing temperature. The mechanical properties estimated for PPS/Vectra A950 were lower than that of TLCP and no fibrillation of the TLCP phase in the matrix was found. Previous studies^{7,8} lead to the conclusion that maximum fibrillation occurs when the melt viscosity ratio of the original components is close to unity. The presence of fibres seems to be a necessary attribute for improving the mechanical properties. Thus, the viscosity ratio between the dispersed phase and the matrix is an important factor for the phase morphology of the blends. Magagnini et. al⁷ found that the melt viscosity of PPS was considerably reduced in the presence of Vectra B950. The inherent low melt viscosity of the TLCP melt is one reason for this reduction. Change of flow pattern of the blend is another reason. Heino and Seppala^{8,9} reported that PPS/Vectra A950 blends were two phase systems and that the properties were dependent on miscibility, interfacial adhesion between the blend components and orientation of the TLCP phase. The melting, crystallisation and phase behaviour of the blend have very significant role in determining its processing characteristics and properties.

This Chapter deals with a systematic and comprehensive study on the effect of poly(ethylene terephthalate-co-oxybenzoate) (PET-OB), an aliphatic-aromatic thermotropic liquid crystalline polymer (TLCP) on the thermal behaviour, phase behaviour and morphology of PPS/PET-OB blends. The manner in which two polymers are blended together is of vital importance in controlling the phase morphology and to the

ensuing properties of blends. Most common techniques for preparing the blends are melt-mixing, solution blending and co-precipitation. Published literature regarding the effect of blending techniques and conditions on the morphology and phase behaviour of PPS/PET-OB blend system is rather limited. A comparative study on the thermal properties, phase behaviour and morphology of PPS/PET-OB blends produced using different blending techniques is also presented. Thermal analysis by differential scanning calorimetry (DSC) was employed to compare the melting and crystallisation behaviour of the blends. The influence of blending techniques on the phase behaviour were investigated with polarised light optical microscopy (PLOM) and scanning electron microscopy (SEM).

2.2 EXPERIMENTAL

2.2.1 Materials

PPS used was a commercial grade Ryton V-1 manufactured by Phillips Petroleum Company. This material shows a melting point of 282.0 °C and ΔH 43.2 J/g. Poly(ethylene terephthalate-co-oxybenzoate) (PET-OB), an aliphatic-aromatic thermotropic liquid crystalline polymer (TLCP), was synthesised from poly(ethylene terephthalate) (70 mole %) and 4-acetoxy benzoic acid (30 mole %).¹⁴ It was termed as P37. The intrinsic viscosity of the PET used in the synthesis was 0.6 dL/g. PET-OB exhibited birefringence when it was heated up to 300 °C and then cooled down. PET-OB showed a glass transition temperature of 65 °C and crystal to nematic transition at 197 °C. 1-Chloro naphthalene obtained from Aldrich Chemical Co., U.S.A was used without further purification.

2.2.2 Preparation of blends

(a). **Melt mixing:** Powders of the liquid crystalline PET-OB and PPS were dried at 130 °C under vacuum for 48 h prior to mixing. The PPS/PET-OB blends with a PET-OB content in the range 3, 5, 10, 20, 30, 50, 75 and 90% (wt./wt.) were prepared in a 30 ml mixer attached to a Brabender Plasticorder at 300 °C and 100 rpm for 5 min. under nitrogen. Blank samples of both PPS and PET-OB were subjected to the same treatment.

(b). **By co-precipitation:** The autoclave (made by Parr reactor company, U.S.A) was charged with PPS and PET-OB (blend compositions same as melt-mixed blends) in 1-chloro naphthalene and heated at 260 °C for 5 minutes under nitrogen atmosphere. The reactor was cooled to room temperature and the polymer mixture was precipitated in acetone. Blends were dried at 150 °C in vacuum oven for one week to remove 1-chloro naphthalene.

2.2.3 Thermal analysis

Thermal properties were measured by a *Mettler TA4000* series DSC. The apparatus was calibrated with Indium at different scanning rates. The lag between sample and pan holder temperature was also taken into account and computed through Indium crystallisation tests as described by Elder and Wlochowicz.¹⁵ The weight of samples were kept constant (6.0 ± 0.1 mg) throughout the analysis so that the effect of weight change

on the enthalpy change could be minimised. The heat of fusion and heat of crystallisation were determined from the peak area of the DSC thermograms.

The samples were heated at a rate of 20 °C/min. to 320 °C held there for 10 minutes in order to ensure that it melts completely and quenched to different isothermal crystallisation temperatures, (T_c): 230, 235, 240, 245, 250 and 255 °C. The samples were kept for one hour at each crystallisation temperature¹⁵⁻¹⁷ and then heated to 320 °C at the rate of 20 °C/min. The melting points corresponding to this heating cycle were noted.

2.2.4 Polarised light optical microscopy

The morphology of spherulites of neat PPS and the PPS phase in PPS/PET-OB blends were observed with a hot stage coupled *Leitz* microscope and under crossed polarisers. The blend samples were sandwiched between a microslide and a cover glass and melted at 320 °C on a hot plate for 1 minute under slight pressure. The slides containing thin film were then quickly transferred to the preheated hot stage. The spherulite growth and its impingement were observed at various temperatures under differing magnifications.

2.2.5 Scanning electron microscopy

Morphology of the freeze-fractured surfaces of the compression moulded samples were studied using a *Leica Stereoscan 440* scanning electron microscope. The fractured surface of the samples were coated with thin layer of gold prior to the observations.

2.3 RESULTS AND DISCUSSION

2.3.1 Melting and crystallisation behaviour

DSC heating thermograms (second heating) of PPS, PPS/PET-OB blends are shown in *Figure 2.1*. Thermal data corresponding transitions are tabulated in *Table 2.1*. The glass transition temperature of PPS is not clear due to its semicrystalline nature. The absence of any change in glass transition temperature (T_g , 65 °C) and crystal \leftrightarrow nematic transition (197 °C) (ascribable to PET-OB phase) or in melting transition (282 °C) corresponding to PPS phase from those of blend components indicates poor degree of phase mixing between the two phases.

The degree of super cooling, ($\Delta T = T_m - T_{c_{\text{onset}}}$, T_m is the melting peak temperature and $T_{c_{\text{onset}}}$ is the onset temperature of crystallisation), (*Table 2.1*) decreases at lower PET-OB content (upto 30%), but increased slightly on further addition of PET-OB as a result of phase inversion and heterogeneous nucleation.¹⁻³

The equilibrium melting temperature is probably the macroscopic quantity most suited to characterise a given crystal of a flexible linear macromolecule, especially in blends with another polymer.¹⁶⁻²¹ Therefore, we determined the equilibrium melting points T_m^0 of pure PPS as well as of PPS phase in PPS/PET-OB blends by Hoffman-Weeks analysis.¹⁶ This analysis involves isothermal crystallisation of the sample at various temperatures (T_c) and plotting the observed melting point (T_m) as a function of

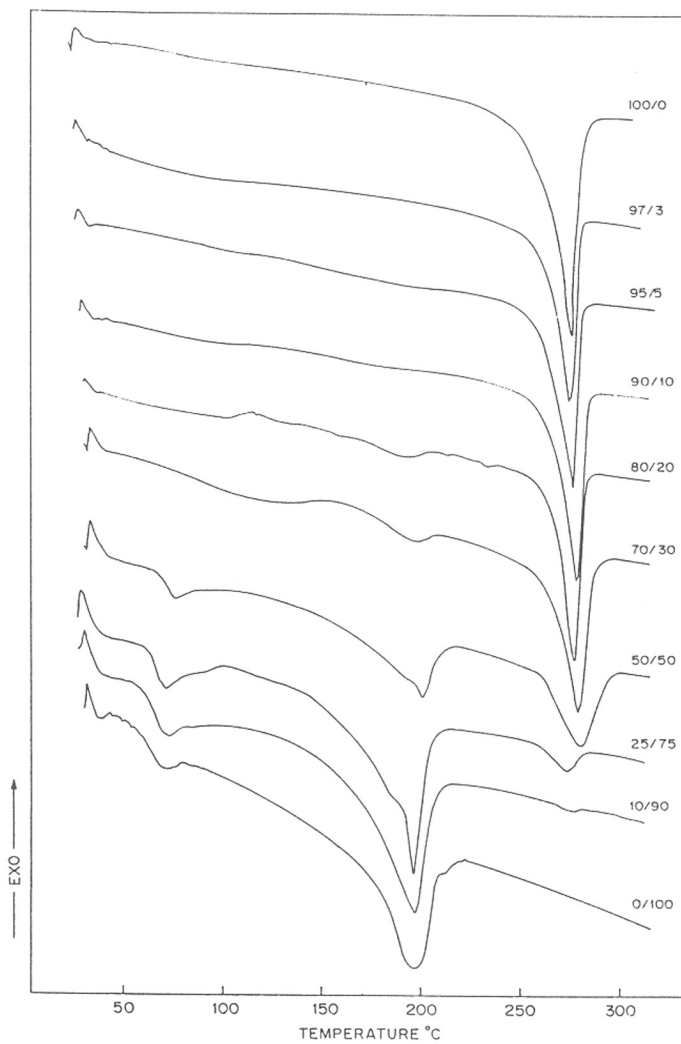


Figure 2.1 DSC thermograms of PPS/PET-OB blends at a heating rate of 20 °C/min.

Table.2.1: Thermal data of PPS and the PPS phase in of PPS/PET-OB Blends

PPS/PET-OB %(wt/wt)	T _m °C (a)	ΔH _m J/gm	T _c °C	T _{c_{onset}} °C (b)	ΔH _c J/gm	ΔT °C (a)-(b)
100/0	282	43.4	237	244	44.8	38
97/3	282	41.6	249	262	42.3	19
95/5	280	39.3	250	260	44.5	21
90/10	278	40.7	252	261	44.9	19
80/20	277	37.9	251	265	43.1	14
70/30	274	38.2	252	262	38.9	19
50/50	274	28.5	246	251	29.9	29
25/75	271	26.7	244	248	25.6	28
10/90	267	22.8	243	247	25.7	30

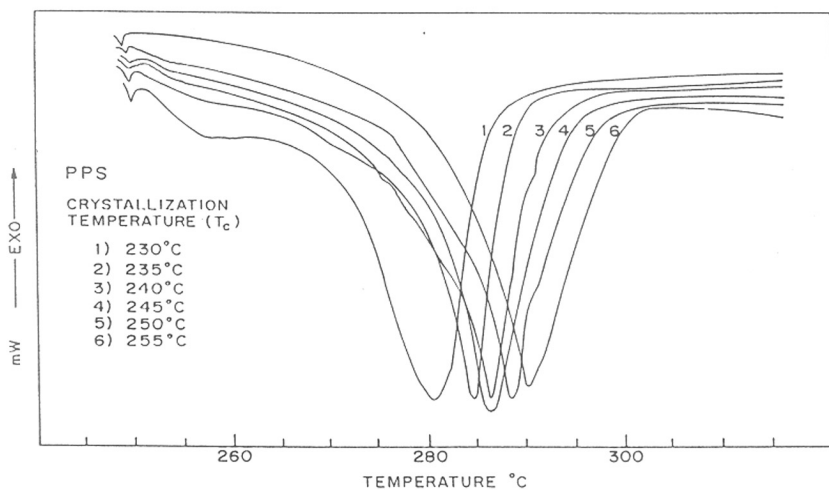
T_m: Melting peak temperature

T_{c_{onset}}: Onset temperature of crystallisation

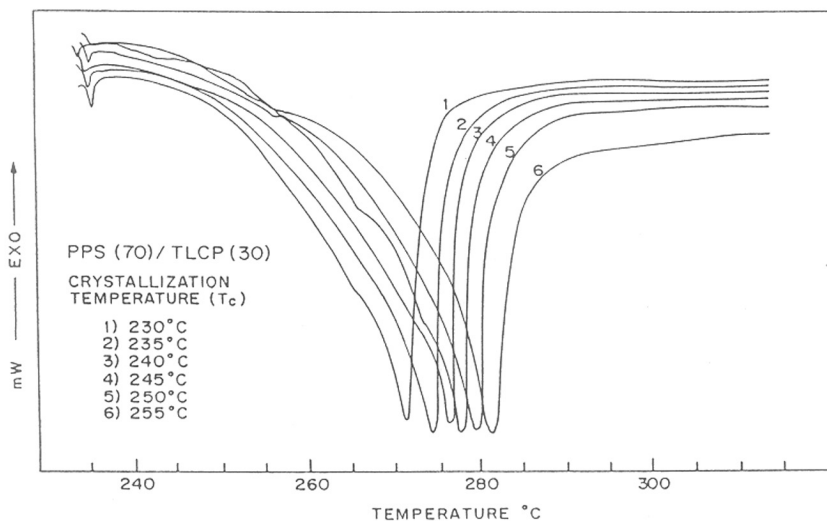
T_c: Crystallisation peak temperature

ΔT: Degree of supercooling

T_c. Figure 2.2 shows typical DSC endotherms of PPS and PPS (70)/PET-OB (30) blends obtained after isothermal crystallisation at 230, 235, 240, 245, 250 and 255 °C for one hour. The melting transition temperatures (T_m) of PPS and PPS/PET-OB blend increased with the crystallisation temperature (T_c).



(a)



(b)

Figure 2.2 Typical DSC thermograms obtained after isothermal crystallisation at various temperatures for one hour: (a) PPS and (b) PPS(70)/PET-OB (30) blend.

The Hoffman-Weeks equation

$$T_m = \eta T_c + (1 - \eta)T_m^0 \quad 2.1$$

predicts a linear relation between T_m and T_c . The equilibrium melting point, T_m^0 , is obtained from the intersection of this line with the $T_m = T_c$ equation as shown in *Figure 2.3*. The slope of the Hoffman-Weeks plot, η , assumes values between 0 and 1 and may be regarded as a measure of the stability, i.e., the lamellar thickness of the crystals undergoing the melting process.¹⁶ A value of $\eta = 0$ implies that the crystals are perfectly stable ($T_m = T_m^0$ at all T_c), whereas a value of $\eta = 1$ reflects inherently unstable crystals.

Figure 2.3 shows the Hoffman-Weeks plots for neat PPS as well as of PPS phase in PPS/PET-OB blends. The T_m^0 and η values are tabulated in *Table 2.2*. The value of the equilibrium melting point of pure PPS obtained (304.1 °C) is in good agreement with previously reported values²⁰⁻²³ which are in the range of 303-315 °C. It is clear that the equilibrium melting point of PPS in PPS/PET-OB blends decreases with increase PET-OB concentration and the slope of Hoffman-Weeks plots, η , increases with PET-OB content. This is indicative of a decrease in lamellar thickness of PPS on blending with PET-OB.

The analysis of the melting behaviour of a crystalline component in semicrystalline polymer blends is an important tool in the study of the phase behaviour of polymer mixtures.^{20,21} In miscible blends the melting point of the crystalline component

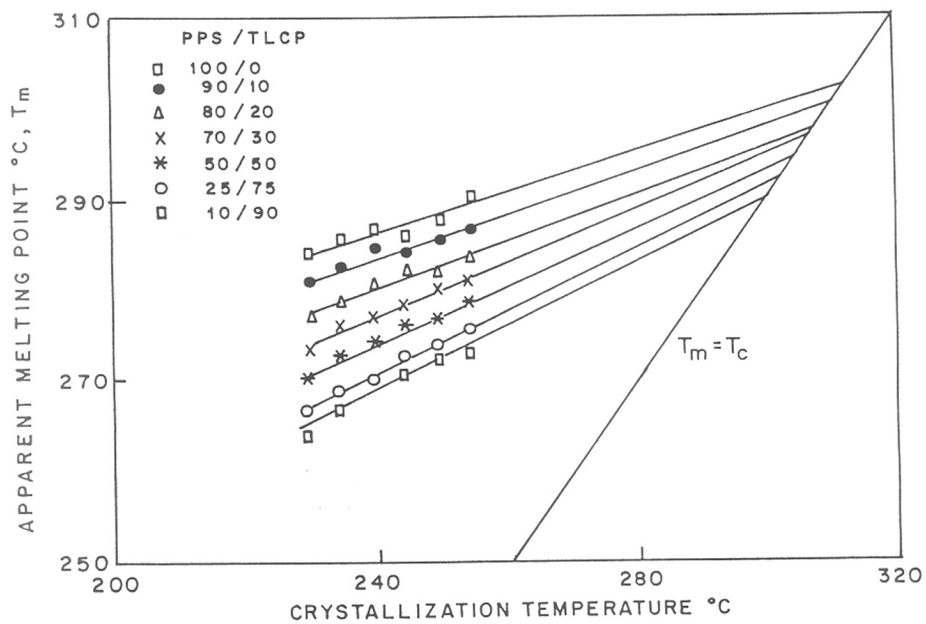


Figure 2.3 Hoffman-Weeks plots for pure PPS and PPS/PET-OB blends.

Table 2.2: Hoffman-Weeks Analysis

PPS/PET-OB Blends	Equilibrium melting point $T^{\circ}m$	Slope, η
100/0	304.1	0.179
90/10	301.3	0.229
80/20	299.6	0.263
70/30	298.5	0.303
50/50	296.0	0.348
25/75	294.1	0.360
10/90	289.1	0.374

is usually lowered with respect to that in parent homopolymer as a result of thermodynamically favourable interactions.²² However, it is difficult to determine the existence of any specific interaction, either chemical or physical, between PPS and PET-OB in the PPS/PET-OB blend system. The depression in the equilibrium melting point of PPS/PET-OB blends with respect to that in neat PPS can be ascribed to the nucleating effect of PET-OB on the spherulitic growth of PPS phase. In the presence of

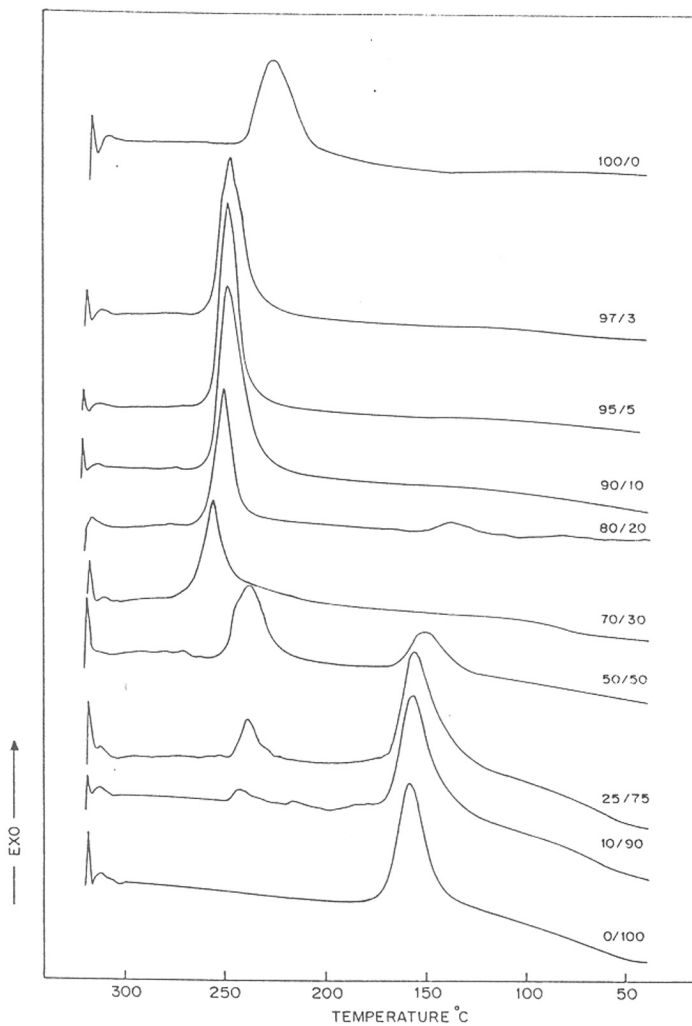


Figure 2.4 DSC crystallisation exotherms of PPS/PET-OB blends at the cooling rate of 20 °C/min.

PET-OB phase the thermal nucleated process in PPS is known to lead to rod-shaped growth²⁵ and thereby cause a reduction in the spherulite size. In the molten state PET-OB chains could diffuse into the PPS phase and get entrapped within its spherulite during crystallisation. This will lead to the formation of less stable crystals. We had observed a similar reduction in the Avrami exponent of PPS phase in PPS/ PET-OB blends with increase in PET-OB content.¹

The crystallisation exotherms of pure PPS and PPS/PET-OB blends during cooling are shown in *Figure 2.4*. The crystallisation temperature (T_c) and the heat of melt crystallisation (ΔH_c), (Table 2.1) increase with PET-OB content up to 30% due to its nucleating effect on the spherulitic growth of PPS phase.^{23,24} On the other hand, (T_c) and ΔH_c (and hence the degree of crystallinity) of PPS are depressed on further addition of PET-OB. Therefore, the crystallisation of each of the two blend components represent phase separation processes in which the two polymers crystallise from the mixture to form separate phases. Ultimately the PPS/PET-OB blend system exists as two phases. The T_c (maximum of crystallisation exotherm PPS phase) shifts to a higher temperature range [237 °C for PPS and 251 °C for PPS phase in 90/10 % (wt./wt.) PPS/ PET-OB blends].

2.3.2 Phase behaviour

The effect of the concentration of the minor component on the melting behaviour of major component is usually expressed in the form of temperature-concentration phase diagram.^{18,19} Penning^{20,21} et. al constructed a phase diagram to study the phase behaviour

of poly(vinylidene fluoride)/poly(1,4-butylene adipate) blends. In *Figure 2.5* we present a similar temperature-concentration phase diagram describing the overall thermal behaviour of PPS/PET-OB blend system, as studied by DSC. According to the phase diagram, the blend can be classified as completely anisotropic PET-OB liquid phase/isotropic PPS liquid phase (I, both component in the molten state), anisotropic PET-OB liquid phase/isotropic crystalline solid phase (II, PET-OB in molten state and PPS in crystallised state), or liquid crystalline/semicrystalline solid (III, both in solid state) depending on temperature and composition. The phase diagram shows equilibrium melting transition corresponding to the PPS phase, the crystal \leftrightarrow nematic transition of PET-OB (197 °C), two crystallisation transitions (PPS phase crystallises at 250 °C and PET-OB phase crystallises at 150 °C) and one glass transition (at 65 °C, ascribable to PET-OB phase). The T_c (corresponding to the maximum of the crystallisation exotherm of PPS phase and PET-OB phase) shows that both PPS and PET-OB crystallise from the mixture over a wide range of composition. It is clear that the crystallisation of PPS takes place at temperatures well above the crystal \leftrightarrow nematic transition of PET-OB. This means that the PPS/PET-OB blends crystallise in well separated temperature regimes and that the PPS component will always be solidified before the crystallisation of PET-OB begins.

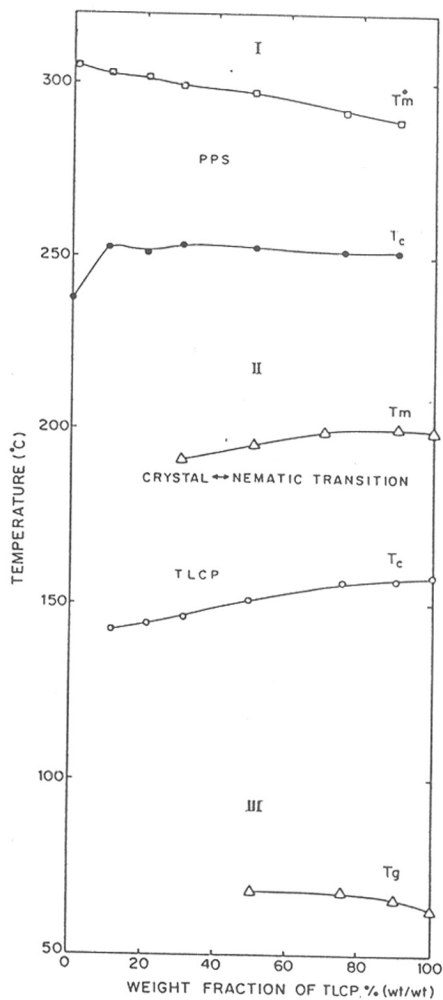


Figure 2.5 Phase diagram of the PPS/PET-OB blend system, showing the equilibrium melting transition (T_m^*) of PPS and the crystallisation temperatures (T_c) of both PPS and PET-OB, crystal↔nematic transition as well as single glass transition temperature (T_g) of PET-OB.

2.3.3 Morphology

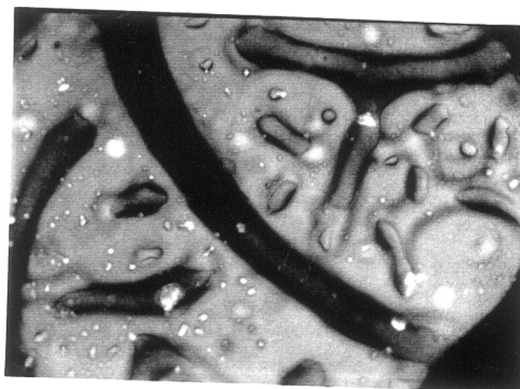
The morphological studies are very important in order to establish how the processing condition may govern the morphological features and hence the end-use properties of these blends. Polarised light optical microscopy (PLOM) offers a convenient method to follow the phase separation and crystallisation mechanism of PPS/TLCP blends as a direct consequence of remarkable phase contrast between optically isotropic PPS phase and optically anisotropic TLCP phase. Scanning electron microscopy (SEM) can reveal the level of interfacial adhesion of different phases in polymer blends. The shape, size and extent of mixing of dispersed phase can be investigated by SEM.

2.3.3.1 Polarised light optical microscopy

Three factors are known to influence the crystalline morphology of the blends.²⁵ These are: (1) Separate crystallisation of blend components, (2) Liquid-liquid phase separations in the melt and (3) Differing crystallisation rates as a function of crystallisation temperature. A liquid-liquid phase separation in the melt prior to crystallisation is observed in the PPS/PET-OB blend system, as seen from *Figures 2.6 (a) and (b)*. Above equilibrium melting temperature of PPS (T^0_m , 304.1 °C), the PET-OB phase exists as anisotropic oriented droplets, as seen in *Figure 2.6 (a)*. This morphology is responsible for the rheological properties, low thermal expansion coefficients and



(a)

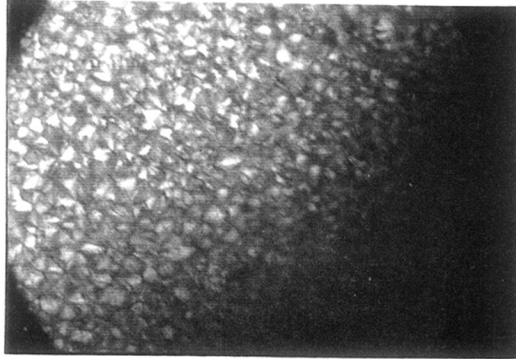


(b)

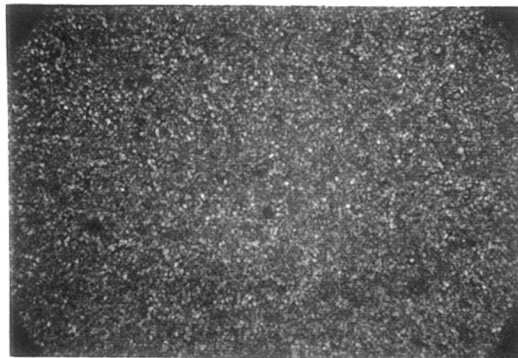
Figure 2.6 Optical micrographs (same magnification = 100 X) showing phase behaviour of 70/30 % wt./wt. PPS/PET-OB blend in molten state (at 320 °C).

processing characteristics of the blends containing PET-OB as one component. Due to its low crystal \leftrightarrow nematic transition temperature and low melt-viscosity, PET-OB phase will provide enough thermal mobility for the rapid crystallisation of PPS phase.

A spherulitically crystallising polymer is most easily studied between crossed polarisers in an optical microscope. Spherulites form easily from melts with relatively high viscosity, i.e., under circumstances where the diffusion rates are low and the ratio of the diffusion constant to the crystal growth is small.²⁶ *Figure 2.7* shows the optical micrographs of PPS and PPS/PET-OB blends. *Figure 2.7 (a)* shows large spherulites of neat PPS. Blends exhibited smaller and greater number of spherulites than neat PPS as shown in *Figure 2.7 (b)* [same magnification 100 X]. This means that the number of nucleating sites in PPS matrix increased in the presence of PET-OB. In molten state PET-OB molecules exist as nematic rigid rods which will form the nucleus for the nucleation and growth of PPS spherulites. The PPS spherulites start crystallising from the nuclei in a three-dimensional way, but the growing entities soon meet oriented PET-OB phase and grow in the form of fibres, discs, or tubes which results in the transcrystalline morphology.²⁷ This observation indicates that the presence of PET-OB has a profound effect on the crystallisation behaviour of PPS. Improvements in the rate of PPS crystallisation have been observed in the presence of inorganic fillers²³,



(a)



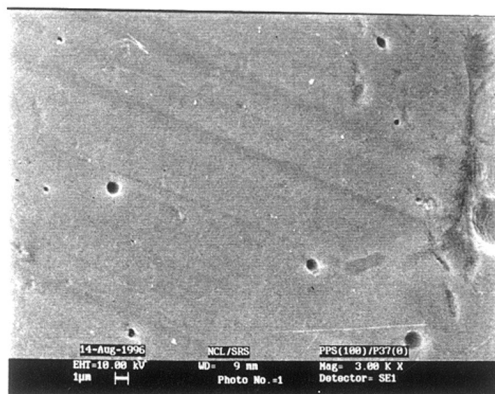
(b)

Figure 2.7 Optical micrographs (same magnification, bar 100 X) of the spherulite morphology of PPS in blends with PET-OB at various compositions: (a) pure PPS after 20 min. at 238 °C; (b) 70/30 PPS/PET-OB blends

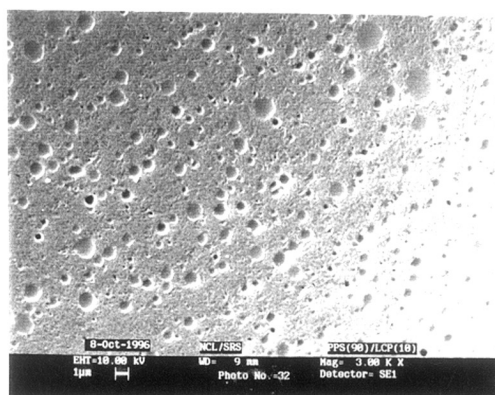
thermoplastics^{28,29} and commercial wholly aromatic TLCPs.³⁰⁻³² This reduction in spherulite size is in accordance with results in the observed depression in equilibrium melting temperature of PPS. This means that the number of nucleating sites in PPS matrix increase in the presence of PET-OB as a result of heterogeneous nucleation.^{10,30-32} The crystallisation temperature (T_c) and hence the rate of crystallisation of PPS phase increases with the addition of PET-OB as observed in phase diagram (*Figure 2.5*). These observations are very significant from technological perspectives because the enhanced crystallisation rate on the addition of nucleating agents improves the productivity by shortening the moulding cycle and improves the properties of the moulded parts by developing finer grain structures.²⁴

2.3.3.2 Scanning electron microscopy

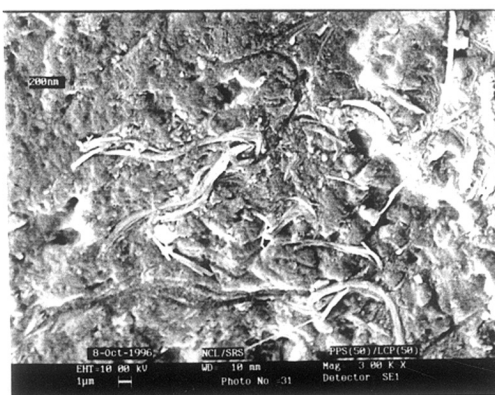
SEM micrographs of freeze-fractured surface of pure PPS and PET-OB blends are shown in *Figure 2.8 (a, b, c)*. The macrophase separated-morphology observed [*Figure 2.8(b)*] for a blend having 10 wt./wt.% of PET-OB is due to poor interfacial adhesion. With increasing PET-OB content, a higher orientability of the dispersed phase is thus confirmed. This is clear in the blend containing 50% PET-OB [*Figure 2.8(c)*], where the PET-OB phase exists as fibrils. The presence of fibres seems to be necessary to improve the mechanical properties of blends containing PET-OB.^{1,7-9} As PET-OB content is further increased, the morphology becomes complicated as a direct consequence of phase inversion.



(a)



(b)



(c)

Figure 2.8 SEM micrographs showing morphology of PPS in blends with PET-OB at various compositions: (a) pure PPS; (b) 90/10; (c) 50/50 (wt./wt.) PPS/PET-OB blends.

Some authors have recently claimed that the extent of fibrillation of TLCP phase can be improved effectively by using compatibilising agents such as sulfonated polystyrene ionomers (SPSs)³³, controlled transesterification reaction³⁴ or by the reaction between the functional groups of PPS and TLCP using a catalytic mixture.³⁵ Factors such as melt viscosity ratios of the blend components, deformation force and interfacial tension greatly affect the morphology of microcomposites containing TLCP. The properties of blends are strongly influenced by their morphology as a consequence of incompatibility and phase separation. The phase stabilisation of PPS blends with TLCP can be improved by the use of compatibilisers.

2.4 Comparative study of blends generated by different techniques

The manner in which two polymers are blended together is of vital importance in controlling the phase morphology and to the ensuing properties of blends. Most common techniques for preparing the blends are melt-mixing, solution blending and co-precipitation. This section describes a comparative study on the thermal properties, phase behaviour and morphology of PPS/PET-OB blends produced using different blending techniques.

2.4.1 Thermal properties

Melting behaviour: DSC heating thermograms of PPS, PET-OB as well as PPS/PET-OB blends prepared by melt-mixing and co-precipitation methods are shown in *Figure 2.9*. In co-precipitated blends the endothermic peaks corresponding to the melting

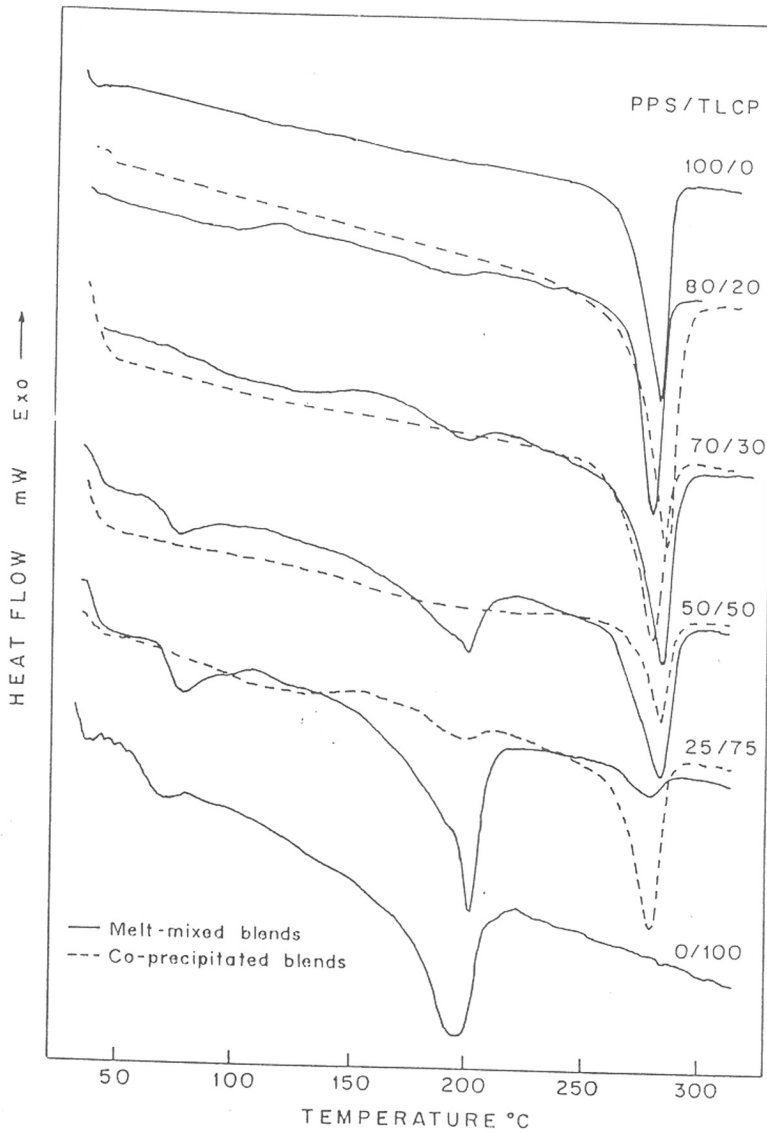


Figure 2.9 DSC thermograms (second heating scan) of melt-mixed and co-precipitated PPS/PET-OB blends at the heating rate of 20 °C/min.

Table 2.3: Comparison of thermal data of PPS phase in melt-mixed and co-precipitated PPS/PET-OB Blends

PPS/ PET-OB % (wt/wt)	Melt-mixed blends			Co-precipitated blends		
	T _m °C	T _c °C	ΔH _m J/g	T _m °C	T _c °C	ΔH _m J/g
100/0	282	237	43.9	282	237	43.9
90/10	280	252	43.8	281	239	35.1
80/20	279	251	44.0	280	243	33.6
70/30	281	252	35.1	278	249	32.1
50/50	280	246	32.1	279	251	26.3
25/75	278	244	26.2	279	251	24.9
10/90	277	243	23.4	278	249	22.0

transition of PET-OB are absent whereas in melt-mixed blends the intensity of melting transition peak of PET-OB increased with its concentration.

The occurrence of phase separation in blends is observable in DSC thermograms by the absence of any change in the glass transition temperature, the melting transition temperature or enthalpy of transitions from those corresponding to the original polymer components.³⁶

The absence of the endothermic peak corresponding to melting transition (T_m) of PET-OB in the co-precipitated PPS/PET-OB blends of 80/20, 70/30 and 50/50 compositions in *Figure 2.9* could be due to (i) the absence of phase separation or (ii) due to microphase separation not detectable by DSC. But, in the present blend system it is difficult to interpret any interactions, either chemical or physical, between the PPS and PET-OB^{8,9}. Moreover, in the case of homogeneous miscible blends the melting endotherm should have shifted to temperatures intermediate between that of the two homopolymers^{11,37} and this shift is not observable for the PPS/PET-OB blends in *Figure 2.9*. Therefore, the hypothesis (ii) namely, microphase separation not detectable by DSC is more appropriate to describe the blends prepared by co-precipitation.

The minimum domain size required for the detection of phase separation by DSC is considered to be of the order of 20 nm.³⁸ Sehurer et. al³⁹ have reported that in DSC thermograms the transition corresponding to the minor component may appear reduced in intensity if the dispersed phase is smaller. In the case of melt-mixed blends, the domains of dispersed TLCP phase are comparatively large in size and therefore it can be easily detected by DSC, as shown in the heating thermogram presented in *Figure 2.9*.

2.4.2 Crystallisation behaviour

The crystallisation exotherms of pure PPS and PPS/PET-OB blends prepared by melt-mixing and co-precipitation methods are shown in *Figure 2.10*. The crystallisation temperatures (T_c), presented in *Table 2.3*, are those corresponding to the exothermic peak maxima and are corrected as described by Elder and Wlochowicz.¹⁵ In co-precipitated blends the exothermic peaks corresponding to the PET-OB

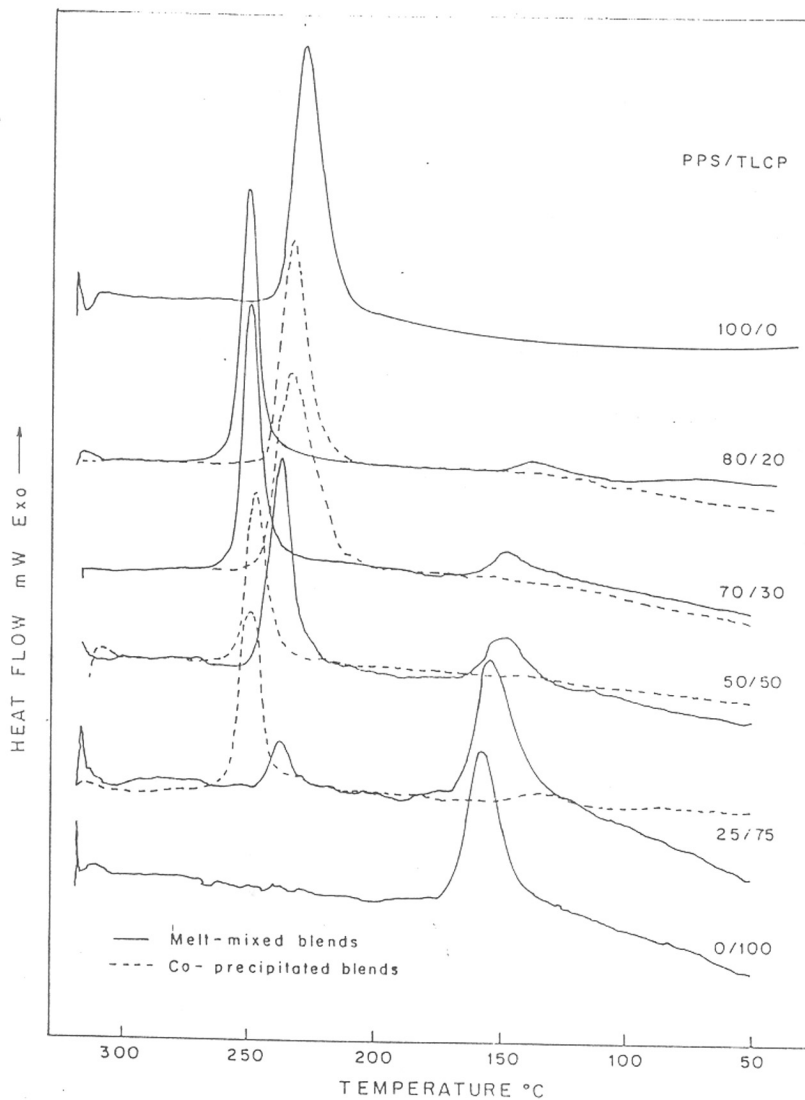


Figure 2.10 DSC crystallisation exotherms (second cooling scan) of melt-mixed and co-precipitated PPS/PET-OB blends at the cooling rate of 20 °C/min.

crystallisation are absent whereas in melt-mixed blends the peak intensity of crystallisation exotherm of PET-OB increased with its concentration. The crystallisation temperature (T_c) and hence the rate of crystallisation of PPS phase increased with PET-OB content upto 30% and decreased on further addition of PET-OB for melt-mixed blends. On the other hand, T_c and hence the rate of crystallisation of PPS phase in co-precipitated blends steadily increased with PET-OB content as shown in *Figure 2.10*.

These observations are similar to the melting behaviour discussed in **Section 2.4.1**. The dispersed PET-OB phase in co-precipitated blends crystallises to form microphase not detectable by DSC whereas in melt-mixed blends the PPS and PET-OB crystallise into separate phases as seen in DSC exotherm presented in *Figure 2.10*. The PET-OB phase accelerates the crystallisation of PPS phase in both melt-mixed and co-precipitated blends. Due to its low melt-viscosity,^{2,3} the molten PET-OB phase provides enough chain mobility to cause rapid crystallisation of PPS phase.

2.4.3 Degree of crystallinity

The degree of crystallinity, α , of the PPS phase in both melt-mixed and co-precipitated blends were plotted against the PET-OB content as presented in *Figure 2.11*. The degree of crystallinity, α , was calculated from the enthalpy of melting (ΔH_m) normalised to the PPS content, assuming that the contribution of the PET-OB phase is negligible.²⁰ A value of 146.2 J/g was estimated by Maemura et al.⁴¹ for enthalpy of

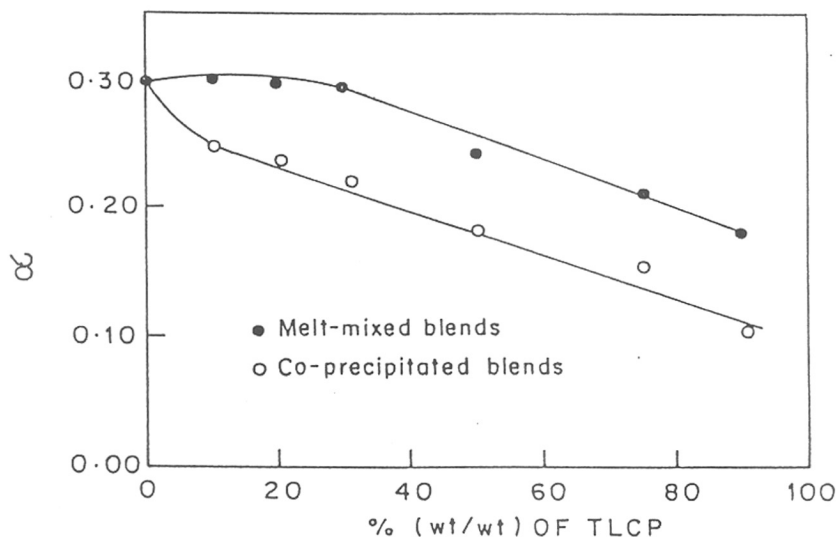


Figure 2.11 Effect of PET-OB content on the degree of crystallinity (α) of PPS phase in both melt-mixed and co-precipitated blends.

fusion of 100% crystalline PPS. In melt-mixed blends the degree of crystallinity of PPS remains almost constant upto 30 wt.% PET-OB content and then reduced with further addition of PET-OB. In the case of co-precipitated blends the degree of crystallinity decreased steadily with PET-OB concentration. This marked difference in the degree of crystallinity may be due to the fact that the degree of mixing is more intimate in co-precipitated blends as compared to the melt-mixed blends of similar composition. The addition of a second polymer to a semicrystalline polymer can act as a diluent, which could either decrease crystallinity by decreasing concentration and number of nuclei, or increase crystallinity by enhancing nucleation or increasing the chain mobility.⁴² Degree of crystallinity, α , is known to be a measure of degree of phase mixing.^{9,43} The degree of crystallinity is known to decrease on compatibilisation of incompatible blends.⁴³ From these observations, we may conclude that the degree of crystallinity of PPS phase depends on the extent of phase separation between the PPS phase and PET-OB phase, which in turn, depends on the blending technique used for the preparation of PPS/PET-OB blends.

2.4.3 Morphology

2.4.3.1 Polarised light optical microscopy

Figure 2.12 (a)-(f) show the optical micrographs under cross polarisers of PPS and PPS/PET-OB blends (in molten state at 320 °C) produced by melt-mixing and co-

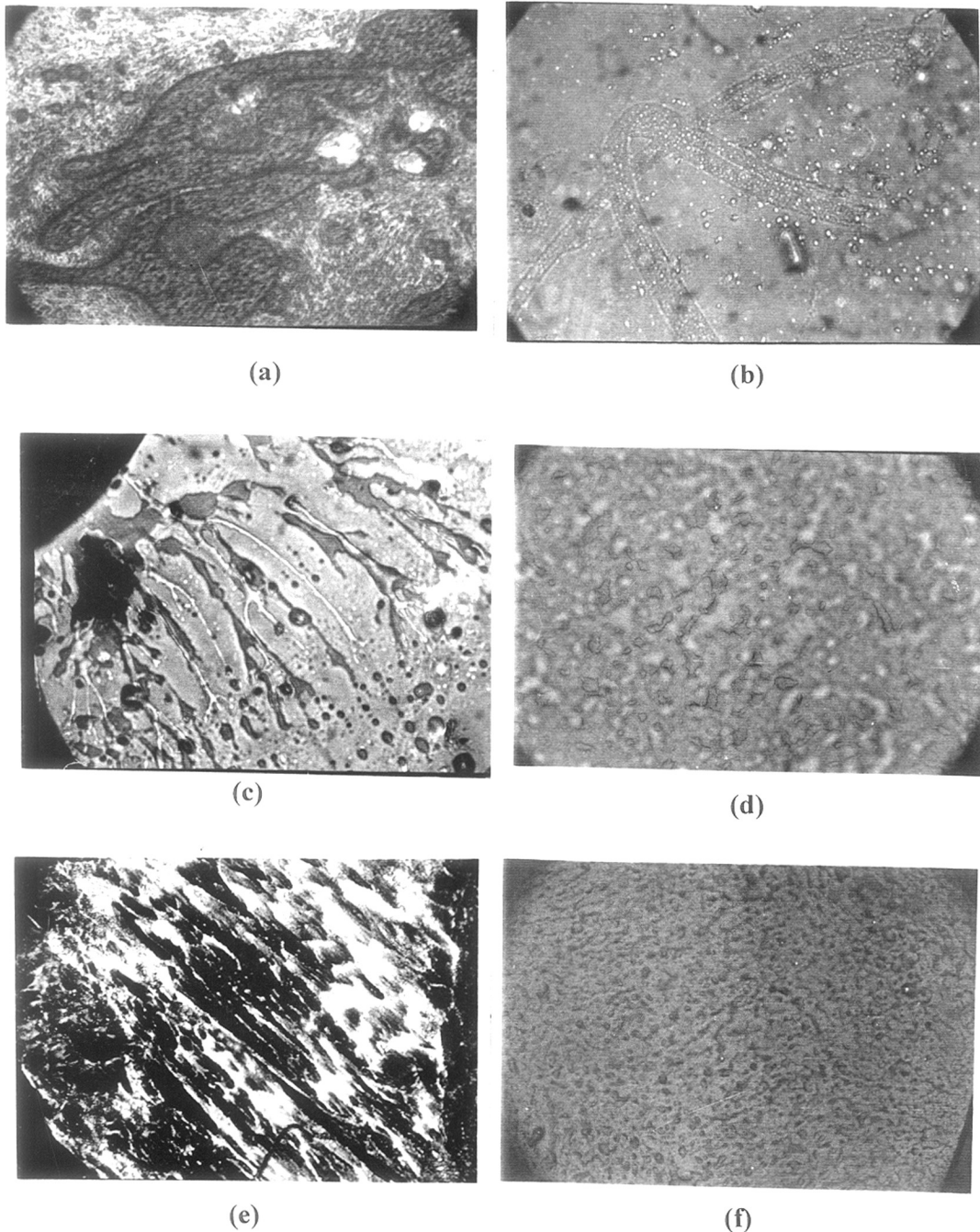


Figure 2.12 Optical micrographs (same magnification, 100 X) of the phase behaviour and morphology of melt-mixed and co-precipitated PPS/PET-OB blends at various compositions at 320 °C. (a) melt-mixed [(a) 90/10, (c) 70/30 & (e) 50/50 % (wt./wt)] and co-precipitated [(b) 90/10, (d) 70/30 & (f) 50/50 % (wt./wt.)] PPS/PET-OB blends.

precipitation. At this temperature, the domains of PET-OB alone are observable under cross polarisers as these are in the anisotropic nematic state. The liquid-liquid phase separation *via* spinodal decomposition is observable in PPS/PET-OB blends produced by melt-mixing as well as by co-precipitation. *Figure 2.12 (c)* and *(d)* show a comparison between the PET-OB domain size of melt-mixed and co-precipitated blends under identical conditions. In co-precipitated blends the PET-OB domains are relatively smaller and are more uniformly dispersed within PPS matrix whereas in the melt-mixed blends a wide size distribution is noted due to distinctive phase separation and an aggregation of the PET-OB phase.

2.4.3.2 Scanning electron microscopy

Figure 2.13 (a)-(f) show the SEM micrographs of PPS and PPS/PET-OB blends prepared by melt-mixing and co-precipitation. The melt-mixed blends show macrophase-separated-morphology in *Figure 2.13 (a), (c) and (e)* indicating poor phase mixing whereas the co-precipitated blends of the same composition [*Figure 2.13 (b), (d) and (f)*] exhibit a disperse type morphology. In the blend containing 50% PET-OB [*Figure 2.13 (e)*], the PET-OB phase exists as fibrils whereas in the corresponding co-precipitated blend [*Figure 2.13 (f)*] fibrils are not observable. The fibrillation observed in the melt-mixed blend [*Figure 2.13 (e)*] is due to deformation force which plays a major role in the melt-mixing of polymers. The more uniform and continuous morphology of co-precipitated blends is a consequence of intimate dispersion of PET-OB phase within the

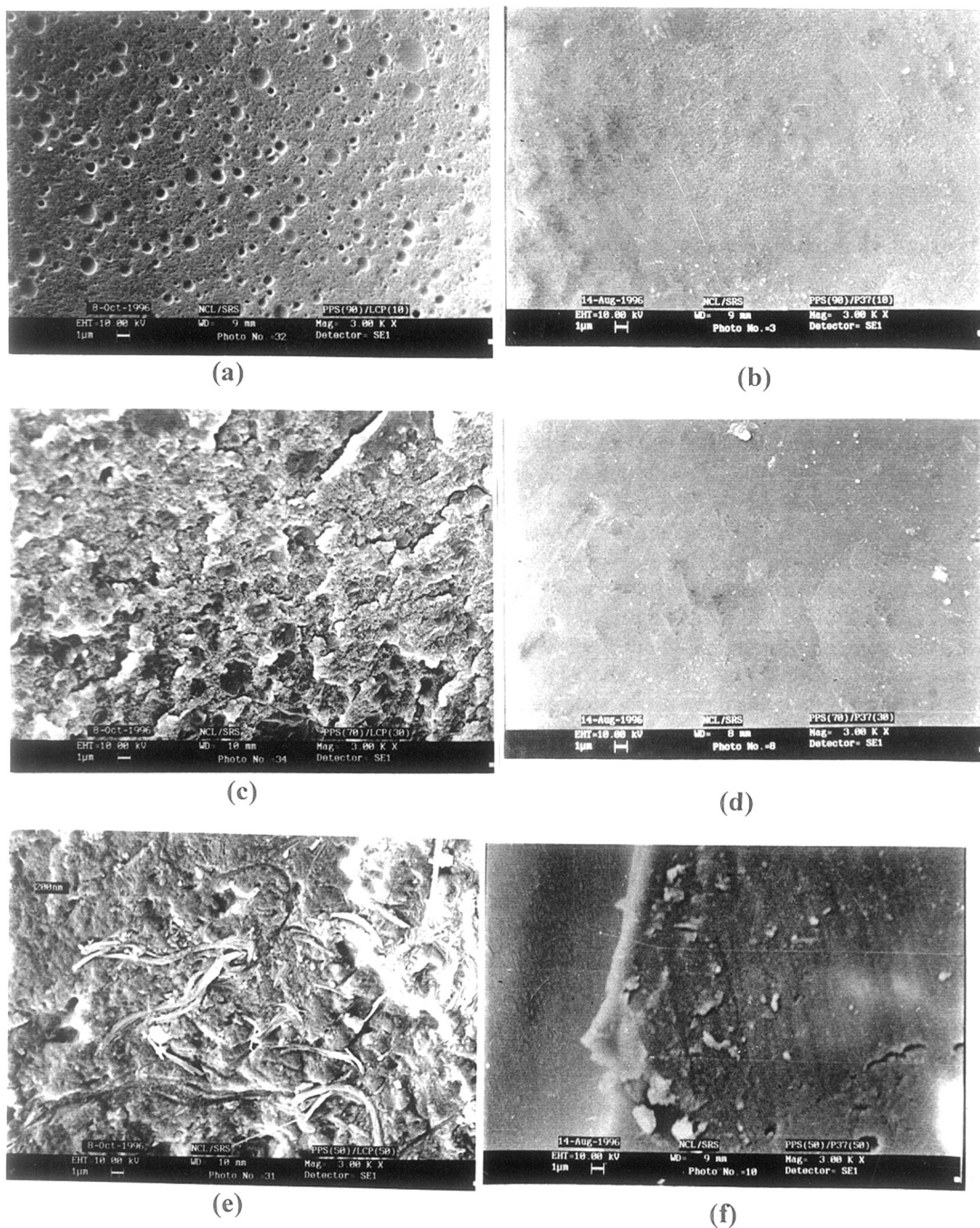


Figure 2.13 SEM micrographs showing morphology of freeze-fractured samples of melt-mixed [(a) 90/10, (c) 70/30 & (e) 50/50] % (wt./wt.) and co-precipitated [(b) 90/10, (d) 70/30 & (f) 50/50] % (wt./wt.) PPS/PET-OB blends (PET-OB was termed as LCP in micrographs of melt-mixed blends and as P37 in micrographs of co-precipitated blends).

PPS matrix. This morphology is comparable to that noted in the case of partially miscible blends. It is difficult to obtain homogeneous mixing of blend components with melt-mixing as a direct consequence of restricted motion of polymer chains in the molten state. In that case, the dispersion process is controlled by the shear viscosity of the two polymers. The properties of melt-mixed blends are also strongly influenced by the temperature, time and speed of mixing.

Two polymers which are indeed miscible may form a phase separated system when solution cast from certain solvents because of differences in the polymer/solvent interaction parameters of the two polymers.⁴⁴ In co-precipitated blends, mixing of two polymers to a homogeneous level is possible because the free motion of polymer chains is greater in solution as compared to the molten state. Also, on using a nonsolvent rapid removal of solvent from the solution of two polymers by precipitation prevents agglomeration and this leads to the homogenisation of components. Therefore, in relation to melt-mixing and solution casting, the co-precipitation is a more convenient and suitable alternative for generating molecular composites.

The properties of blends are strongly influenced by their morphology as a consequence of incompatibility and phase separation.^{36,45,46} In order to develop an ideal fibril-reinforced microcomposite based on thermoplastics (TP)/thermotropic liquid crystalline polymer (TLCP), the formation of longer and finer TLCP fibrils with a higher aspect ratio with TP matrix and increased interfacial adhesion are the two most important factors.^{9,43} The phase stabilisation of PPS blends with PET-OB can be improved by the

use of compatibilisers. However, recent studies^{3,33-35,41} have shown that most of the compatibilised TP/TLCP blends tend to hinder TLCP fibril formation, due to lower interfacial tension and finer dispersed phase domains, even though enhanced interfacial adhesion is obtained. The compatibilisation must not cause the loss of fibrous morphology.

2.5 CONCLUSION

Thermal properties, phase behaviour and morphology of blends of poly(phenylene sulphide) and poly(ethylene terephthalate-co-oxybenzoate) (PET-OB), an aliphatic-aromatic thermotropic liquid crystalline polymer (TLCP), were investigated. DSC studies showed that the crystallisation temperature (T_c) and the heat of melt crystallisation (ΔH_c), increased whereas the degree of super cooling (ΔT) first reduced marginally with PET-OB content up to 30% and then more dramatically with further increase in PET-OB content. Melting, crystallisation and phase behaviour of blends were investigated using DSC and PLOM. The equilibrium melting temperature (T_m^0) of PPS phase and the crystal lamellar thickness decreased with increase in PET-OB concentration. Phase diagram showed that the PPS phase crystallises at a temperature well above the crystal-nematic transition of PET-OB. The crystallisation temperature (T_{max}) of PPS phase increased with the addition of PET-OB. PLOM observation revealed that the PPS spherulite size reduced in the presence of PET-OB. SEM observation indicated a macrophase separated-morphology for blends.

The following conclusions can be drawn: i) the blend exists as immiscible and phase separated; ii) the PET-OB phase could act as nucleating agent for the PPS

crystallisation; iii) the PET-OB phase influences the spherulitic growth rate as well as the overall crystallisation rate of PPS.

From the comparative study of thermal properties, phase behaviour and morphology of melt-mixed and co-precipitated blends, we could reach in the following conclusions: (a) the extent of phase separation is more in melt-mixed blends as compared to co-precipitated blends; (b) the PET-OB phase accelerates crystallisation of PPS phase in both melt-mixed and co-precipitated blends and (c) the effect of PET-OB phase on crystallinity of PPS varied with extent of phase separation between the two components.

2.6 REFERENCES AND NOTES

1. T.G. Gopakumar, R.S. Ghadage, C.R. Rajan, S. Ponrathnam and A. Fradet, *Polymer* (in press).
2. T.G. Gopakumar, C.R. Rajan, S. Ponrathnam and A. Fradet, *Polym. J.* (in Press).
3. T.G. Gopakumar, C.R. Rajan, S. Ponrathnam and A. Fradet, *J. Appl. Polym. Sci.*, (communicated).
4. C.S. Brown and P.T. Alder, "Blends containing liquid crystal polymers", in M.J. Folkes and P.S. Hope, Eds., *Polymer Blends and Alloys*, Chap. 8. Chapman & Hall, London, (1993).
5. D.G. Baird, T. Sun, D.S. Done and R. Ramanathan, *Polym. Prepr.*, (Am. Chem. Soc.), Div. Polym. Chem., **30**, 1989, 546.
6. P.R. Subramaniam and A.I. Isayev, *Polymer*, **32**, 1991, 1961.
7. P.L. Magagnini, S. De Petris, M. Paci, M. Pracella, M.L. Minkova, A. Valenza and F.P. La Mantia, *Proceedings of Eighth Annual meeting, Polymer processing Society*, New Delhi (India), 1992, p.356.
8. M.T. Heino and J.V. Seppala, *J. Appl. Polym. Sci.*, **44**, 1992, 1051.
9. M.T. Heino and J.V. Seppala, *J. Appl. Polym. Sci.*, **44**, 1992, 2185.
10. B.C. Kim, S.M. Hong, S.S. Hwang and K.U. Kim, *Polym. Eng. Sci.*, **36**, 1996, 574.
11. G.O. Shonaike, S. Yamaguchi, M. Ohta, H. Hamada, Z. Maekawa, M. Nakamichi and W. Kosaka, *Eur. Polym. J.*, **30**, 1994, 413.
12. G.O. Shonaike, S. Yamaguchi, M. Ohta, H. Hamada, Z. Maekawa, M. Nakamichi, W. Kosaka and K. Toi, *Polym. Eng. Sci.*, **35**, 1995, 240.
13. G. Gabellini, M.B. de Moraes and R.E.S. Bretas, *J. Appl. Polym. Sci.*, **60**, 1996, 21.
14. J. Mathew, R.S. Ghadage, S. Ponrathnam and S.D. Prasad, *Macromolecules*, **27**, 1994, 4021.
15. M. Elder and A. Wlochowicz, *Polymer*, **24**, 1983, 1593.
16. J.D. Hoffman and J.J. Weeks, *J. Res. Natl. Bur. Stand. A.*, **66**, 1962, 13.

- 17 D. Lovinger, D. Davis and F.J. Padden, Jr., *Polymer*, **26**, 1985, 1595.
- 18 B. Wunderlich, *Macromolecular Physics: Crystal Melting*, Vol. 3, Ch. 8, Academic Press, New York, (1973).
- 19 T. Nishi and T.T. Wang, *Macromolecules*, **8**, 1975, 909.
- 20 J.P. Penning and R.S. Manley, *Macromolecules*, **29**, 1996, 76.
- 21 J.P. Penning and R.S. Manley, *Macromolecules*, **29**, 1996, 84.
- 22 P.J. Flory, *Principles of Polymer chemistry*; Cornell University Press; Ithaca, New York, (1953).
- 23 D.P. Desio and L. Rebenfeld, *J. Appl. Polym. Sci.*, **39**, 1990, 825.
- 24 V.M. Nadkarni and J.P. Jog, *J. Appl. Polym. Sci.*, **32**, 1986, 5817.
- 25 R. Thomann, J. Kressler, S. Setz, Ch. Wang and R. Mulhaupt, *Polymer*, **37**, 1996, 2631.
- 26 B. Wunderlich, *Macromolecular Physics: Crystal Structure, Morphology, Defects*, Vol. 1, Academic Press, New York, (1973).
- 27 B. Wunderlich, *Macromolecular Physics: Crystal Nucleation, Growth, Annealing*, Vol. 2, Academic Press, New York, (1973).
- 28 V.M. Nadkarni, V.L. Shingankuli and J.P. Jog, *Int. Polym. Proc.*, **2**, 1987, 53.
- 29 V.L. Shingankuli, J.P. Jog and V.M. Nadkarni, *J. Appl. Polym. Sci.*, **36**, 1988, 335.
- 30 S.M. Hong, B.C. Kim, K.U. Kim and I.L. Chung, *Polym. J*, **24**, 1992, 727.
- 31 L.I. Minkova, M. Paci, M. Pracella and P. Magagnini, *Polym. Eng. Sci.*, **32**, 1992, 57.
- 32 L.I. Minkova and P.L. Magagnini, *Polymer*, **36**, 1995, 2059.
- 33 D. Dutta, R.A. Weiss and J. He, *Polymer*, **37**, 1996, 435.
- 34 R.S. Porter and L.H. Wang, *Polymer*, **33**, 1992, 2019.
- 35 P. Chen, V. Sullivan, T. Dolce and M. Jaffe, *U. S. Patent, US. 5,182,334*, assigned to Hoechst Celanese Corp., Somerville, N.J (1993).

36. O. Olabisi, L.M. Robeson and M.T. Shaw, *Polymer-Polymer Miscibility*, Academic Press, New York, (1979).
37. J.R. Fried, F.E. Karasz and W.J. MacKnight, *Macromolecules*, **11**, 1978, 150
38. L.A. Utracki, *Polymer blends and Alloys: Thermodynamics and Rheology*, Hanser Publishers, New York (1989).
39. W.J. Schurer, A. DeBoer and G. Challa, *Polymer*, **19**, 1978, 201.
40. L.I. Minkova, S. De Petris, M. Paci, M. Pracella, P.L. Magagnini, "Characterisation of blends of poly(phenylene sulphide) with thermotropic liquid crystalline copolyesteramide" in D. Acierno, F.P. La Mantia, Eds., *Processing and Properties of Liquid Crystalline Polymers and LCP Based Blends*, Chem Tec Publishing, Canada, 1993, 153.
41. E. Maemura, M. Cakmak and L.J. White, *J. Intern. Polym. Proc.*, **3**, 1990, 79.
42. L.I. Long, R.A. Shanks and Z.H. Stachurski, *Prog. Polym. Sci.*, **20**, 1995, 651.
43. Y.P. Chiou, K.C. Chiou and F.C. Chang, *Polymer*, **37**, 1996, 4099.
44. G. Das, A.N. Banerjee and B.C. Mitra, *Eur. Polym. J.*, **32**, 1996, 179.
45. D.R. Paul and S. Newman, *Polymer Blends*, Vol. 1 Academic Press, New York, (1978).

CHAPTER 3

CRYSTALLISATION KINETICS
OF PPS AND PPS/PET-OB
BLENDS^{1,2}

ABSTRACT

The effect of annealing, isothermal and non-isothermal crystallisation kinetics of Poly(phenylene sulphide) [PPS] were studied using differential scanning calorimetry (DSC). The study clearly indicated that there should be a minimum annealing time of 10 minutes at a temperature of 320 °C to obtain consistent thermal behaviour for PPS. The value of Avrami exponent 'n' was found to have temperature dependence. The Ozawa equation was found valid not only for neat PPS but also for blends containing PET-OB. The PPS crystallisation temperature was seen to increase markedly upon the addition of PET-OB. A notable reduction in Avrami exponent for the PPS/PET-OB blend systems suggests that the nucleated process leads to rod-shaped growth with thermal nucleation. The cooling crystallisation function, which represents the rate of non-isothermal crystallisation, was found to decrease with decreasing temperature and/or increase in PET-OB content.

3.1 INTRODUCTION

The study of the kinetics of crystallisation is necessary to optimise the process conditions and establishing the structure-property correlations in polymers.³ During fabrication of thermoplastic composites the polymer invariably undergoes repeated melting, quenching and crystallisation. The mechanical and physical properties of the moulded and extruded products of crystalline polymers are governed by the supermolecular morphology, which, in turn, is controlled by the crystallisation process. The properties of semicrystalline polymers such as PPS depend on their crystallisation behaviour. It is important, therefore, to understand the effects of the process cycles on the crystallisation kinetics of PPS.

The crystallisation behaviour of neat PPS⁴, of PPS with solid fillers⁵⁻⁷ and of PPS blended with thermoplastic polymers^{8,9} has been studied extensively by isothermal methods. The study of non-isothermal crystallisation of polymers is of great technological significance, since most practical processing techniques proceed under non-isothermal conditions. The non-isothermal experiments would provide more insight into the understanding of the crystallisation behaviour of polymer, because the more extremely employed isothermal methods are often restricted to narrow temperature ranges.¹⁰ The non-isothermal crystallisation kinetics of linear and branched PPS were studied by Lopez and Wilkes.⁴ They found that the Avrami exponent, determined by Ozawa equation¹¹ from non-isothermal measurements are in good agreement with those achieved by isothermal methods.

Liquid crystalline polymer (LCP) blends have been studied extensively in recent years.¹²⁻²⁰ The motivation was first to use the high-tensile modulus of the LCPs in the solid state to reinforce the polymer matrix. Secondly, the low viscosity of the LCPs can reduce the overall viscosity of the blend and thus act as a good processing aid. The thermotropic liquid crystalline polymer, which is initially dispersed as spheres or droplets, can be elongated in adequate flow fields to give an *in-situ* reinforcement. Elongated fine fibrils can effectively reinforce the matrix polymer. Moreover, the LCP phase has been shown to influence the crystallisability of the matrix.¹⁴⁻¹⁸ Minkova et. al¹⁹ found that blending PPS with Vectra B950, a wholly aromatic commercial LCP from Hoechst Celanese, leads to an increase of the non-isothermal crystallisation temperature without any reduction of the degree of crystallinity. Minkova and Magagnini¹⁰ found that the non-isothermal crystallisation of PPS is strongly accelerated by Vectra B950 without any change in the type of nucleation and the geometry of crystal growth. Hong et. al²⁰ studied non-isothermal crystallisation kinetics of PPS/Vectra B950 blends. This study revealed a notable reduction in Avrami exponent, indicating that the nucleated process leads to rod-shaped growth with thermal nucleation.

In this Chapter the following studies are presented: (i) the effects of annealing on the thermal behaviour of PPS; (ii) the isothermal and non-isothermal crystallisation kinetics of neat PPS and (iii) the non-isothermal crystallisation behaviour of PPS blended with an aliphatic-aromatic thermotropic liquid crystalline copolyester, poly(oxybenzoate-co-ethylene terephthalate) (PET-OB) by analysing Differential scanning calorimetry (DSC) data adopting Avrami and Ozawa equations.

3.2 EXPERIMENTAL

3.2.1 Materials

PPS used was a commercial grade Ryton (V - I) manufactured by Phillips Petroleum Company. The melt flow index (MFI) of this material was 79.8 g/10 minutes (ASTM 1238, 5 Kg, 316 °C). Thermotropic liquid crystalline poly(oxybenzoate-co-ethylene terephthalate) (PET-OB) was synthesised from PET and 4-acetoxy benzoic acid according to an established procedure.²¹ The intrinsic viscosity of PET used in the synthesis was 0.6 dL/g. PET-OB was characterised as described in **Section 2.2.1**.

3.2.2 Effect of annealing on the thermal behaviour of PPS

Thermal properties were measured by a *Mettler TA4000* series DSC. The DSC apparatus was calibrated by the procedure described in **Section 2.2.3**. Annealing was done by heating the sample to the melt-temperature for a pre-defined time to destroy any residual crystal structure. A definite amount of the sample was weighed in the DSC pan and kept in the DSC cell. It was heated from 30 °C to 320 °C at the rate of 10 °C/minutes under nitrogen atmosphere. The sample was held for 5 minutes at that temperature to ensure complete melting. Then it was cooled to 30 °C at the rate of 10 °C/minutes. This was repeated six times. The above programme was performed for different samples with two more annealing times of 10 minutes and 20 minutes. Thus thermograms corresponding to heating and cooling cycles with three different annealing times were obtained. The values of ΔH and peak values were calculated.

3.2.3 Isothermal crystallisation kinetics of PPS

The isothermal crystallisation studies were carried out over a wide temperature range (245-270 °C). The weighed sample of PPS was first heated from 30 °C to 320 °C at the rate of 10 °C/minute under constant nitrogen atmosphere. The sample was held at this temperature for 10 minutes (annealed) to impart constant thermal history. Then it was quenched at a rate of 70 °C/minute to the isothermal crystallisation temperature of 267 °C and the exothermic crystallisation peak was recorded on time base at this temperature for 15 minutes. The sample was then cooled to 30 °C at the rate of 70 °C/minutes. The DSC scans were collected and analysed.

3.2.4 Preparation of blends

Powders of the liquid crystalline PET-OB and PPS were dried at 130 °C under vacuum for 8 h prior to mixing. The PPS/PET-OB blends, with PET-OB content in the range 3, 5, 10, 20, 30% wt./wt., were prepared by blending in a 30 mL mixer attached to a Brabender Plasticorder, at 290 °C and 100 rpm for 5 minutes under nitrogen. Blank samples of both PPS and PET-OB were subjected to the same treatment.

3.2.5 Non-isothermal crystallisation kinetics of PPS/PET-OB blends

About 10 mg of the polymer sample was weighed very accurately in aluminium DSC pan and placed in the DSC cell. It was heated from 30 °C to the melt temperature of 320 °C at the rate of 10 °C/minute under nitrogen atmosphere. The sample was held for 10 minutes at this temperature to destroy any residual nuclei, before cooling at a specified

cooling rate. The constant cooling rates of 10, 15, 20, 25 and 30 °C/minute were applied. The thermograms corresponding to heating and cooling cycles were recorded and analysed to estimate the non-isothermal crystallisation kinetics.

3.3 RESULTS AND DISCUSSION

3.3.1 Effect of annealing

Annealing is a process by which one can impart certain property by heat treatment with or without complete melting.²² Annealing can destroy the thermal history of the crystal and it can achieve the equilibrium perfection. The annealing of semicrystalline polymers may change their degree of crystallinity, the size and orientation of the crystallites and the structural morphology. Upon annealing, crystallites grow and mechanical properties change significantly. The average degree of crystallisation after annealing depends on the annealing temperature and time.

First, the PPS sample was heated to 320 °C at a heating rate of 10 °C/minute, held at this temperature for 5 minutes and then cooled to room temperature at 10 °C/minute. This procedure was repeated for six times on each sample. The *Figure 3.1* shows superimposed plot of six cooling cycles annealed for 5 minutes at 320 °C. The shift in the value of crystallisation peak temperature (T_c) indicates that annealing of 5 minutes time is not sufficient to achieve a constant thermal behaviour. The superimposed plot of six cooling cycles of the sample annealed for 10 minutes at 320 °C is presented in *Figure 3.2*.

After two cooling cycles, the T_c of the sample was almost constant. This result indicates that there should be a minimum time of 30 minutes (three 10 minute cycles) to

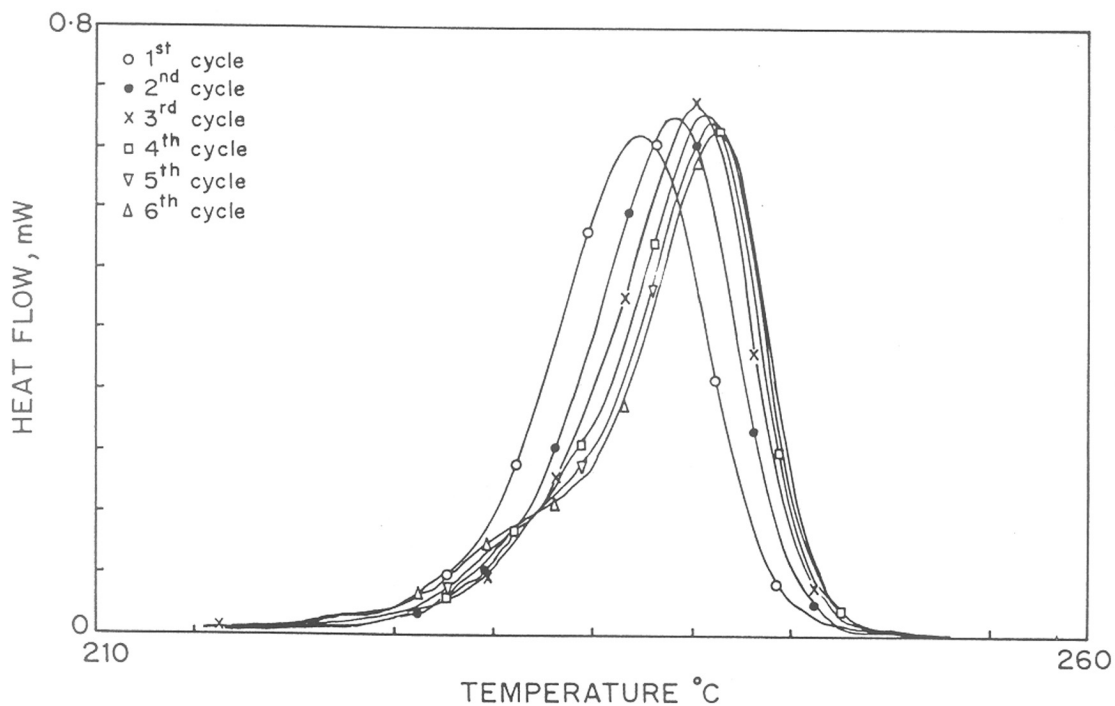


Figure 3.1 Superimposed plot of six heating cycles showing effect of annealing on T_m in PPS (sample annealed for 5 minutes at 320 °C)

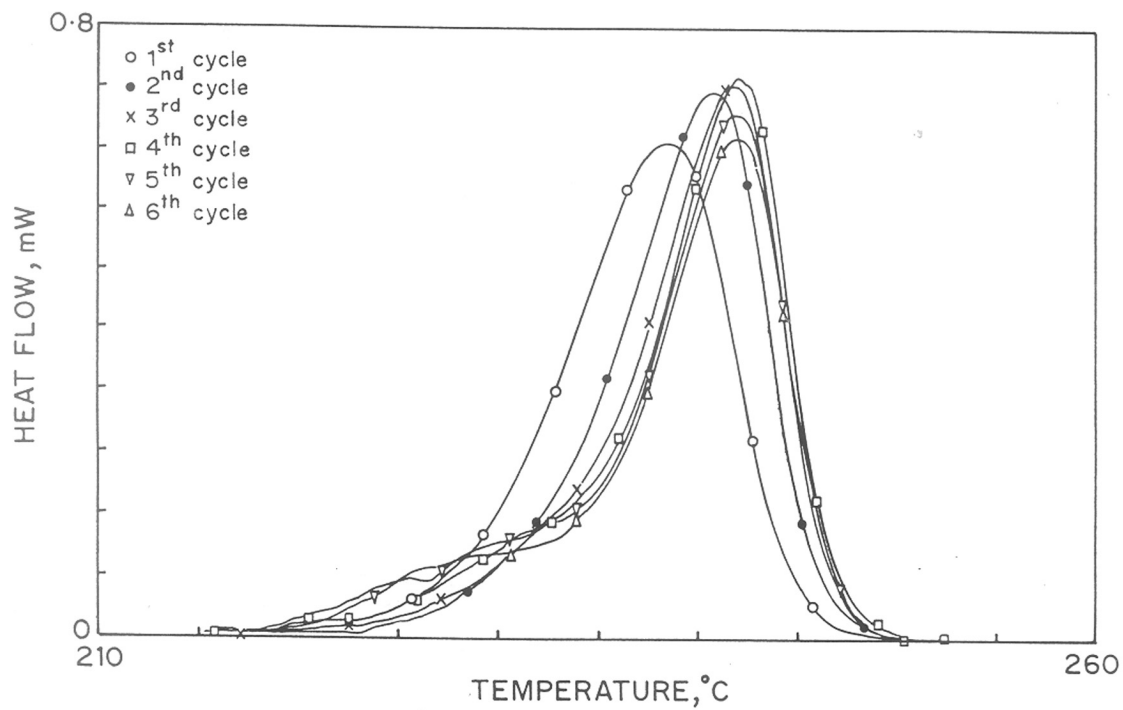


Figure 3.2 Superimposed plot of six heating cycles showing effect of annealing on T_m in PPS (sample annealed for 10 minutes at 320 °C)

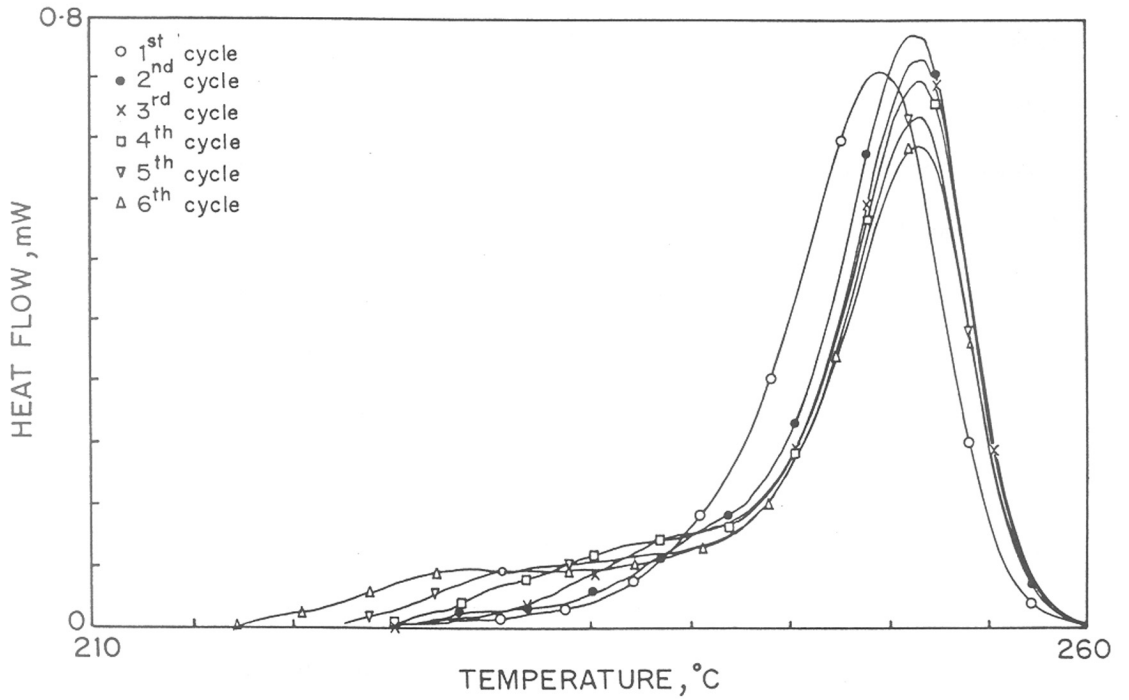


Figure 3.3 Superimposed plot of six heating cycles showing effect of annealing on T_m in PPS (sample annealed for 20 minutes at 320 °C)

get rid of possible post-polycondensation problems. After that, 10 minute annealing time is sufficient to obtain a constant thermal behaviour. Similarly, superimposed plot of six cooling cycles of a sample annealed for 20 minutes at 320 °C is presented in *Figure 3.3*. It is obvious from the figure that there is no change in the crystallisation peak temperature (T_c) from the second 20 minutes annealing cycle onwards. This is also in agreement with the value of the minimum time required to achieve constant thermal behaviour sample as deduced from *Figure 3.2*. These results show that there should be a minimum time of 20 minutes at 320 °C to overcome possible post-polycondensation problems and 10 minute annealing time to obtain a constant thermal behaviour sample.

3.3.2 Isothermal crystallisation kinetics of PPS

The isothermal crystallisation of PPS was studied over the temperature range of 230 °C to 260 °C. The onset of crystallisation in PPS takes place at around 255 °C. A typical isothermal crystallisation peak of PPS at 267 °C is shown in *Figure 3.4*. The crystallisation isotherm of PPS at 267 °C is presented in *Figure 3.5*.

The crystallisation-time dependence was analysed graphically by means of the Avrami equation²³ which describes isothermal crystallisation kinetics and is defined as:

$$X_c(t) = 1 - e^{-kt^n} \quad (3.1)$$

where $X_c(t)$ denotes the weight fraction of crystals at time t and at a constant temperature T ; k is a rate constant that includes the combined effects of nucleation and crystal growth rate; and n , the Avrami exponent depends on the dimension of crystal growth and the type of nucleation.²⁴ The linear form of this equation can be given by

$$\log \{ -\ln [1 - X_c(t)] \} = \log k + n \log t \quad (3.2)$$

The crystallisation kinetic parameters k and n are dependent on molecular weight, polymer structure, molecular weight distribution, degree of tacticity and presence of impurities. The extent of crystallisation $X_c(t)$ at a fixed time was determined from point by point area measurement at the isothermal crystallisation peak, assuming that the fractional crystallisation at a given time is proportional to the ratio of the crystallisation peak area up to that time to the total peak area.

The plot of $\log \{ -\ln [1 - X_c(t)] \}$ vs. $\log t$ for the PPS sample is shown in *Figure 3.6*. The values of Avrami exponent n obtained from this plot is 1.65. The extent of crystallisation vs. time at 267 °C is represented in *Figure 3.7*. It shows the time dependence of crystallisation of PPS.

The rate constant k was calculated by using the equation,

$$k = \ln 2 / (t_{1/2})^n \quad (3.3)$$

where $t_{1/2}$ denotes the crystallisation half time. The value of the Avrami exponent obtained from the plot is 1.65 and the rate constant k is $1.74 \times 10^{-4} \text{ sec}^{-n}$. The crystallisation half time is 152 seconds in this case. It is clear from the graph that the Avrami equation describes the isothermal crystallisation behaviour of PPS fairly well. The low value of Avrami exponent ' n ' can be attributed to the excessive crystallisation of sample during the initial non-isothermal process up to first 50 sec. (*Figure 3.5*). This excessive crystallisation observed during non-isothermal mode results in the reduction of crystal growth dimensionality. The crystallites formed during first 50

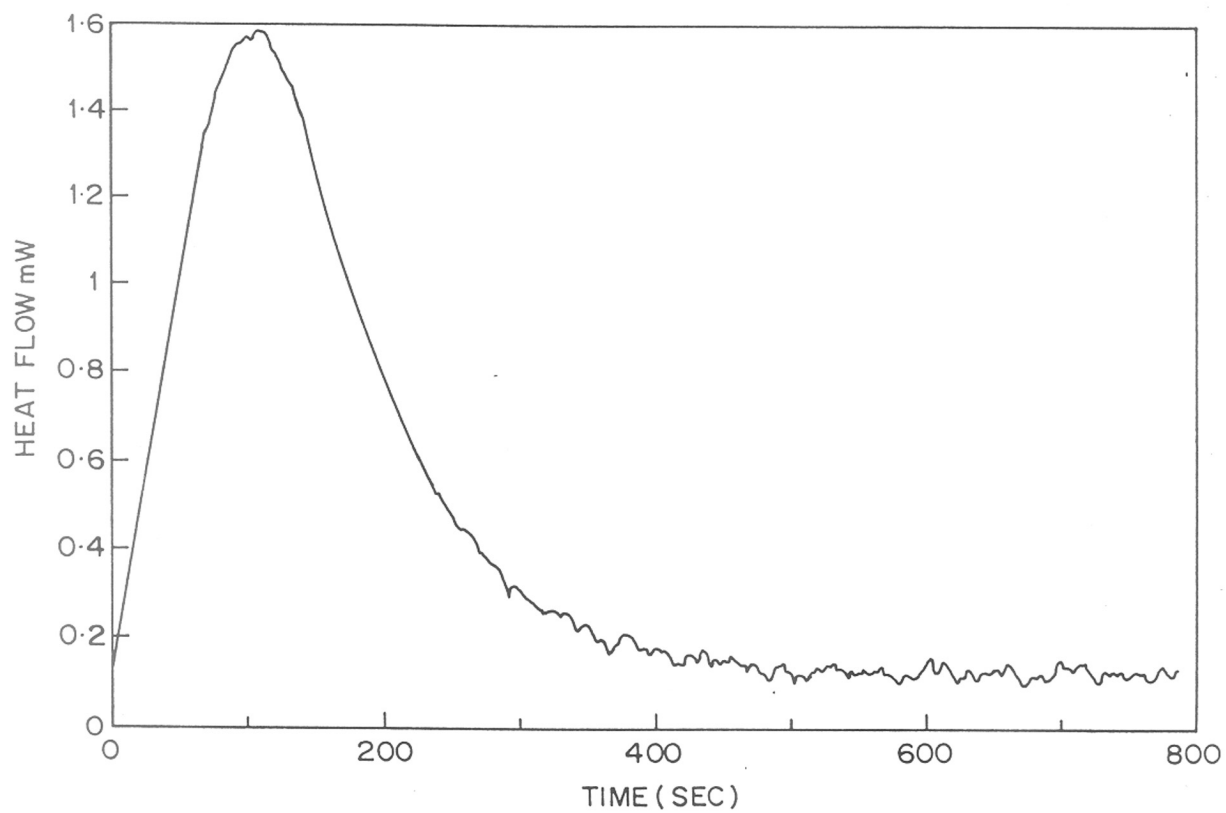


Figure 3.4 A typical isothermal crystallisation peak at 267 °C.

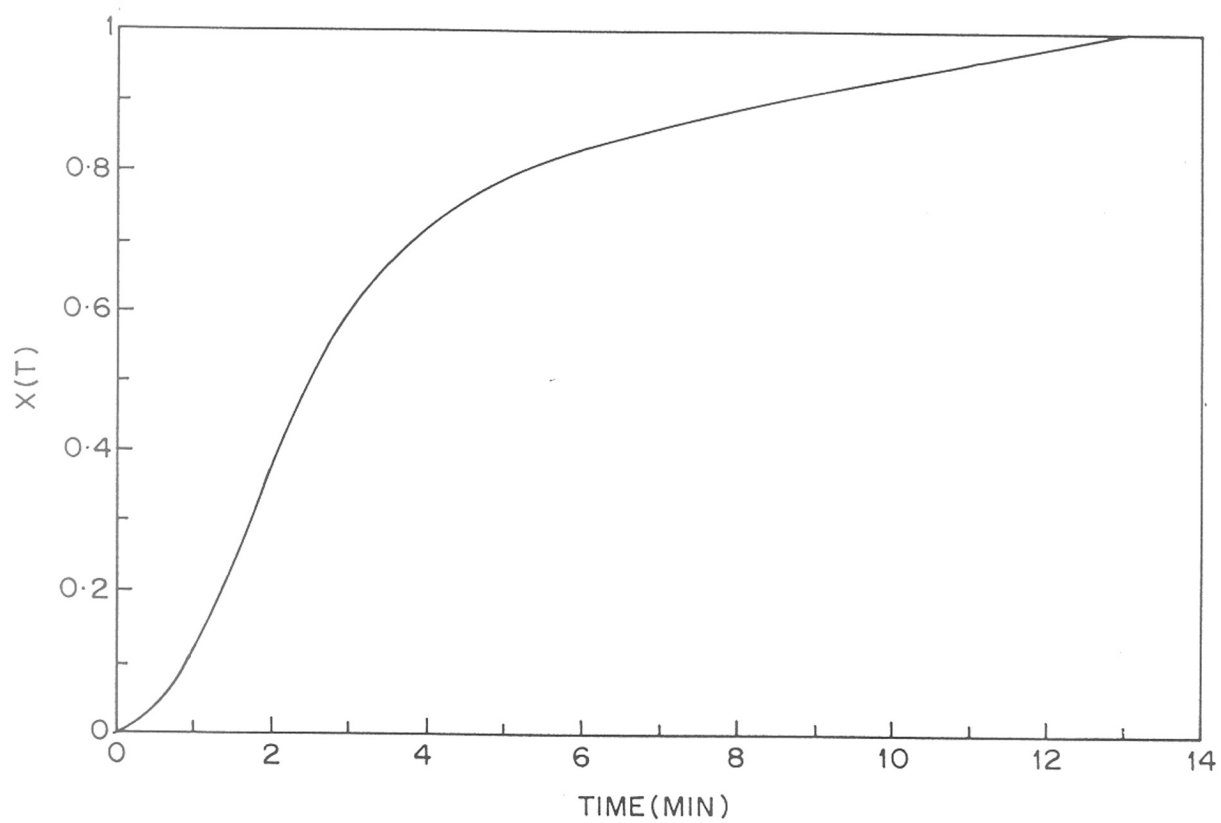


Figure 3.5 Crystallisation isotherm of PPS at 267 °C.

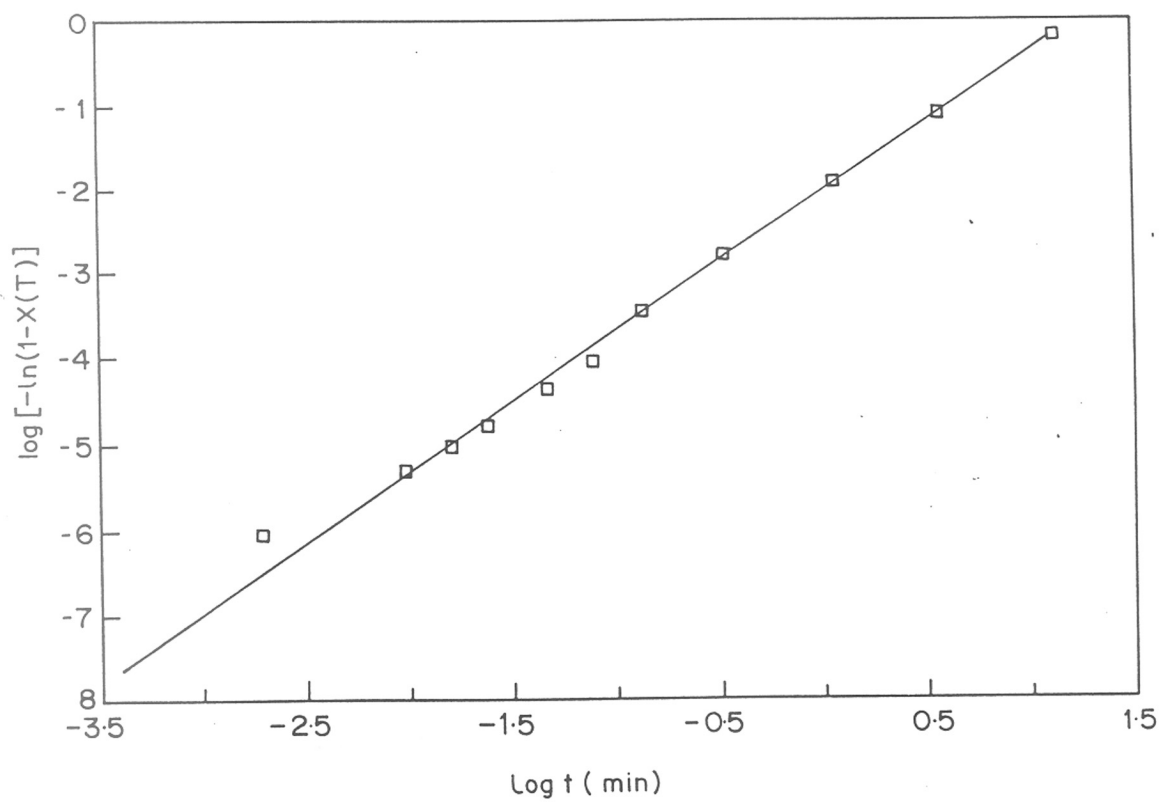


Figure 3.6 Avrami plot of PPS at 267 °C.

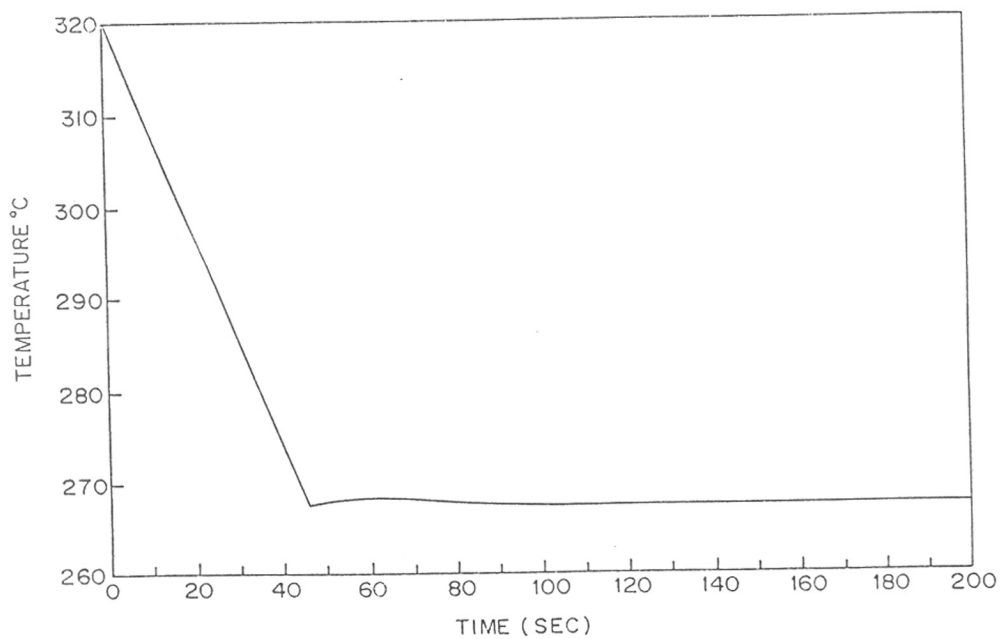


Figure 3.7 The extent of crystallisation vs. time at 267 °C

seconds (non-isothermal mode) can act as nucleation points for the further crystallisation of sample during isothermal crystallisation. Additional experimentation such as scanning electron microscopy of surface and bulk morphology are necessary to obtain a more detailed information on this dual mode crystallisation.

3.4 Non-isothermal crystallisation kinetics of PPS and PPS/PET-OB blends

In the processing of polymers, such as fibre spinning, injection moulding and extrusion, the crystallisation occurs under non-isothermal conditions. Non-isothermal studies are used to elucidate structure development in the melt processing of polymers. It is therefore obvious that predicting crystallisation kinetics under continuous cooling conditions is of primary practical importance. In addition, isothermal measurements are often restricted to narrow temperature range because the response time of the measuring instrument becomes comparable to the overall time for crystallisation. Also, non-isothermal experiments during cooling can offer a clue to understand the crystallisation behaviour of polymers.^{11,23}

Non-isothermal crystallisation kinetics can be obtained by applying the non-isothermal DSC data to the Ozawa equation,¹¹ an extended Avrami equation.²³ Ozawa assumes that crystallisation occurs at a constant cooling rate and that crystallisation originates from a distribution of nuclei that grow as spherulites with constant radial growth rate at a given temperature.

The overall non-isothermal crystallisation kinetics of PPS was studied using the Ozawa equation(3.4).¹¹

$$\ln \{ -\ln [1 - X(T)] \} = \chi - n \ln \varphi \quad (3.4)$$

where X is the volume fraction of material crystallised at temperature T , φ is the constant cooling rate; n , the Avrami exponent, depends on the nucleation density and on the spherulitic radial growth rate for both instantaneous and sporadic nucleation and χ is the cooling crystallisation function.

The DSC thermograms obtained at a cooling rate of 10 °C/minutes for neat PPS and its blends with TLCP content of up to 30 wt./wt.% are shown in *Figure 3.8*. The exothermic crystallisation peaks are monomodal and their shapes indicate that secondary crystallisation does not play an important role in these blends. It was observed that the blend exotherms are much sharper than that of pure PPS and are located at a higher temperature with respect to the latter. The PPS crystallisation temperature was found to increase from 241 °C to 251 °C upon the addition of 3-30% PET-OB.

The crystallisation temperature, T_c , the half widths of the crystallisation peaks ΔT and the degrees of crystallinity α of the PPS phase obtained at different cooling rates for the blends with PET-OB content in the range 3-30% are presented in *Table 3.1*.

The crystallisation temperatures T_c are those corresponding to the exothermic peak maxima, corrected as described by method Elder and Wlochowicz.²⁶ The degree of crystallinity α was calculated from the enthalpy of crystallisation normalised to the PPS content, assuming that the contribution of the TLCP phase is negligible.²⁷ The value of 146.2 J/g was estimated by Maemura et al.²⁸ for the enthalpy of fusion of 100% crystalline PPS. It is noticed that α remains constant which suggests that the addition of PET-OB does not affect the degree of crystallinity of PPS. At a fixed PET-OB level,

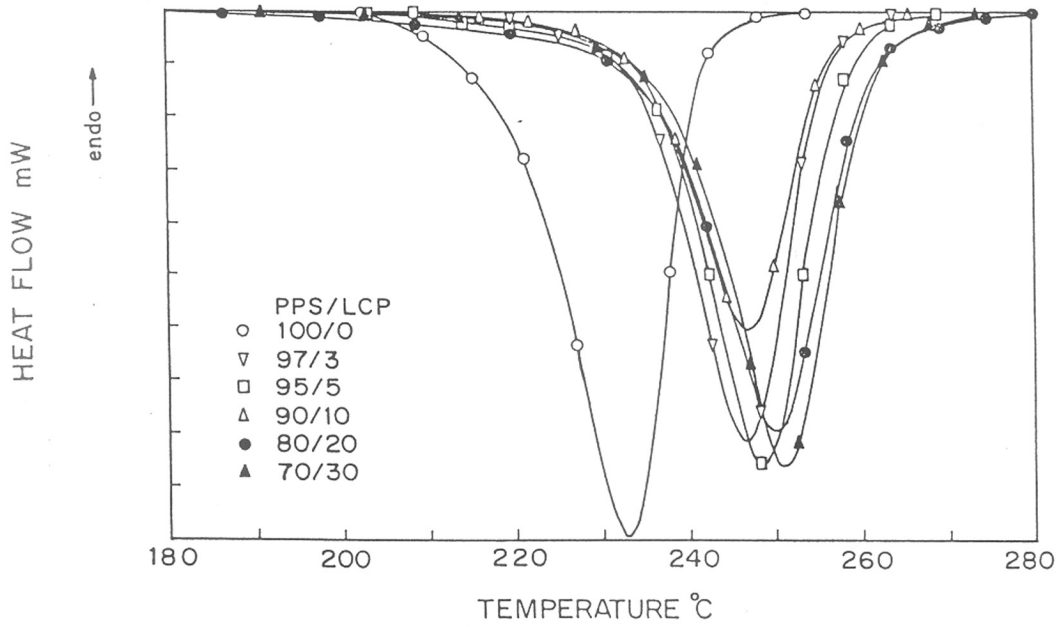


Figure 3.8 DSC cooling traces of PPS/PET-OB blends at 10 °C/minute

the crystallisation peak temperature (T_c) decreased with increasing cooling rate, whereas at a given cooling rate the T_c increased as PET-OB content increased.

The crystallisation temperature increases upon the addition of PET-OB to PPS whereas it decreases on increasing the cooling rate, as could be expected for the polymer crystallisation controlled by nucleation.²⁵ The sharpness of the crystallisation peaks, as measured by ΔT , is considerably higher for the blends than for pure PPS. This suggests that the rate of non-isothermal crystallisation of PPS increases appreciably in the presence of PET-OB.

The overall non-isothermal crystallisation kinetics of PPS was studied¹¹ using the Ozawa equation 3.4.¹¹ The amorphous fractions $[1 - X(T)]$ of the PPS phase in PPS/PET-OB blends with PET-OB content between 0 and 30% were calculated from the DSC traces and plotted against T for different cooling rates. The plots drawn for pure PPS and for 90/10 PPS/PET-OB blend are shown in *Figures 3.9* and *3.10* respectively. The Ozawa plots can be obtained by plotting double logarithm of the reciprocal amorphous fractions of the PPS phase against cooling rate, for different temperatures, as shown in *Figures 3.11* and *3.12* for neat PPS and for 90/10 wt./wt.% PPS/PET-OB blend respectively. It can be seen that these plots as well as those of all other blends studied represent straight lines, which means that the Ozawa equation satisfactorily describes the non-isothermal crystallisation behaviour of these blends.

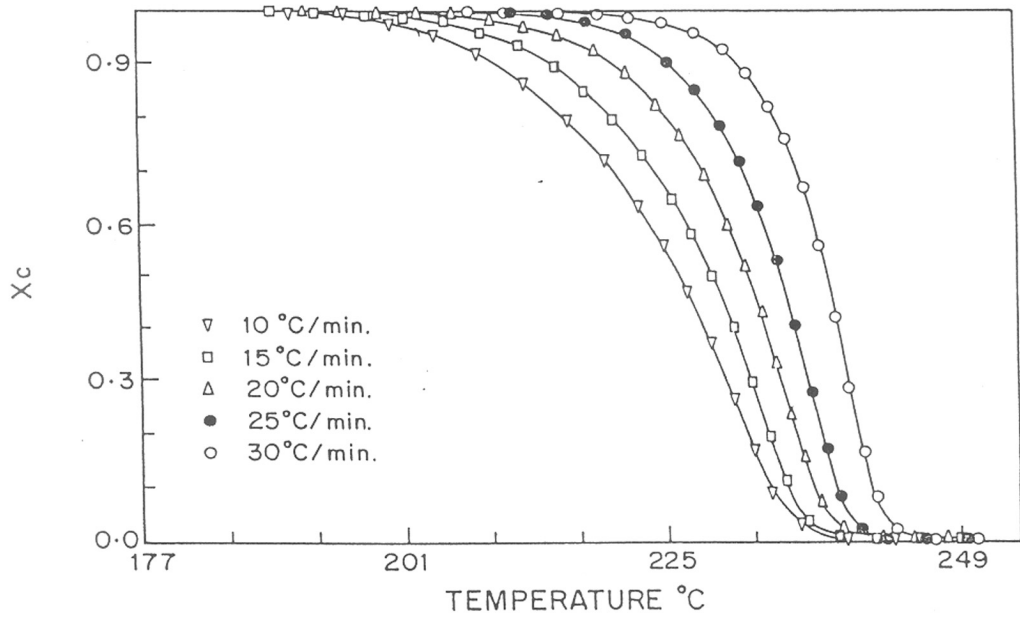


Figure 3.9 Fraction of crystallised PPS vs. crystallisation time.

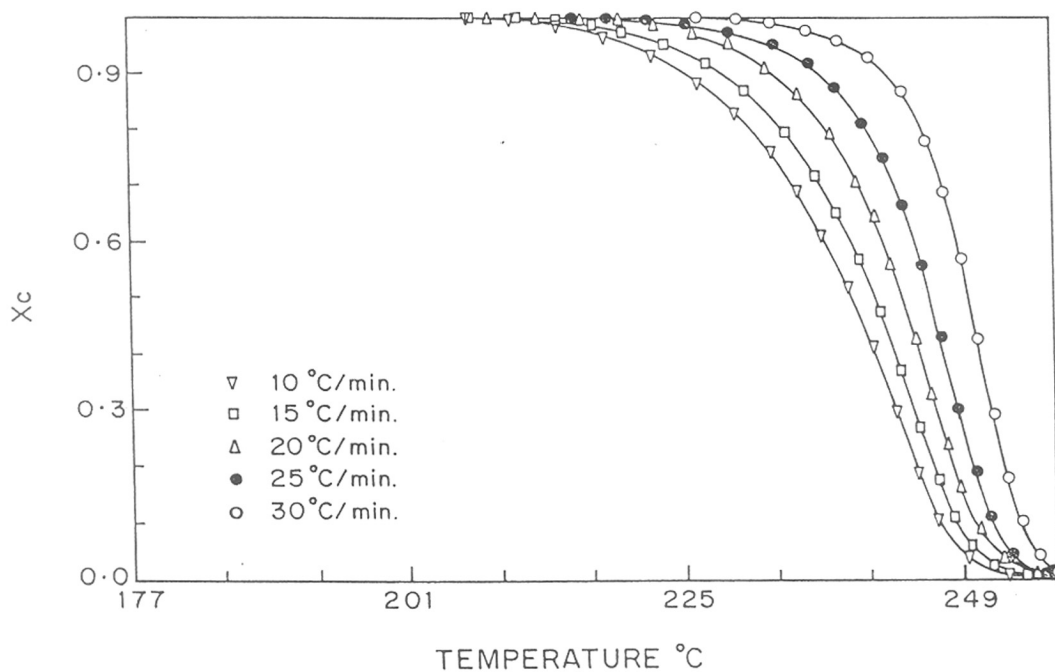


Figure 3.10 Fraction of crystallised PPS phase in PPS (90%)/PET-OB (10%) vs. crystallisation time.

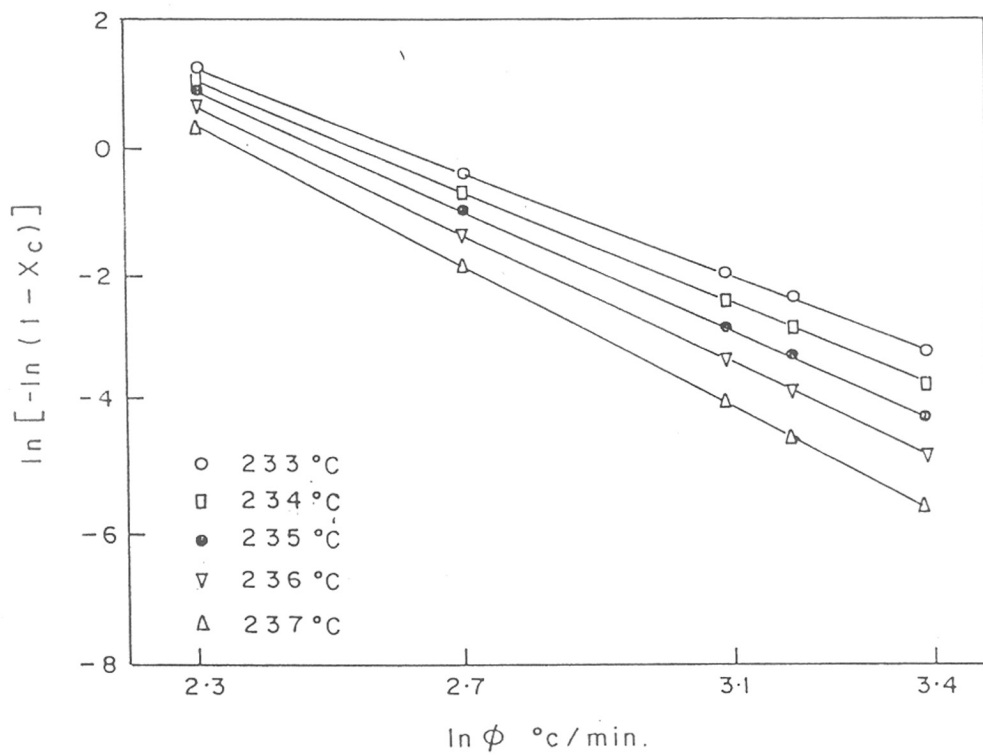


Figure 3.11 Ozawa plots of non-isothermal crystallisation for neat PPS.

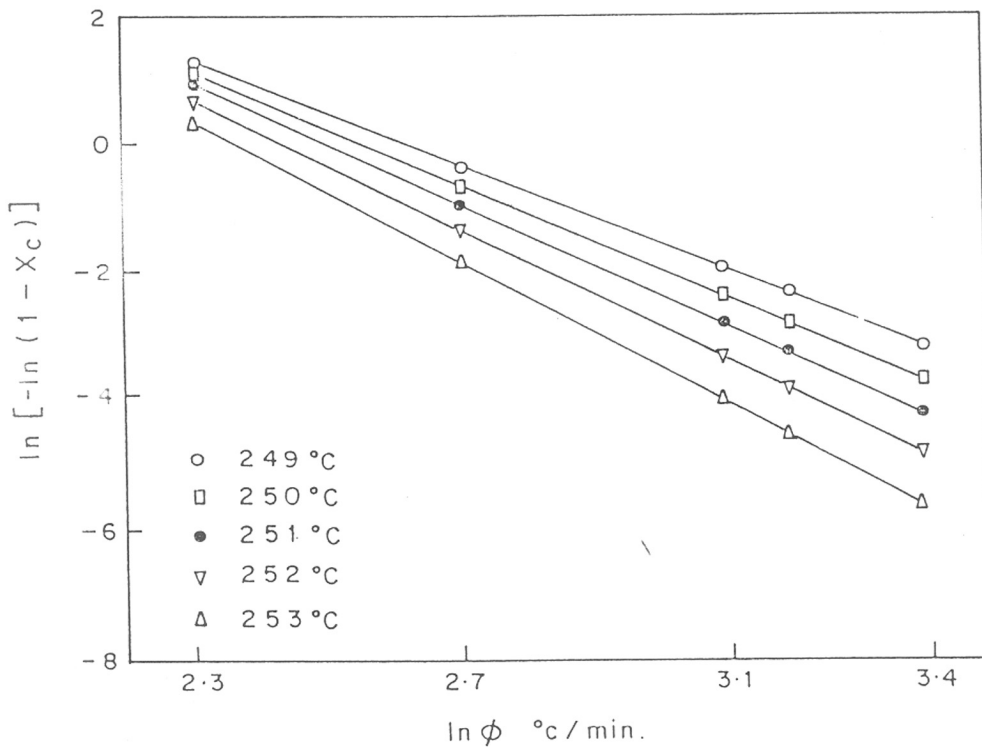


Figure 3.12 Ozawa plots of non-isothermal crystallisation for PPS/PET-OB blends.

Table 3.1 Effect of PET-OB on the crystallisation temperature (T_c), degree of crystallinity (α), half-width of crystallisation peak (ΔT) and Avrami exponent (n) of PPS in PPS/PET-OB blends.

Blend PPS/TLCP No.	wt./wt. %	10 °C/min ⁻¹			15 °C/min ⁻¹			20 °C/min ⁻¹			25 °C/min ⁻¹			30 °C/min ⁻¹			
		T_c °C	α	ΔT °C	T_c °C	α	ΔT °C	T_c °C	α	ΔT °C	T_c °C	α	ΔT °C	T_c °C	α	ΔT °C	n
1	100/0	243.3	0.30	21.4	339.4	0.28	23.5	237.1	0.31	26.7	235.2	0.31	29.3	232.0	0.31	36.6	2.97
2	97/3	250.9	0.31	14.4	250.1	0.28	16.0	249.6	0.30	15.3	248.9	0.29	16.4	247.7	0.29	16.9	2.68
3	95/5	252.2	0.29	14.0	250.6	0.30	16.0	250.8	0.29	15.5	250.3	0.30	16.4	249.8	0.30	16.4	2.50
4	90/10	253.0	0.30	14.5	252.6	0.29	15.7	252.1	0.29	14.9	251.3	0.30	15.3	250.8	0.29	14.8	2.45
5	80/20	253.9	0.28	11.4	252.1	0.29	12.4	251.3	0.30	14.4	250.0	0.32	14.9	249.6	0.31	13.4	2.23
6	70/30	254.2	0.29	12.4	253.9	0.29	12.4	252.8	0.29	13.2	251.6	0.28	14.2	250.8	0.30	12.3	2.01

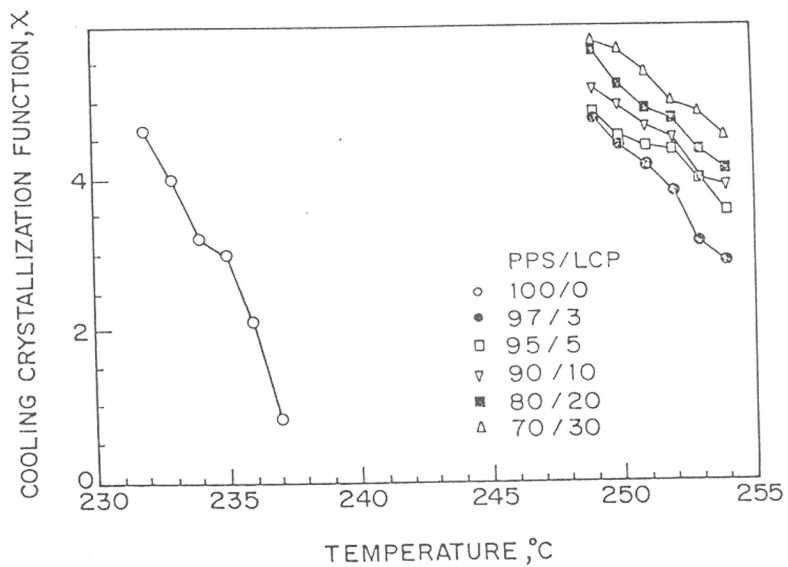


Figure 3.13 Plot of cooling crystallisation function for PPS/PET-OB blends.

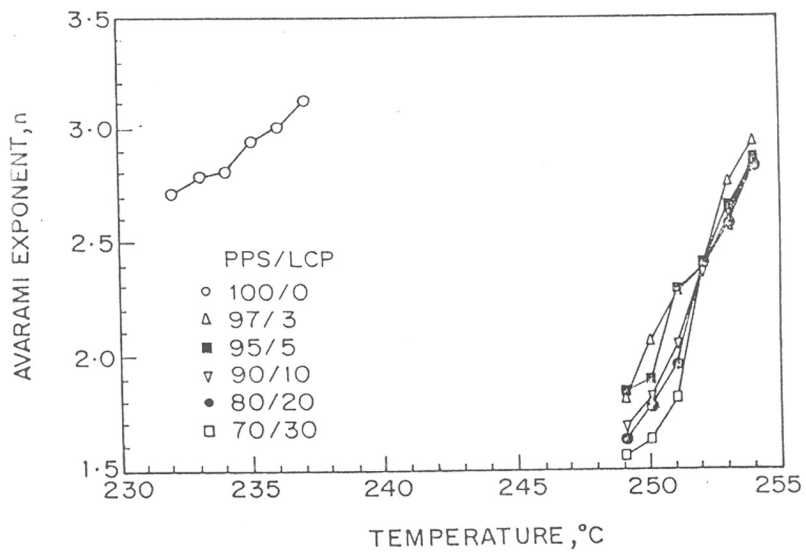


Figure 3.14 Plot of Avrami exponent $[n]$ vs. temperature for PPS/PET-OB blends.

The intercept of the Ozawa plots gives the cooling crystallisation function which represents the rate of non-isothermal crystallisation.^{11,25,29} The plot of cooling crystallisation against temperature is presented in *Figure 3.13*. The function decreased with a decreasing in temperature or increase in PET-OB content. The values of χ measured are in good agreement with those given by Ozawa¹¹ for PET, Kozlowski²⁹ for polyamides, Elder et al.²⁶ for PP and Lopez et al.²⁵ for PPS. The measured χ values for the blends are of the same order of magnitude as those obtained for pure PPS, but they appear in the plot at a higher temperature range due to the higher crystallisation temperature of the blends.

The Avrami exponent, n , was obtained from the slope of the Ozawa plots. The Avrami exponents so obtained are plotted against temperature in *Figure 3.14*. PPS gives a value of three, suggesting that the nucleated process leads to a spherulitic growth with thermal nucleation.³⁰⁻³² In case of PPS/PET-OB blend systems, however, the Avrami exponent decreases as the temperature decreases, particularly at low temperatures. This clearly indicates that the nucleated process leads to rod-shaped growth with thermal nucleation.³¹ Hong et al. reported²⁰ similar results for PPS/Vectra B950 blends. Two factors may lower the value of Avrami exponent, n : (1) fast crystallisation rate of the blend systems at lower temperatures prevents the spherulite from developing into 3-dimensional crystallites²⁵; (2) Growth site impingement, truncation of spherulites, impurity segregation, and slightly slow secondary crystallisation^{3, 24, 32-35} may change the crystallisation mechanism if the crystalline weight fraction exceeds 0.5.

However at higher crystallisation temperatures, e.g., 246-247 °C, the Avrami exponent approximates to 3 because the predetermined nuclei grows into 3-dimensional spherulites before being cooled.³⁶ This indicates that the type of nucleation and the geometry of crystal growth markedly changes in presence of PET-OB. The deviation of Avrami exponent n could be attributed to factors such as time-dependent nucleation, variant growth rate constant as well as combination of homogeneous and heterogeneous nucleation. However, in general, it is difficult to elucidate the growth geometry and the nucleation type solely from the n value. On the basis of Mandelkern's analysis³ the crystallisation of PPS may involve homogeneous nucleation whereas in the blends it may be heterogeneous nucleation with two directional diffusion controlled growths.

3.4 CONCLUSION

The crystallisation kinetics of neat poly(phenylene sulphide) (PPS) and PPS in blends with PET-OB was studied by means of differential scanning calorimetry. The non-isothermal crystallisation studies showed that the theory of Ozawa is a suitable method for PPS crystallisation. The value of Avrami exponent n was found to have temperature dependence. The observed deviations in the value of n obtained in above kinetic studies were attributed to factors such as time-dependent nucleation, variant growth rate constant and a combination of homogeneous and heterogeneous nucleations. The PPS crystallisation temperature was found to increase markedly upon addition of 3-30% PET-OB. A notable reduction in Avrami exponent for the PPS/PET-OB blend system suggests that the nucleated process leads to rod-shaped growth with thermal nucleation. The cooling crystallisation function, which represents the rate of non-

isothermal crystallisation, decreases with lowering of temperature or increase in PET-OB content.

3.5 REFERENCES

- 1 T.G. Gopakumar, R.S. Ghadage, S. Ponrathnam, C.R. Rajan and P. Sini. "Thermal and crystallisation behavior of poly(phenylene sulphide)" in D. Joseph Francis, K.E. George and S.K. Narayanankutty, Eds., *Advances in Polymer Technology*, Allied Publishers, New Delhi, p.151 (1996).
- 2 T.G. Gopakumar, R.S. Ghadage, S. Ponrathnam, C.R. Rajan and A. Fradet, *Polymer*, **38**, 1997, 2209.
- 3 L. Mandelkern, *Crystallization of Polymers*, McGraw-Hill Book Company, New York (1964).
- 4 L.C. Lopez and G.L. Wilkes, *Polymer*, **29**, 1988, 106.
- 5 V.M. Nadkarni and J.P. Jog, *J. Appl. Polym. Sci.*, **30**, 1985, 997.
- 6 G.P. Desio and L. Rebenfeld, *J. Appl. Polym. Sci.*, **39**, 1990, 825.
- 7 S.S. Song., L.J. White and M. Cakmak, *Polym. Eng. Sci.*, **30**, 1990, 994.
- 8 V.M. Nadkarni, V.L. Shingankuli and J.P. Jog, *Intern. Polym. Proc.*, **2**, 1987, 53.
- 9 V.L. Shingankuli, J.P. Jog and V.M. Nadkarni, *J. Appl. Polym. Sci.*, **36**, 1988, 335.
- 10 L.I. Minkova and P.L. Magagnini, *Polymer*, **36**, 1995, 2059.
- 11 T. Ozawa, *Polymer*, **12**, 1971, 150.
- 12 G. Kiss, *Polym. Eng. Sci.*, **27**, 1987, 410.
- 13 A. Kolhi, N. Chung and R.A. Weiss, *Polym. Eng. Sci.*, **29**, 1989, 573.
- 14 M. Kimura, R.S. Porter and G. Salee, *J. Polym. Sci., Polym. Phys.*, **21**, 1983, 367.
- 15 E.G. Joseph, G.L. Wilkes and D.G. Baird, in A. Blumstein, Ed., *Polymer Liquid Crystals*, Plenum Press, New York (1984).
- 16 S.K. Bhattacharya, A. Tandolkar and A. Misra, *Molec. Cryst., Liq. Cryst.*, **153**, 1987, 501.

- 17 M. Paci, C. Barone and P.L. Magagnini, *J. Polym. Sci., Polym. Phys.*, **25**, 1987, 1595.
- 18 M. Pracella, E. Chielini and D. Dainelli, *Makromol. Chem.*, **190**, 1989, 175.
- 19 L.I. Minkova, M. Paci, M. Pracella and P.L. Magagnini, *Polym. Eng. Sci.*, **32**, 1992, 57.
- 20 S.M. Hong, B.C. Kim, K.U. Kim and I.J. Chung, *Polym. J.*, **24**, 1992, 727.
- 21 J. Mathew, R.V. Bahulekar, R.S. Ghadage, C.R. Rajan, S. Ponrathnam and S.D. Prasad, *Macromolecules*, **27**, 1994, 4021.
- 22 B. Wunderlich, *Macromolecular Physics: Crystal melting and nucleation*, Vol. 1, Academic Press, New York (1973).
- 23 M.J. Avrami, *Chem. Phys.*, **7**, 1941, 1103.
- 24 C.N. Velsaris and J.C. Seferis, *Polym. Eng. Sci.*, **26**, 1986, 1574.
- 25 L.C. Lopez and G.L. Wilkes, *Polymer*, **30**, 1989, 882.
- 26 M. Elder and A. Wlochowicz, *Polymer*, **24**, 1983, 1593.
- 27 L.I. Minkova, S. De Petris, M. Pracella, P.L. Magagnini, "Characterisation of blends of poly(phenylene sulphide) with a liquid crystalline copolyesteramide" in D. Acierno, F.P. La Mantia, Eds., "Processing and Properties of Liquid Crystalline Polymers and LCP Based Blends", ChemTec Publishing, Canada, 153 (1993).
- 28 E. Maemura, M. Cakmak and L.J. White, *Intern. Polym. Proc.*, **3**, 1990, 79.
- 29 W. Kozolowski, *J. Polym. Sci., C*, **38**, 1970, 47.
- 30 M. Day, T. Suprunchuk, J.D. Cooney and D.M. Wiles, *J. Appl. Polym. Sci.*, **36**, 1988, 1097.
- 31 Y. Deslandes, M. Dat, N.F. Sabir and T. Suprunchuk, *Polym. Composites*, **10**, 1989, 360.
- 32 S. Kumar, D.P. Anderson and W.W. Adams, *Polymer*, **27**, 1986, 329.
- 33 P. Cebe and S.D. Hong, *Polymer*, **27**, 1986, 1183.

- 34 M.C. Tobin, *J. Polym. Sci., Polym. Phys.*, **14**, 1976, 2253.
- 35 S.P. Kim and S.C. Kim, *Polym. Eng. Sci.*, **31**, 1990, 110.
- 36 S.A. Jabarin, *J. Appl. Polym. Sci.*, **34**, 1987, 85.

CHAPTER 4

SYNTHESIS OF
COMPATIBILISER¹ AND
COMPATIBILISATION OF
PPS/PET-OB BLENDS²

ABSTRACT

In this chapter the synthesis and characterisation of a compatibiliser for poly(phenylene sulphide) (PPS)/poly(ethylene terephthalate-co-oxybenzoate) (PET/OB) blend system is presented. The block copolymers synthesised by melt-transesterification of dicarboxyl terminated (PPS) with PET/OB, a semi-aromatic thermotropic liquid crystalline polymer (TLCP), were characterised using Fourier transform infra-red spectroscopy (FTIR), differential scanning calorimetry (DSC), x-ray diffraction (XRD) and polarised light optical microscopy (PLOM). The effect of factors such as mole percent of oxybenzoate, weight percent of PPS to PET/OB content and melt-transesterification time at 300 °C on the thermotropic character and crystallisability of the copolymers were also investigated. The crystallisability and thermotropic character were observed to depend on the extent of interchange reactions between the respective segments, which in turn, are dictated by the composition of PET-OB and the transesterification time. The thermotropic character and crystallisability of the copolymers were significantly influenced by factors such as mole percent of oxybenzoate, weight percent of PPS to PET/OB content and melt-transesterification time (at 300 °C) etc. The efficiency of this copolymer to compatibilise PPS/PET-OB blends was tested. While compatibilised blends appeared monophasic, uncompatibilised blends were seen to be clearly phase separated. The uncompatibilised blends showed macrophase-separated-morphology indicating poor phase mixing whereas the compatibilised blends of the same composition exhibited a disperse type morphology, as observed by PLOM.

4.1 INTRODUCTION

Blending conventional thermoplastic polymers with thermotropic liquid crystalline polymers (TLCPs) can lead to easier processing and *in situ* matrix reinforcement.³⁻¹² The properties of blends are strongly influenced by the morphology as a consequence of incompatibility and phase separation.¹³ The addition of block or graft copolymers represents the most researched approach to the compatibilisation of blends.⁵ Daccord and Sillion¹⁴ reported the preparation of block copolymers of PPS telechelics with other polymers. Heitz et al^{15,16} reported block copolymers of carboxyl terminated telechelic PPS with polyamides and polyesters.

An ideal fibril-reinforced microcomposite based on thermoplastics (TP)/thermotropic liquid crystalline polymer (TLCP) blend should comprise of a TP matrix and longer and finer TLCP fibrils (with high aspect ratio) with good interfacial adhesion between the two.¹⁷ The phase stabilisation of PPS blends with TLCPs can be improved by using compatibilisers. However, recent studies^{9-11,18-20} have shown that most of the compatibilised TP/TLCP blends tend to hinder TLCP fibril formation, due to lower interfacial tension and finer dispersed phase domains, even though enhanced interfacial adhesion is obtained. The compatibilisation must not cause the loss of fibrous morphology.

In this Chapter, the synthesis and characterisation of block copolymers of dicarboxyl terminated poly(phenylene sulphide) (DCTPPS) and poly(ethylene terephthalate-co-oxybenzoate) (PET/OB), a semi-aromatic thermotropic liquid crystalline

polymer, are discussed. The compatibilising efficiency of these block copolymers for PPS/PET-OB blend system was evaluated. Thermal analysis by differential scanning calorimetry (DSC) was employed to compare the melting and crystallisation behaviour of the uncompatibilised and compatibilised blends. The influence of compatibilisation on the phase behaviour were investigated with polarised light optical microscopy (PLOM) and scanning electron microscopy (SEM).

4.2 EXPERIMENTAL

4.2.1 Materials

PPS used was a commercial grade Ryton V-1 manufactured by Phillips Petroleum Company, U.S.A. The 4-chlorobenzoic acid, sodium sulphide and N-methyl pyrrolidinone procured from commercial source were used after purification. This material showed a melting point of 282 °C and the ΔH was 43.2 J/g. The aliphatic-aromatic thermotropic liquid crystalline polymer (TLCP) was synthesised and characterised as described in **Section 2.2.1**.

Dicarboxyl terminated poly(phenylene sulphide) (DCTPPS) of varying statistically average chain length ($n = 6, 9$ and 12) and poly(ethylene terephthalate-co-oxybenzoate) (PET-OB), an aliphatic-aromatic thermotropic liquid crystalline polymer (TLCP) with oxybenzoate content 30, 45 and 60 mole percent, were synthesised by established procedures.^{16,21} Block copolymers of DCTPPS and PET-OB (75/25, 50/50, 25/75 wt./wt.%) were synthesised by melt-transesterification at 300 °C under reduced nitrogen pressure for varied times in the range of 60, 90, 120 and 180 minutes. A 80 mL

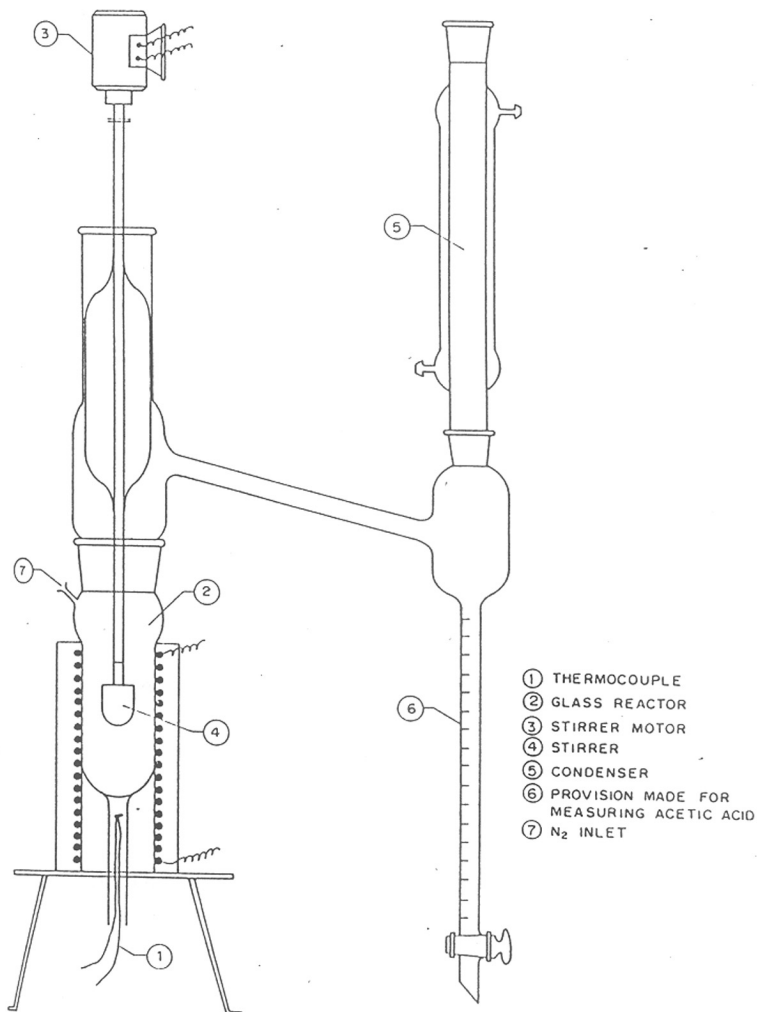


Figure 4.1 Laboratory scale reaction set-up for the synthesis of PPS-PET/OB block copolymer.

glass lined electrically heated reactor depicted in *Figure 4.1* was used for polymer synthesis. The reactor had two parts for charging/stirring the reactants and for nitrogen purging. It could be maintained isothermally at any temperature between ambient temperature and 400 °C. A provision for measuring the side product was made as shown in *Figure 4.1*.

4.2.2 Measurements

IR spectra of PPS-PET/OB block copolymers were recorded on a *Perkin Elmer 16 PC* FTIR spectrometer using potassium bromide discs. Thermal transitions in copolymers were estimated with a *Mettler DSC 30* differential scanning calorimeter under nitrogen atmosphere using sample weight of 6.0 ± 0.1 mg. Samples were analysed in the temperature range of 30-350 °C in both heating and cooling cycles at a rate of 20 °C/minute. Melting transition temperatures determined from the peak maxima and the enthalpy changes (ΔH) corresponding to heating and cooling were calculated from the area under the peak of the DSC thermogram. Instrument calibrations made were as described in **Section 2.2.3**. The block copolymers were observed by a hot stage coupled *Leitz* microscope under crossed polarisers in the temperature range over which transitions were observed by DSC. X-ray diffraction study of copolymer samples were performed with *Philips PW 1730* X-ray diffractometer using Cu $K\alpha$ -radiation.

4.2.3 Preparation of Blends

Powders of the PET-OB and PPS were dried at 130 °C under vacuum for 48 h prior to mixing. The uncompatibilised and compatibilised PPS/PET-OB blends with a PET-OB content in the range 10, 20, 30, 50, 75 and 90 % (wt./wt.) were prepared in a 30 ml mixer attached to a Brabender Plasticorder at 300 °C and 100 rpm for 5 minutes under nitrogen atmosphere. The amount of compatibiliser fixed to 10 wt.% with respect to PET-OB concentration. Blank samples of both PPS and PET-OB were subjected to the same treatment.

4.2.4 Polarised light optical microscopy

The phase behaviour of compatibilised and uncompatibilised PPS/PET-OB blends was investigated by a hot stage coupled *Leitz* microscope under crossed polarisers by the procedure described in **Section 2.2.4**.

4.2.5 Scanning electron microscopy

Morphology of the blend surfaces were studied using a *Leica Stereoscan 440* scanning electron microscope as discussed in **Section 2.2.5**.

4.3 RESULTS AND DISCUSSION

Dicarboxyl terminated poly(phenylene sulphide) (DCTPPS) of varied statistically average degree of polymerisation were synthesised by reacting 4-chloro benzoic acid, 1,4-dichloro benzene and sodium sulphide (Na_2S) in N-methyl-2-pyrrolidone (NMP) at 250 °C in a Parr reactor.^{15,16} The mole ratio of 4-chloro benzoic acid : 1,4-dichloro

benzene was varied to prepare dicarboxyl terminated PPS telechelics of varied chain length ($n=6, 9, 12$) (*Scheme 1*). While the empirical formula of the telechelics are supported by the elemental analysis, the actual block length within the given system would indeed be a varied one, with an average corresponding to that dictated by the 4-chloro benzoic acid:1,4-dichloro benzene mole ratio. The melting transition occurs at 280 °C.

The PET/OB copolymers were synthesised from virgin fibre grade poly(ethylene terephthalate) (PET, intrinsic viscosity = 0.6 dL/g) and 4-acetoxy benzoic acid at 275 °C, first at atmospheric pressure and later at 0.5 Torr till the removal of final traces of acetic acid. Three random copolymers of PET:OB 70:30, 55:45 and 40:60 were synthesised. The intrinsic viscosity in 60/40 (v/v) phenol/1,1,2,2-tetrachloro ethane ranged from 0.33 for 70:30 to 0.65 dL/g for 40:60 PET:OB. The generalised structure of this random copolymer is presented in *Scheme 1*. The liquid crystalline transition of PET/OB is around 200 °C and glass transition temperature is around 70 °C.

The PPS-PET/OB block copolymers were synthesised by uncatalysed melt-transesterification between DCTPPS and PET/OB at 300 °C. The composition of DCTPPS, PET/OB as well as the weight ratio of DCTPPS and PET/OB were all varied to synthesise a rich variety of block copolymers. In addition, a definite weight ratio of PPS : PET/OB, from DCTPPS of a specific chain length and PET/OB of a particular composition, was allowed to react for varied times at 300 °C to alter the PET/OB sequence as well as its block length.

The PPS-PET/OB copolymers were suspended in 60:40 (v/v) phenol : 1,1,2,2-tetrachloro ethane mixture under stirring for 24 hours at room temperature. PET/OB is soluble in this solvent system at a concentration of 0.5 gm/dL. The insolubles were filtered off and the filtrate was poured into a number of solvents like methanol in which PET/OB is insoluble. No precipitation was observed indicating the absence of unreacted PET/OB in the final product. This indicates of the formation of PPS-PET/OB copolymer. IR spectra of PPS-PET/OB copolymer exhibited the characteristic aliphatic and aromatic ester C=O stretching occurring at 1718 and 1738 cm^{-1} respectively and the sulphur linkage (-S-) at 814 cm^{-1} . A typical polarised light optical microscope photograph at 300 °C of 50/50 wt./wt.% PPS-PET/OB block copolymer from 55/45 mole ratio PET/OB is shown in *Figure 4.2*. The dark domains correspond to isotropic PPS rich phase while an anisotropic PET/OB rich phase was observed in the form of a thread-like texture. This observation further supports the formation of block copolymer comprising PPS blocks and PET/OB blocks. Similar morphology has been observed for segmented block copolymers with crystallisable hard segments and amorphous soft segments. Wilkes and coworkers²³ studied microstructure of various copolymers comprising crystallisable hard segments and non-crystallisable soft segments and observed copolymer exists as phase separated.

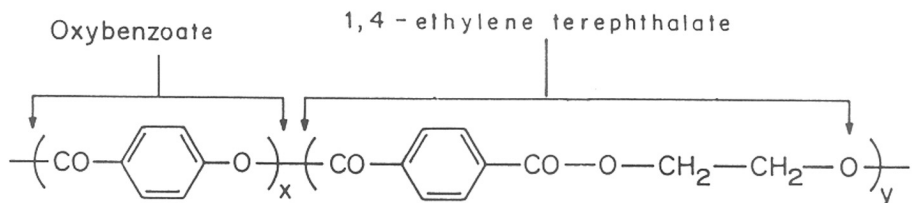
4.3.1 Effect of oxybenzoate (OB) content

The liquid crystallinity as well as liquid crystalline transition of PET/OB segment is sensitive to the mole % of OB. At OB content ≤ 28 mole %, the mesogenic unit, carboxy-

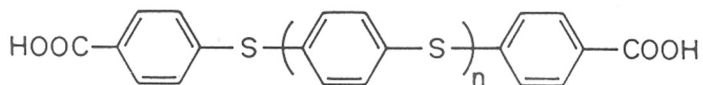
1,4-phenylene oxy carboxy-1,4-phenylene carboxy, is diluted at the expense of increasing concentration of PET and the thermotropic character disappears. Above 50 mole % of OB the average mesogen length increases while the flexible spacer remains unchanged

Scheme 1

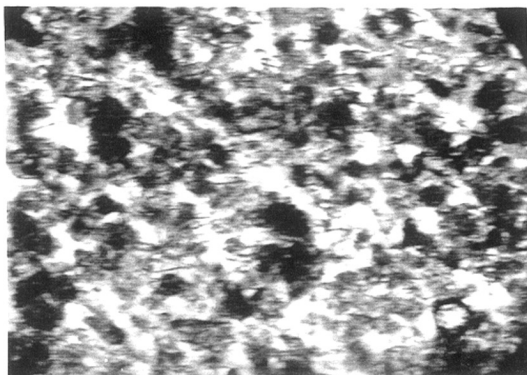
SCHEME I



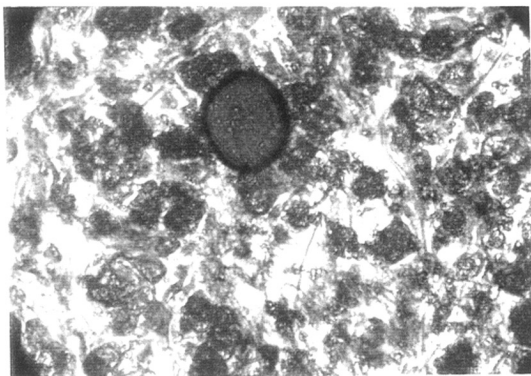
DiCarboxyl terminated polyphenylene sulfide (DCTPPS)



where $\bar{n}=6,9,12$

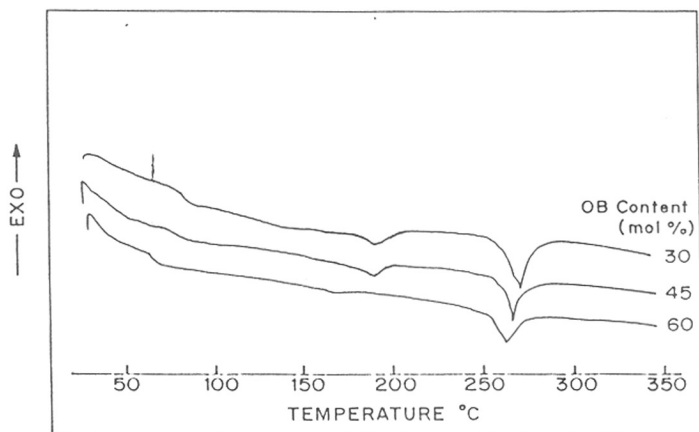


(a)

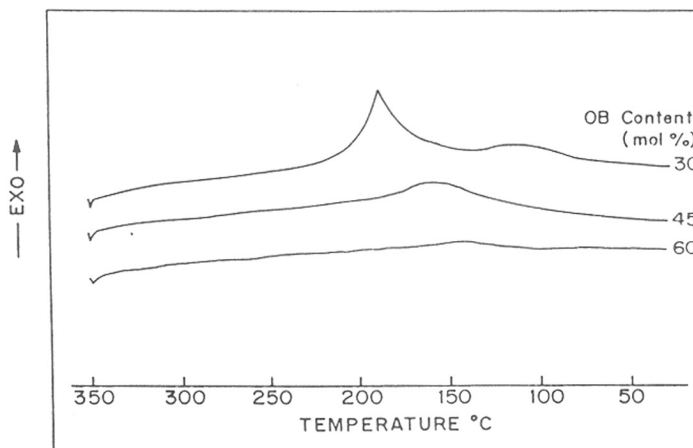


(b)

Figure 4.2 Typical optical micrograph of 50/50 (wt./wt.%) PPS-PET/OB (containing 45 mole % OB) block copolymer.



(a)



(b)

Figure 4.3 DSC thermograms (second heating) showing the effect of oxybenzoate content (with respect to the PET content) on the thermal behaviour of block copolymer; (a) Heating scans; (b) Cooling scans.

and consists of dimethylene units arising from 1,2-ethanediol. Above 60 mole % of OB non-melting oxybenzoate blocks are formed and thermotropic character disappears. This study has been restricted to 30-60 mole % of OB.

The DSC thermograms corresponding to heating and cooling scans of typical 50:50 (wt./wt.%) PPS:PET/OB with 30, 45 and 60 mole % OB (with respect to PET) are shown in *Figure 4.3(a) and (b)*. The thermal properties tabulated in *Table 4.1*.

The T_g , ascribable to PET/OB in PPS-PET/OB block copolymer, decreases marginally with increase in OB content. This decrease in glass transition temperature of PET/OB (T_g of PET is 80 °C) with OB mole % has been attributed to an enhanced randomisation which increases the segmental mobility within PET/OB.¹⁷ The nematic

Table 4.1: Effect of oxybenzoate content on the thermal behaviour of PPS-PET/OB block copolymer

OB content. mole %	T_g °C	T_m °C	L.C.transition °C	ΔH_m J/gm	T_c °C	ΔH_c J/gm
30	71	272	194	23.4	198	22.5
45	69	268	192	25.3	179	19.8
60	65	271	191	27.1	159	17.3

T_g: glass transition temperature, *T_m*: melting transition temperature, *L.C.transition*: liquid crystalline transition, ΔH_m : heat of fusion (normalised to weight fraction of DCTPPS), *T_c*: crystallisation temperature, ΔH_c : heat of crystallisation

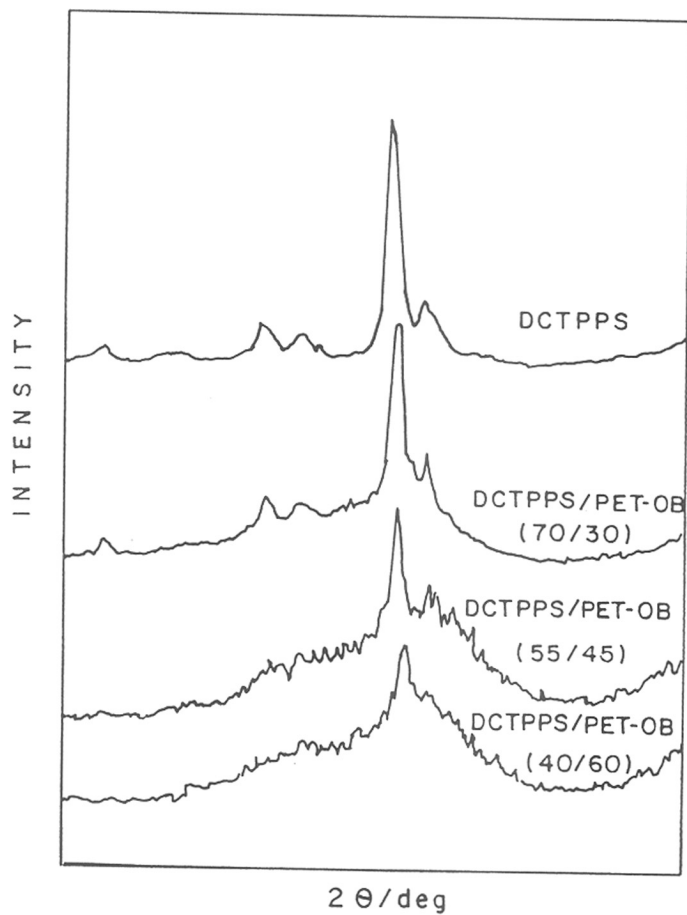


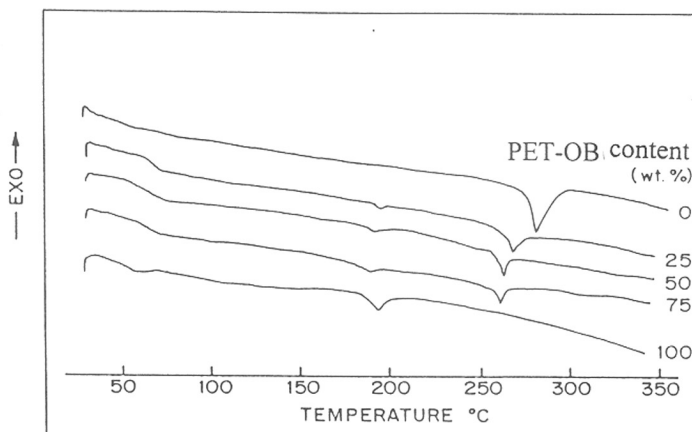
Figure 4.4 X-ray diffraction profiles of 50/50 wt./wt.% PPS-PET/OB block copolymer.

liquid crystalline transition ascribable to PET/OB occurs approximately at 193 °C. The endotherm at 270 °C in *Figure 4.3 (a)* corresponds to melting of PPS. This points to a microphase separation between the two blocks.

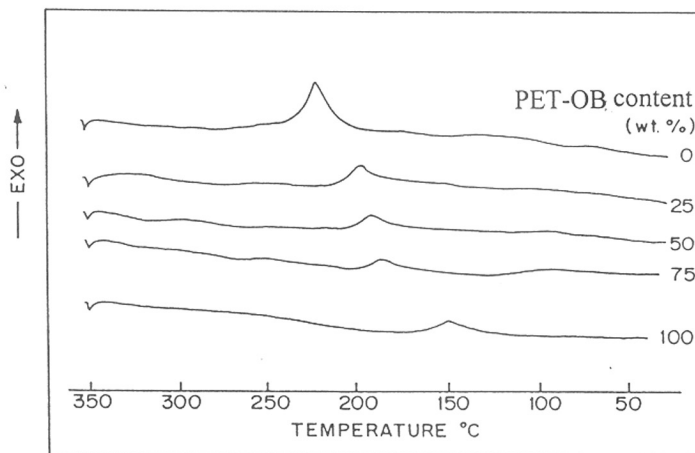
The heat of crystallisation (obtained by integration of exothermic peak corresponding to the crystallisation of PPS segments in the copolymer) reduced with an increase in OB content as observed in *Figure 4.3(b)* and *Table 4.1*. When the OB content attains 60 mole %, the crystallisation peak of PPS segments disappears indicating that the crystallisation of PPS blocks is hindered perhaps due to an interaction between PPS blocks and PET/OB segments in PPS-PET/OB copolymer. The non-melting OB blocks decrease the mobility of crystallisable PPS chains and thereby inhibit their crystallisation. These findings are supported by x-ray powder diffraction studies shown in *Figure 4.4*. Here, the peak height and the area under the peak corresponding to the PPS blocks are seen to reduce with increase in oxybenzoate content indicating a reduction in the crystallinity of PPS segments.

4.3.2 Dependence of DCTPPS:PET/OB composition

The DSC thermograms corresponding to heating and cooling scans of PPS-PET/OB copolymers with 0, 25, 50 and 75 wt.% PET/OB content (OB content fixed at 45 mole %) are shown in *Figure 4.5 (a) and (b)* and thermal properties are compiled in *Table 4.2*.



(a)



(b)

Figure 4.5 DSC thermograms (second heating) showing the effect of PET-OB content on the thermal behaviour of 50/50 wt./wt.% PPS-PET/OB block copolymer: (a) Heating scans; (b) Cooling scans.

Table 4.2: Effect of TLCP content on the thermal behaviour of PPS blocks in copolymer

TLCP content wt. %	Tg °C	Tm °C	L.C.transi tion °C	ΔH_m J/gm	Tc °C	ΔH_c J/gm	$\alpha_{c,PPS}$
0	68	279	-	35.6	222	33.1	0.24
25	72	272	192	24.4	201	22.4	0.16
50	71	267	191	22.1	198	17.4	0.15
75	69	265	192	18.7	193	15.7	0.12

TG: glass transition temperature, Tmb: melting transition temperature, L.C.transition: liquid crystalline transition, ΔH_m : heat of fusion (normalised to weight fraction of DCTPPS), Tc: crystallisation temperature, ΔH_c : heat of crystallisation, $\alpha_{c,PPS}$: degree of crystallinity.

The copolymerisation alters the melting behaviour of both PPS and PET/OB in PPS-PET/OB block copolymer. The intensity of liquid crystalline transition peak is enhanced at higher PET/OB concentration while the melting transition temperature and the corresponding enthalpy values of PPS blocks (normalised to the weight fraction of PPS) are depressed. The existence of distinct endothermic peaks corresponding to the PPS and PET/OB in the DSC thermograms [Figure 4.5 (a)] points to a microphase separation between the PPS and PET/OB in the PPS-PET/OB block copolymer. This observation is further supported by optical microscopy. The intensity of crystal-nematic

transition peak of copolymer reduces with PPS content, as shown in *Figure 4.5 (a)* and *Table 4.2*, as a direct consequence of loss of rigid and axially symmetrical configuration (mesogen) of the copolymer. No glass transition temperature (T_g) corresponding to DCTPPS and PPS blocks in the PPS-PET/OB block copolymer were observable. However, the T_g of PET/OB was found to increase on copolymerisation with DCTPPS perhaps due to an antiplasticising effect of crystallisable PPS blocks on the amorphous phase of PET/OB as observed in block copolymers of PET/OB with polysulphones.²⁴

The degree of crystallinity relative to PPS ($\alpha_{c,PPS}$) segments in PPS-PET/OB was estimated from the heat of fusion (ΔH) determined by DSC according to the following equation:

$$\alpha_{c,PPS} = \Delta H / \Delta H^0_m$$

where ΔH^0_m is the heat of fusion of 100% crystalline PPS, $\Delta H^0_m = 146 \text{ J/g}$.²⁵ $\alpha_{c,PPS}$, the degree of crystallinity of PPS segment in PPS-PET/OB copolymer with 25, 50, 75 wt.% PET/OB were 0.16, 0.15, 0.12 while that of the pure DCTPPS was 0.24 (*Table 4.2*).

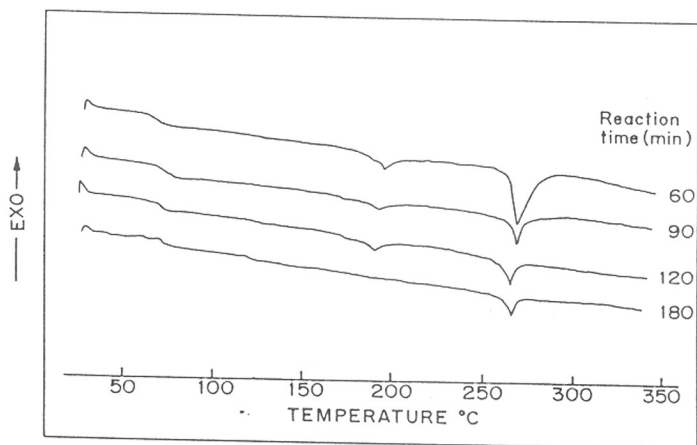
The crystallisation temperature (T_c) of PPS segments in PPS-PET/OB copolymer was found to decrease with an increase in PET/OB content as shown in *Table 4.2*. The PPS segment in PPS-PET/OB copolymer with 25 wt. % PET/OB content crystallises at 201 °C while the DCTPPS crystallises at 222 °C. On copolymerisation, the crystallisability of PPS segments are depressed, probably by the inhibition of the regular chain packing desirable for crystallisation by the introduction of PET/OB through extensive interchange reactions. Heitz and coworkers¹³⁻¹⁵ discussed similar reduction in

the crystallisability of PPS blocks in block copolymers of PPS with polyamides polyesters. The PET/OB segments act as diluent for the crystalline PPS blocks.

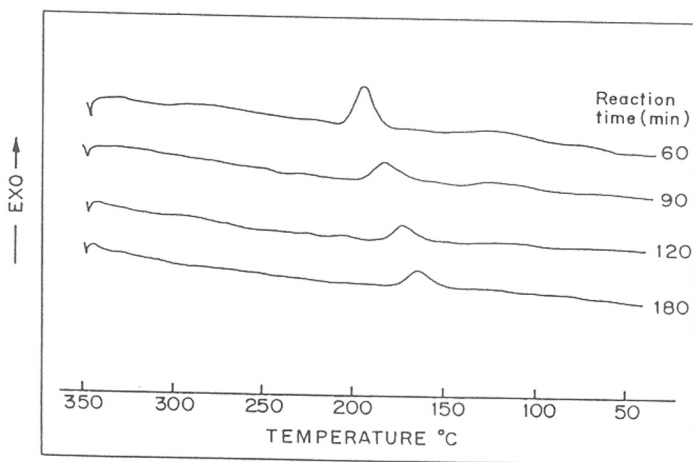
4.3.3 Effect of reaction time

The DSC thermograms corresponding to heating and cooling scans of copolymers (50 wt.% PET/OB composed of 45 mole % OB) synthesised by varying reaction times, 60, 90, 120 and 180 minutes are shown in *Figure 4.6(a) and (b)* and the thermal properties are presented in *Table 4.3*. The longer reaction times would lead to a more randomised PET/OB sequences due to transesterification reactions.

At longer reaction times (120 or 180 minutes), the liquid crystalline transition of the PET/OB segment in copolymer is seen to disappear. This could be explained as follows: At the beginning of reaction (0-15 minutes) acetic acid distills out indicating that DCTPPS preferably reacts with the acetoxy end groups of PET/OB. This leads to the formation of an AB type block copolymer since starting PET/OB is monofunctional in acetoxy end groups. Therefore, PET/OB block retains its initial sequence and hence its liquid crystalline properties. At longer reaction times, interchange reactions occur between terephthaloyl and DCTPPS units which slice PET/OB block and incorporate PPS segments. This slicing lowers the axial ratio and the chain no longer possesses the structure needed to exhibit liquid crystallinity.



(a)



(b)

Figure 4.6 DSC thermograms (second heating) showing the effect reaction time content on the thermal behaviour of 50/50 wt./wt.% PPS-PET/OB block copolymer. (a) Heating scans; (b) Cooling scans.

Table 4.3: Effect of reaction time on the thermal behaviour of copolyester

Reaction time, minutes	T _g	T _m	L.C. transition	ΔH _m	T _c	ΔH _c
60	71	279	193	24.3	202	23.1
90	71	274	192	21.6	195	21.4
120	67	270	189	18.8	185	18.7
180	69	268	-	15.4	178	15.6

T_g: glass transition temperature; *T_m*: melting transition temperature; *L.C.transition*: liquid crystalline transition; *ΔH_m*: heat of fusion (normalised to weight fraction of DCTPPS); *T_c*: crystallisation temperature; *ΔH_c*: heat of crystallisation.

The thermograms corresponding to the cooling scan of the copolymers are presented in *Figure 4.6(b)*. The crystallisation temperature (*T_c*) and heat of crystallisation (*ΔH*) are seen to decrease with increasing transesterification time indicating extensive interchange reactions resulting in a random copolymer.

In conclusion, the liquid crystalline properties and the crystallisability of copolymer are greatly influenced by the extent of interchange reactions, the mole percent of oxybenzoate with respect to the PET, the PPS:PET/OB weight ratio and reaction time.

4.4 Comparison of Uncompatibilised and compatibilised PPS/PET-OB Blends

Compatibilisation can interact in complex ways to influence the final blend properties: (i) Reduce the interfacial tension in the melt causing an emulsification effect and resulting in an extremely fine dispersion of one phase in another; (ii) Increase the adhesion at phase boundaries giving improved stress transfer and (iii) Stabilise the dispersed phase against growth during annealing, modifying the phase boundary interface. Thus, it will be interesting to investigate the effect of compatibilisation of block copolymer comprising PPS blocks and PET-OB blocks on the thermal behaviour and phase morphology of the PPS/PET-OB blends.

4.4.1 Thermal properties

4.4.2 Melting behaviour

DSC heating thermograms of pure PPS, PET-OB, uncompatibilised PPS/PET-OB and compatibilised PPS/PET-OB blends were shown in *Figure 4.7*. In compatibilised blends, the endothermic peaks corresponding to the melting transition of PET-OB are absent whereas in melt-mixed blends the intensity of melting transition peak of PET-OB increases with its concentration. Phase separations in blends can be identified in DSC thermograms by the absence of any change in the glass transition temperature, melting transition temperature or enthalpy of transitions from those corresponding to the original polymer components.¹³ The absence of the endothermic peak corresponding to melting transition of PET-OB in the compatibilised PPS/PET-OB blends in *Figure 4.7* could be due to the absence of phase separation. The degree of

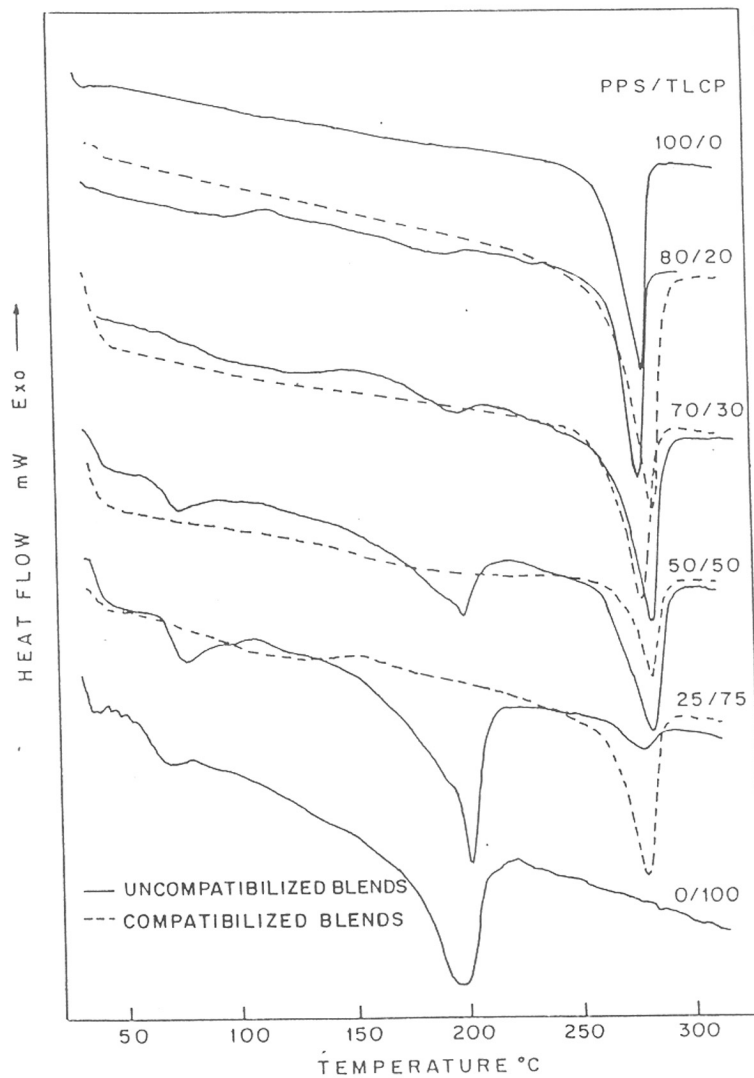


Figure 4.7 DSC thermograms (second heating) of uncompatibilised and compatibilised PPS/PET-OB blends at the heating rate 20 °C/minute.

Table. 4.4. Comparison of thermal data of PPS phase in uncompatibilised and compatibilised PPS/PET-OB Blends

PPS/PET-OB % (wt./wt.)	Uncompatibilised blends				Compatibilised blends (10% w.r.t. PET-OB content)			
	T _m °C	T _c °C	ΔH _f J/g	α	T _m °C	T _c °C	ΔH _f J/g	α
100/0	282	237	43.9	0.30	282	237	43.9	0.30
90/10	280	252	43.4	0.29	281	239	36.6	0.25
80/20	279	251	43.0	0.29	280	241	33.7	0.23
70/30	281	252	40.1	0.27	278	244	29.1	0.20
50/50	280	246	35.1	0.24	279	246	22.3	0.15
25/75	278	244	28.2	0.19	279	243	19.9	0.13
10/90	277	243	24.4	0.16	278	240	17.4	0.11

T_m: Melting peak temperature.
ΔH_f: Heat of Fusion.

T_c: Crystallisation peak temperature.
α: Degree of Crystallinity

interaction between two polymers is described by ΔG, comprising of ΔH and ΔS contributions. For a blend to be a single phase, ΔG<0. Since ΔS is negligible for polymers, ΔH dominates in the free energy of mixing in polymer blends. The introduction of interacting groups by chemical modification of a polymer or by

copolymerisation can result in a negative contribution to the enthalpy of mixing. The enthalpy of mixing (ΔH_{mixing}) of stiff rigid-rod like liquid crystalline segments with a flexible-coil polymer is mostly positive. From *Table 4.4*, it is very clear that the enthalpy of mixing (ΔH_{mixing}) of PPS/PET-OB blend decreases. This points to a favourable interaction between PPS and PET-OB chains on compatibilisation.

4.4.3 Crystallisation behaviour

The crystallisation exotherms of pure PPS, PET-OB, uncompatibilised and compatibilised PPS/PET-OB blends were shown in *Figure 4.8*. The crystallisation temperatures (T_c), presented in *Table 4.4*, were those corresponding to the exothermic peak maxima and are corrected as described by Elder and Wlochowicz.²² In compatibilised blends, the exothermic peaks corresponding to the PET-OB crystallisation are absent whereas in uncompatibilised blends the peak intensity of crystallisation exotherm of PET-OB increases with its concentration. Again, in compatibilised blends the crystallisation temperature (T_c) and hence the rate of crystallisation of PPS phase passes through a maximum corresponding to 30 mole % PET-OB. On the other hand, T_c and hence the rate of crystallisation of PPS phase in compatibilised blends slightly decreases with increase in PET-OB content as shown in *Table 4.4*. The dispersed PET-OB phase in compatibilised blends crystallises to form microphase not detectable by DSC where as in uncompatibilised blends the PPS and PET-OB crystallise into separate phases as shown in the DSC exotherm presented in *Figure 4.8*. The PET-OB phase accelerates

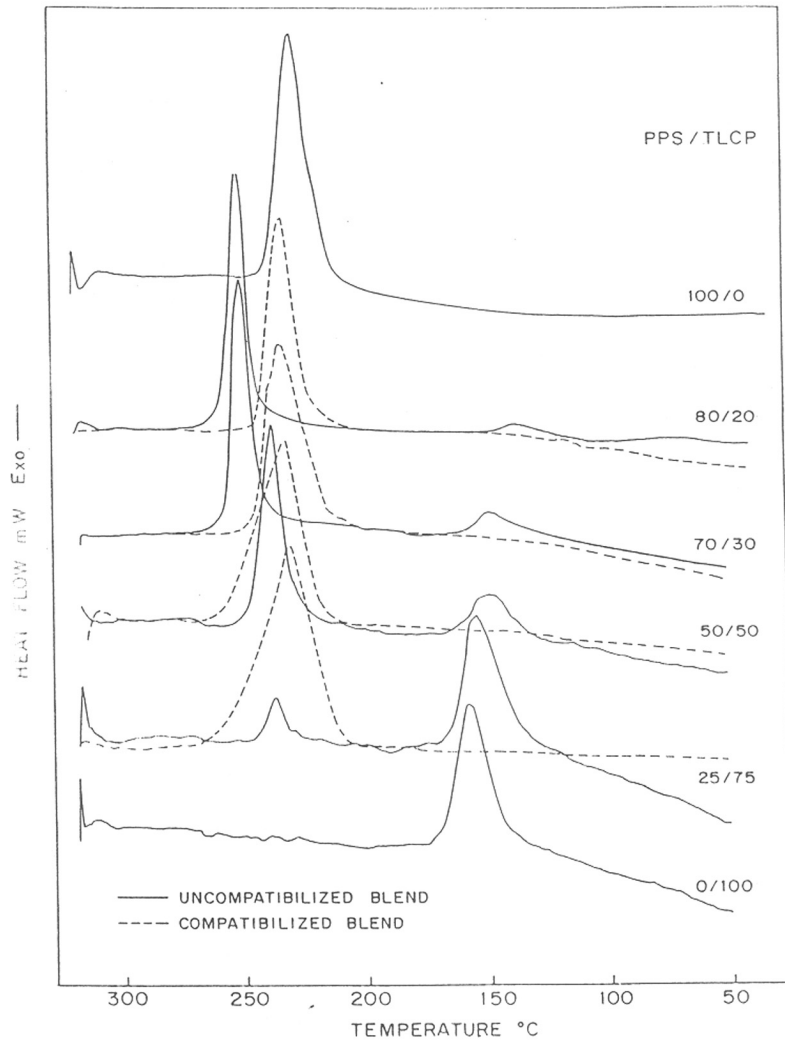


Figure 4.8 DSC exotherms (second cooling) of uncompatibilised and compatibilised PPS/PET-OB blends at the heating rate 20 °C/minute.

the crystallisation of PPS phase in uncompatibilised blends whereas it retards the rate of crystallisation of PPS phase in compatibilised blends. This may be due to the interference of copolymer in the crystallisation of PPS. Similar results of decrease of rate of crystallisation of blends on compatibilisation was reported in earlier studies.²⁶ Chang and coworkers²⁶ investigated the effect of reactive compatibilisation of NORYL [poly(phenylene oxide)/polystyrene]/Vectra A950 using styrene-glycidyl methacrylate (SG) as reactive component. They observed that the crystallisation rate of blend components were decreased by *in situ* formed block copolymer comprising of SG and Vectra A 950.

4.4.4 Degree of Crystallinity

The degree of crystallinity, α , of the PPS phase in both uncompatibilised and compatibilised blends plotted against the PET-OB content were presented in *Table 4.4*. The degree of crystallinity, α , was calculated from the enthalpy of fusion normalised to the PPS content, assuming that the contribution of the PET-OB phase is negligible.²⁷ A value of 146.2 J/g was estimated by Maemura et al²⁵ for enthalpy of fusion of 100% crystalline PPS. For uncompatibilised blends, the degree of crystallinity of PPS remains almost constant up to 30 wt.% PET-OB and then reduces with further increase in PET-OB content. In compatibilised blends, the degree of crystallinity steadily decreases with PET-OB concentration. This observation is consistent with previous reports of

crystallinities of compatibilised blends.²⁸⁻³² Chang and coworkers²⁹ investigated ethylglycidyl methacrylate copolymer (EGMA) as reactive compatibiliser for immiscible blends of polypropylene (PP) and Vectra A900 and observed that the crystallinity of PP phase in compatibilised blends was lower than that of the corresponding incompatibilised blends due to interference in the PP crystallisation by the *in situ* formed EGMA-g-Vectra A900 copolymers.

This marked difference in the degree of crystallinity is due the improved interfacial adhesion in compatibilised blends as compared to the uncompatibilised blends of similar composition. The addition of a second polymer to a semicrystalline polymer acts as a diluent, which could either decrease crystallinity by decreasing concentration and number of nuclei, or increases crystallinity by enhancing nucleation or increasing the chain mobility.²⁹ Degree of crystallinity, α , is known to be a measure of degree of phase mixing.^{11,13} The degree of crystallinity is known to decrease on compatibilisation of incompatible blends.³² Thus, the degree of crystallinity of PPS phase depends on the extent of phase separation between the PPS phase and PET-OB phase.

4.4.5 Morphology

4.4.5.1 Polarised light optical microscopy

The optical micrographs under cross polariser of uncompatibilised and compatibilised PPS/PET-OB blends (in molten state at 320 °C) are presented in *Figure 4.9 (a)-(d)*. At this temperature, the PET-OB domains alone are observable under cross

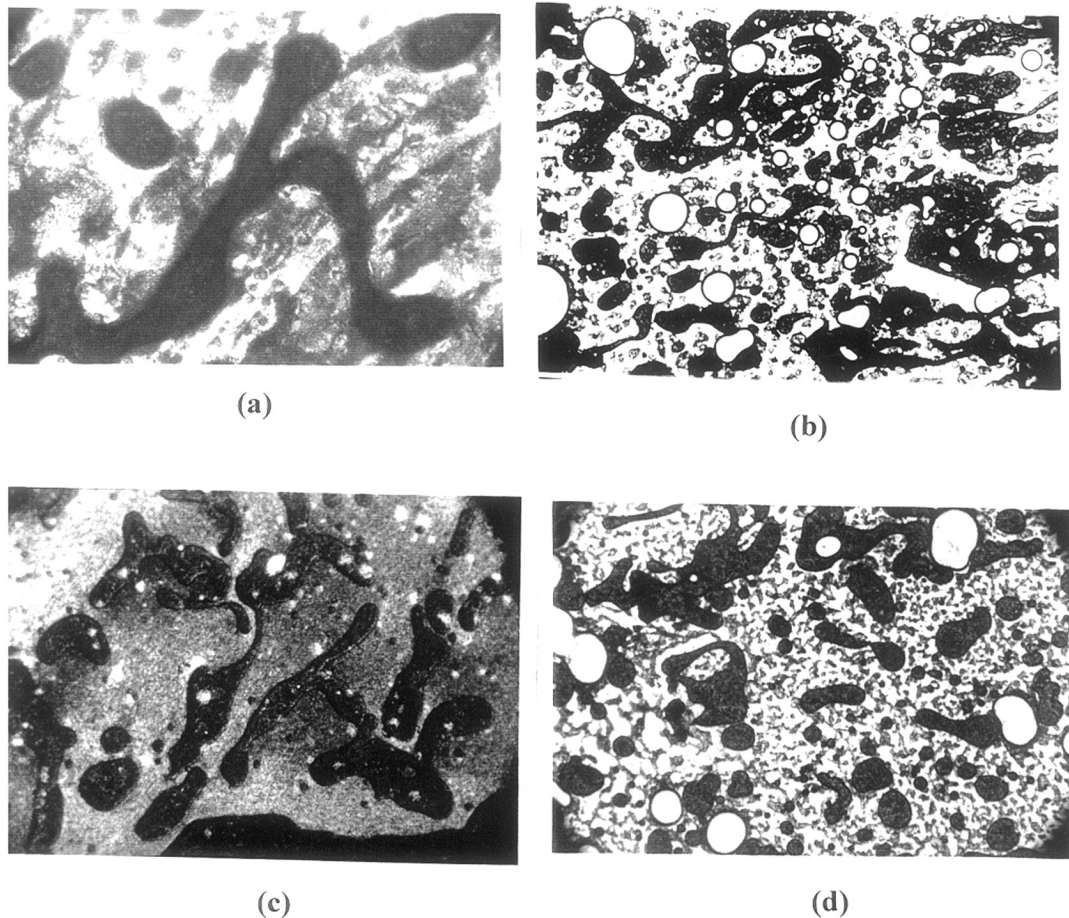
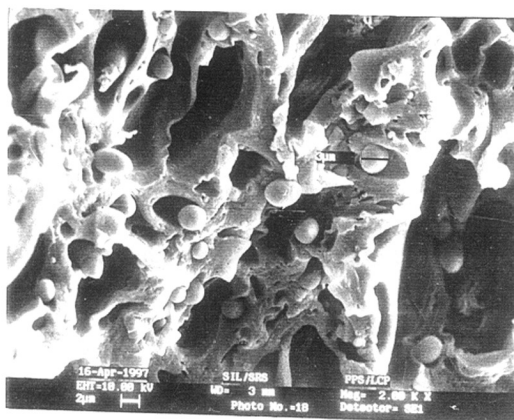


Figure 4.9 Optical micrographs (same magnification; 100 X) of the phase behaviour and morphology of uncompatibilised and compatibilised PPS/PET-OB [% wt./wt.] blends of differing compositions at 320 °C. (a) Pure PPS; (b) uncompatibilised 70/30; (d) uncompatibilised 50/50; (c) compatibilised 70/30 and (e) compatibilised 50/50 blends.

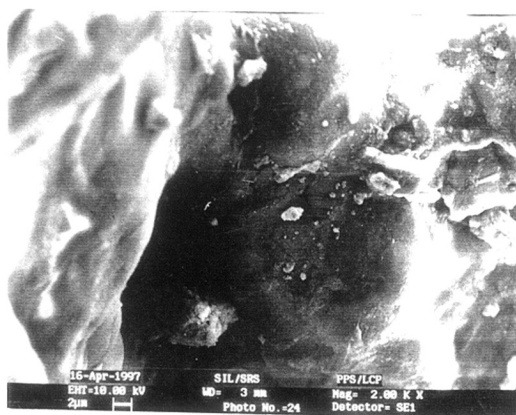
polarisers as these are in the anisotropic nematic state. The liquid-liquid phase separation is observable in both uncompatibilised and compatibilised PPS/PET-OB blends. A comparison can be made between uncompatibilised and compatibilised blends under identical conditions by observing the domain size of PET-OB in *Figure 4.9 (a) and (b)*. In compatibilised blends [*Figure 4.9 (a)*], the PET-OB domains are relatively smaller and are more uniformly dispersed within PPS matrix whereas in the uncompatibilised blends [*Figure 4.9 (b)*] a wide size distribution is noted due to distinctive phase separation and an aggregation of the PET-OB phase.

4.4.5.2 Scanning electron microscopy

The SEM micrographs uncompatibilised and compatibilised PPS/PET-OB blends are shown in *Figures 10 (a) and (b)*. The uncompatibilised blends show macrophase-separated-morphology as seen from *Figures 10 (a)* indicating poor phase mixing whereas in the compatibilised blends of the same composition [*Figures 10 (b)*] disperse type morphology was observed. The more uniform and continuous morphology of compatibilised blends is a consequence of intimate dispersion of PET-OB phase within the PPS matrix.



(a)



(b)

Figure 4.10 SEM micrographs showing morphology of freeze-fractured samples of uncompatibilised [(a) 90/10, (c) 70/30 & (e) 50/50 % (wt./wt.)] and compatibilised [(b) 90/10, (d) 70/30 & (f) 50/50 % (wt./wt.)] PPS/PET-OB blends

4.5 CONCLUSION

The thermotropic character and the crystallisability of the block copolymer, comprising poly(phenylene sulphide) and poly(ethylene terephthalate-oxy benzoate) blocks, were greatly influenced by the extent of interchange reactions, which in turn depends on the mole percent of oxybenzoate (with respect to the PET content), PET/OB content and reaction time.

The compatibilising efficiency of the block copolymer for poly (phenylene sulphide) and poly(ethylene terephthalate-co-oxybenzoate) (PET-OB), an aliphatic-aromatic thermotropic liquid crystalline polymer (TLCP), blend system was tested. Thermal properties, phase behaviour and morphology of uncompatibilised as well as compatibilised blends of PPS and PET-OB were compared using differential scanning calorimetry, polarised light optical microscopy and scanning electron microscopy. From these observations, we concluded: (i) PPS-PET/OB block copolymer is a suitable compatibiliser for PPS-PET/OB blend system; (ii) homogenisation of morphology occurs on compatibilisation; (iii) the PET-OB phase accelerates crystallisation of PPS phase in uncompatibilised blends whereas it retards crystallisation of PPS phase in compatibilised blends and (iv) the effect of PET-OB phase on crystallinity of PPS varied with extent of phase separation between the two components.

4.6 REFERENCES AND NOTES

- 1 T.G. Gopakumar, S. Ponrathnam, C.R. Rajan and A. Fradet, *Macromolecules*, Communicated.
- 2 T.G. Gopakumar, S. Ponrathnam, C.R. Rajan and A. Fradet, *Polymer* Communicated.
- 3 D. Acierno and F.P. La Mantia, Eds., *Processing and properties of Liquid crystalline polymers and LCP blends*, Chem Tech Publishing, Ontario, (1993).
- 4 F.P. La Mantia, Ed., *Thermotropic liquid crystalline polymer blends* Technomic Publishing Company. Inc., Pennsylvania 17604, (1993).
- 5 C.S. Brown and P.T. Alder, "Blends containing liquid crystalline polymers", in M.J. Folkes and P.S. Hope, Eds., *Polymer blends and alloys*, Ch. 8, Blackie Academic and Professional, London, 1993.
- 6 P.R. Subramaniam and A.I. Isayev, *Polymer*, **32**, 1991, 1961
- 7 G.O. Shonaike, S. Yamaguchi, M. Ohta, H. Hamada, Z. Maekawa, M. Nakamichi and W. Kosaka, *Eur. Polym. J.*, **30**, 1994, 413.
- 8 G. Gabellini, M.B. de Moraes and R.E.S. Bretas, *J. Appl. Polym. Sci.*, **60**, 1996, 21.
- 9 T.G. Gopakumar, R.S. Ghadage, C.R. Rajan, S. Ponrathnam and A. Fradet, *Polymer*, **38**, 1997, 2209.
- 10 T.G. Gopakumar, S. Ponrathnam, C.R. Rajan and A. Fradet, *Polymer J.* (in Press).
- 11 T.G. Gopakumar, S. Ponrathnam, C.R. Rajan and A. Fradet, *Polymer* (in Press).
- 12 T.G. Gopakumar, S. Ponrathnam, C.R. Rajan and A. Fradet, *J. Appl. Polym. Sci.*, (communicated).
- 13 O. Olabisi, L.M. Robeson and M.T. Shaw, *Polymer-Polymer Miscibility*, Academic Press, New York (1979).
- 14 G. Daccord and B. Sillion, *Polymer Bull.*, **6**, 1982, 477.
- 15 W. Heitz, *Makromol. Chem. Symp.*, **26**, 1987, 1.

- 16 L. Freund and W. Heitz, *Makromol. Chem.*, **191**, 1990, 815.
- 17 Y.P. Chiou, K.C. Chiou and F.C. Chang, *Polymer*, **37**, 1996, 4099.
- 18 D. Dutta, R.A. Weiss and J. He, *Polymer*, **37**, 1996, 435.
- 19 R.S. Porter and L.H. Wang, *Polymer*, **33**, 1992, 2019.
- 20 P. Chen, V. Sullivan, T. Dolce and M. Jaffe, *U. S. Patent, US 5,182,334*, **1993**, assigned to Hoechst Celanese Corp., Somerville, N.J.
- 21 J. Mathew, R.S. Ghadage, S. Ponrathnam and S.D. Prasad, *Macromolecules*, **27**, 1994, 4021.
- 22 M. Elder and A. Wlochowicz, *Polymer*, **24**, 1983, 1593.
- 23 S. Abouzahr and G.L. Wilkes, "Segmented copolymers with emphasis on segmented polyurethanes" in M.J. Folkes, Ed., *Processing, Structure and Properties of Block copolymers*, Elsevier Applied Science Publishers Ltd., New York, **1985**.
- 24 D. Pospiech, L. Haubler, H. Komber, D. Voigt, D. Jehnichen, A. Janke, A. Baier, K. Ekstein and F. Bohme, *J. Appl. Polym. Sci.*, **62**, 1996, 1819.
- 25 E. Maemura, M. Cakmak and L. White, *J. Intern. Polym. Proc.*, **3**, 1990, 79.
- 26 P.C. Lee, W.F. Kuo and F.C. Chang, *Polymer*, **37**, 1996, 5655.
- 27 L.I. Minkova, S. De Petris, M. Paci, M. Pracella and P.L. Magagnini, "Characterisation of blends of poly(phenylene sulphide) with thermotropic liquid crystalline copolyesteramide" in D. Acierno, and F.P. La Mantia, Eds., *Processing and Properties of Liquid Crystalline Polymers and LCP Based Blends*, ChemTec Publishing, Ontario, (1993); p.153.
- 28 T.G. Gopakumar, C.R. Rajan, S. Ponrathnam and A. Fradet, *Polymer*, (communicated).
- 29 Y.P. Chiou, K.C. Chiou and F.C. Chang, *Polymer*, **37**, 1996, 4099.
- 30 T.O. Ahn, S.C. Hang, H.M. Jeong and J.H. Kim, *Polymer*, **38**, 1997, 214.
- 31 J.L. Rodríguez, J.I. Eguiazabal and J. Nazabal, *Polym. J.*, **28**, 1996, 501.
- 32 L.I. Long, R.A. Shanks and Z.H. Stachurski, *Prog. Polym. Sci.*, **20**, 1995, 651.

CHAPTER 5

REACTIVE
COMPATIBILISATION OF
PPS/VECTRA A950 BLENDS^{1,2}

ABSTRACT

Reactive compatibilisation of immiscible poly(phenylene sulphide) (PPS)/Vectra A950 blends was attempted by *in situ* reactive extrusion of PPS and Vectra A950 in presence of dicarboxyl terminated poly(phenylene sulphide) (DCTPPS) in a twin screw extruder. The chemical reaction between DCTPPS and Vectra A950 during blending in Brabender Plasticorder was confirmed by the change in the torque and by the infra-red spectroscopic analysis of the product. The suitability of block copolymer formed during reactive blending as a compatibiliser was evaluated by studying the morphology, mechanical and thermal properties of the compatibilised PPS/Vectra A950 blends of widely varying compositions. The mechanical properties were found to improve, the crystallisation temperature and heat of crystallisation of PPS phase were observed to decrease marginally while morphology homogenised as a result of improvement in the interfacial adhesion between the two phases on compatibilisation.

5.1 INTRODUCTION

Specific improvement in properties of PPS on blending with wholly aromatic³⁻⁸ and semi-aromatic⁹⁻¹² thermotropic liquid crystalline polymers have been reported in the very recent past. Most blends of thermoplastics and TLCPs show poor interfacial adhesion resulting in inferior mechanical properties. In immiscible polymer blends the desired strong interfacial adhesion and stabilised morphology often require the presence of appropriate interfacial agents.

Recently, increasing efforts have been directed towards *in situ* compatibilisation of immiscible polymer blends by reactive extrusion.¹³⁻¹⁸ Instead of synthesising the compatibilisers in a separate step, these are created during extrusion through interfacial reactions between the respective functionalised polymers. From a technological point of view one step reactive extrusion process is easier to control for cost effective generation of compatible blends from initially immiscible polymers.¹⁸

This is the first report of *in situ* compatibilisation of PPS and Vectra A950, a wholly aromatic TLCP by reactive extrusion in presence of dicarboxyl terminated PPS (DCTPPS). The carboxyl end groups of PPS can undergo transesterification reaction with ester groups in the Vectra A950 in the molten state leading to the *in situ* formation of block copolymer comprising PPS blocks and Vectra A 950 blocks at the interface between the PPS/Vectra A950 blends during extrusion. The chemically identical PPS block is miscible with PPS matrix while the Vectra A950 block is compatible with Vectra A950 component. In this chapter the study of the compatibilising efficiency of this block

copolymer by the investigation of morphology, mechanical and thermal properties of the PPS/ Vectra A950 blends over a wide range of composition is reported.

5.2 EXPERIMENTAL

5.2.1 Materials

Poly(phenylene sulphide) (PPS) (unfilled grade Fortron 0220 A1) and Vectra A950 (unfilled grade) a wholly aromatic thermotropic liquid crystalline polymer (copolyester of 25 mole % of 2-hydroxy-6-naphthoic acid (HNA) and 75 mole % of 4-hydroxy benzoic acid (HBA) were supplied by Hoechst Celanese. Dicarboxyl terminated poly(phenylene sulphide) (DCTPPS) of varying statistically average block length ($n = 6, 9, 12$) were prepared by the procedure described in **Section 4.2.1**.

5.2.2 Methods

Pellets of PPS and Vectra A950 were manually mixed in the ratio 95/5, 90/10, 75/25, 50/50 (wt./wt.) and dried in an air oven dryer at 150 °C. DCTPPS was taken as 10 % (wt./wt.) with respect to Vectra A950 concentration.

5.2.3 Reactive blending

The melt blending of the of PPS, Vectra A950 and DCTPPS was done with *Berstroff co-rotating twin-screw extruder (E0.0004/91)*. The cylinder temperatures of the extruder were varied from 285 to 300 °C and the screw speed was 150 rpm (*Table 5.1*). The transesterification between Vectra A950 and DCTPPS and blending with PPS was carried out in one step. Uncompatibilised PPS/Vectra A950 blends with Vectra A950

content 10 and 25% (wt./wt.) were prepared under identical conditions for comparative study. The hot extrudate was immediately quenched in water bath, and was drawn at varying speeds to form strands of differing diameters, palletised and dried before processing. The draw ratio for each strand was determined as the ratio between the die and the strand cross-sections (S_o/S_s). The dimensions of the round hole capillary die were length (L) 30 mm, diameter (D) 5 mm, and thus L/D 6. The screw speed was maintained at 100 rpm for all blends.

Table 5.1: Cylinder Temperature (°C) of the extruder

	1st zone	2nd zone	3rd zone	4th T die
PPS	285	285	290	290
Blends	285	285	290	290
Vectra A950	280	280	285	295

The reaction between DCTPPS and Vectra A950 was tested at 300 °C and 40 rpm on the basis of viscosity increase in a *Brabender Plasticorder* blending machine. The torque developed during mixing of DCTPPS and Vectra A950 was recorded relative to time. The Infra-red spectroscopy of blends and blend components were carried out using potassium bromide pellets on *Shimadzu IR-470* spectrometer.

5.2.4 Processing

Injection moulding: The blends as well as respective polymers were injection moulded into test specimen after drying in an air oven at 150 °C for 8 hours. Injection moulding was performed with a *Arburg all rounder 220-90-350 injection molding machine*. The parent polymers were processed under conditions recommended by the manufacturers (*Table 5.2*). The condition chosen for the processing of blends was a suitable compromise between those used for the respective homopolymers. The moulded specimen consisted of standard test bars for tensile and impact tests.

Table 5.2: Processing conditions

	1st zone	2nd zone	3rd zone	4th zone	5th zone	mould temp.
PPS	310	320	325	325	325	130
Blends	310	310	325	325	325	130
Vectra A950	280	285	285	295	295	290

5.2.5 Testing and Analysis

5.2.5.1 Thermal properties

Thermal properties of extruded PPS/Vectra A950 blend samples were measured by *Mettler TA4000* series differential scanning calorimeter. The apparatus was calibrated with Indium at different scanning rates. The lag between sample and pan holder

temperature was also taken into account, and computed through Indium crystallisation tests as described by Elder and Wlochowicz.¹⁹ The sample mass were kept constant (6.0 ± 0.1 mg) through out the analysis so as to minimise the effect of mass change on the enthalpy change. The heats of fusion and crystallisation were determined from the peak area in the DSC thermogram. The melting transition temperature (T_m) and crystallisation temperature (T_c) were calculated from the peak maxima of the thermograms of samples in the second heating and cooling scan respectively.

5.2.5.2 Tensile properties

Tensile properties were measured according to *ASTM D-638* using an *Instron testing machine* (4204). The strain rate was 5 mm/minute for tensile strength and elongation measurements and 1 mm/minute for determining elastic modulus. The dimensions of the test bars were 15.4 cm \times 1.2 cm \times 0.3 cm.

5.2.5.3 Impact properties

The impact strength of notched and unnotched test specimen were determined according to *ASTM D-253 C* using a *CEAST* impact testing machine. The dimensions of the test specimen were 5.0 \times 0.6 \times 0.3 cm. For PPS and its blends a pendulum of 40 kpcm was used.

5.2.5.4 Scanning electron microscope

The morphology of the fractured surfaces of the extruded and injection moulded tensile specimen were observed by SEM as presented in **Section 2.2.4**.

5.2.5.5 Rheology

The melt-rheology of pure components, uncompatibilised and compatibilised blends were studied by measuring their melt viscosities in shear flow at 310 °C using *CEAST RHEOVIS capillary viscometer*. The L/D ratio for the die was 20 mm/5 mm. The shear rate was 100 to about 10,000 1/s.

5.2.5.6 Polarised light optical microscope

The molten morphology of the PPS/Vectra A950 blends was investigated as described in **Section 2.2.5**.

5.3 RESULTS AND DISCUSSION

5.3.1 *In situ* reactive compatibilisation

Our approach was to extrude the PPS and Vectra A950 in presence of dicarboxyl poly(phenylene sulphide) (DCTPPS) taken in proportion to Vectra A950 concentration using a twin screw extruder. The block copolymer formed during reactive blending, by transesterification between the carboxyl group of the DCTPPS and ester linkages of Vectra A950, could play the role of compatibiliser through its preferential location at the interface with consistent blocks and thereby diffusing into the corresponding phase of the same chemical structure and promote the miscibility by reducing the interfacial tension.

Figure 5.1 illustrates the comparative torque vs. time curves for pure Vectra A950, DCTPPS and 50/50 % (wt./wt.) DCTPPS/Vectra A950 blend. The torque observed for pure Vectra A950 and DCTPPS shows a continuous decrease with time whereas

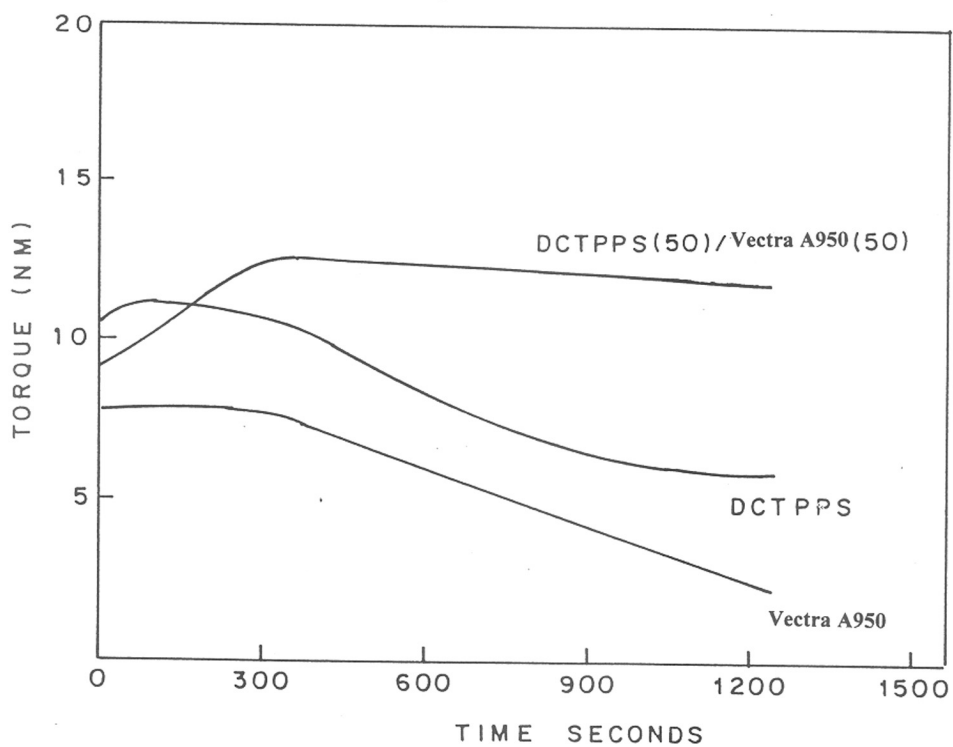


Figure 5.1 Torque vs. Time graph for Vectra A950, DCTPPS and (50/50 % wt./wt.) DCTPPS/Vectra A950 blend.

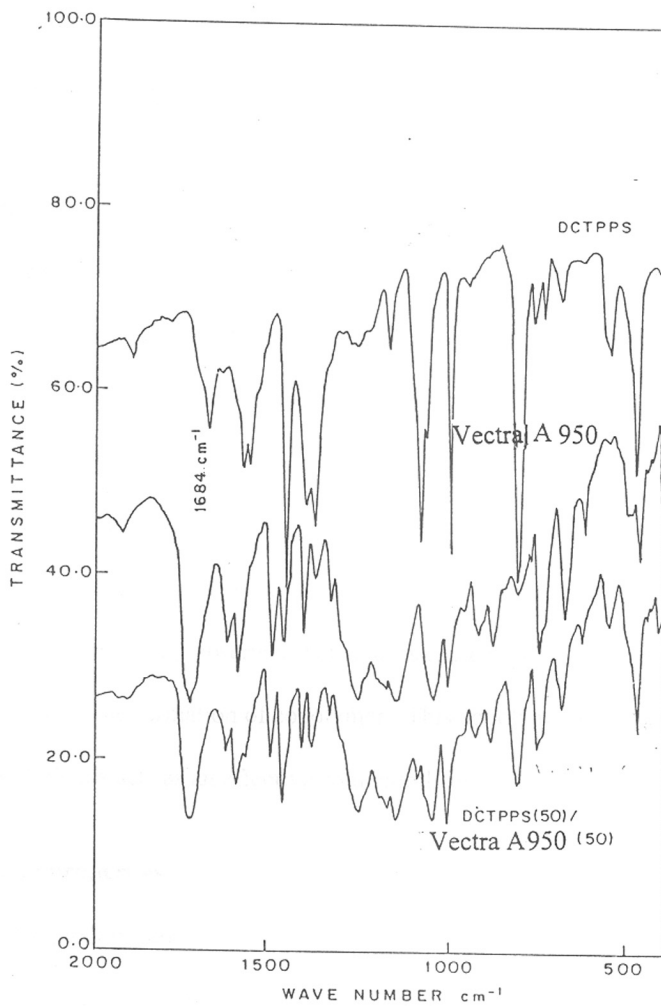


Figure 5.2 IR spectra of pure Vectra A950, DCTPPS and (50/50 % wt./wt.) DCTPPS/Vectra A950 blend.

the torque of DCTPPS/Vectra A950 blend increases with time. This increase in torque of DCTPPS/Vectra A950 blend with time is indicative of an increase in chain length brought forth by transesterification reaction between the carboxyl groups of DCTPPS and ester linkages of the Vectra A950. This observation is further supported by the IR spectra of pure Vectra A950, DCTPPS and melt blend of 50/50 % (wt./wt.) DCTPPS/Vectra A950 blend (*Figure 5.2*). The characteristic peak of carboxyl group of DCTPPS is very clear at 1684 cm^{-1} whereas it is absent in melt blended product of DCTPPS and Vectra A950. Similar results of transesterification reaction between Vectra A950 and various reactive components have been reported.^{15,20-22} Chang and coworkers^{15,21,23} investigated the effect of *in situ* compatibilisation on the various properties of Noryl [poly(phenylene oxide)/polystyrene blend]/Vectra A950 blends using styrene-glycidyl methacrylate (SG) as reactive component. They observed that transesterification reaction between SG and Vectra A950 leads to the formation of copolymer. This copolymer comprising SG blocks and Vectra A950 blocks acts as an effective compatibiliser for Noryl/Vectra A950 blends.

5.3.2 Thermal properties

5.3.2.1 Melting behaviour

Figure 5.3 showed typical DSC curves corresponding to second heating scans of PPS, Vectra A950, uncompatibilised and compatibilised 75/25 % (wt./wt.) PPS/Vectra A950 blends containing 10% DCTPPS with respect to Vectra A950 concentration. Thermal properties are tabulated in *Table 5.3*.

Table 5.3: Thermal properties of PPS/Vectra A950 blends

PPS/TLCP /DCTPPS (wt/wt. %)	Uncompatibilised						Compatibilised [10 % (wt./wt.) of Vectra A950 content]					
	T _m °C	ΔH _m J/m	T _c °C	ΔH _c J/m	T _m -T _c °C	α	T _m °C	ΔH _m J/m	T _c °C	ΔH _c J/m	T _m -T _c °C	α
100/0	279	36.0	227	41.4	52	0.25	-	-	-	-	-	-
90/10	279	33.2	232	36.0	47	0.23	280	26.1	229	34.0	51	0.18
75/25	280	24.8	238	29.7	42	0.17	279	17.4	232	23.4	47	0.12
50/50	279	20.3	242	25.8	37	0.14	280	16.1	240	23.0	40	0.11
0/0/100	282	1.8	238	1.5	-	-	-	-	-	-	-	-

T_m: Melting peak temperature

ΔH_m: Heat of fusion

ΔH_c: Heat of Crystallisation

T_m-T_c=ΔT: Degree of super cooling

T_c: Crystallisation Temperature

α: Degree of crystallinity

It is seen from the *Table 5.3* that the heat of melting (*ΔH_m* of neat PPS =36.0 J/m, uncompatibilised 50/50 wt./wt.% PPS/Vectra A950 blend = 20.3 J/m and compatibilised 50/50 wt./wt.% PPS/Vectra A950 blend=16.1 J/m) was decreased on reactive compatibilisation. The miscibility between polymers is determined by a balance of enthalpic and entropic contributions to the free energy of mixing.³ For polymers the entropy is almost zero, causing enthalpy to be decisive in determining miscibility. As described in **Section 4.4.2**, for a miscible system, $\Delta H \leq 0$. The introduction of

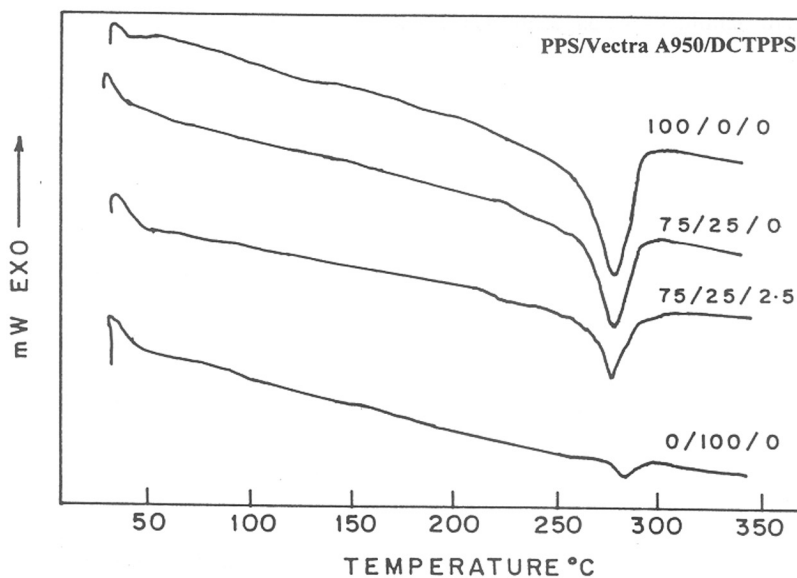


Figure 5.3 DSC curves corresponding to second heating scans of PPS, Vectra A950, uncompatibilised 75/25 % (wt./wt.) PPS/Vectra A950 blend and 75/25 % (wt./wt.) PPS/Vectra A950 blend compatibilised with 10 wt.% DCTPPS with respect to Vectra A950.

interacting groups by chemical modification of a polymer or by copolymerisation can result in a negative contribution to the enthalpy of mixing. A decrease in the enthalpy of PPS/Vectra A950 blend (ΔH_{mixing}) on reactive compatibilisation indicates the presence of favourable interactions between PPS and Vectra A950.

Usually the melting transition and glass transition of blend components undergo an inward migration on compatibilisation as a direct consequence of mutual dissolution of the components. Here, these transitions of PPS and Vectra A950 occur in the same range (280 °C). The glass transition temperatures (T_g) of the individual components in the blends are not distinguishable due to the close proximity of T_g of both components (~100 °C). The melting endotherms of the two materials also overlap, with the melting point of neat Vectra A950 being the range of 282 °C and the PPS being around 279 °C. Therefore, compatibilisation does not affect melting transition of the respective blend components in PPS/Vectra A950 blends.

5.3.2.2 Crystallisation behaviour

Figure 5.4 showed typical DSC curves corresponding to second cooling scans of PPS, Vectra A950 and 75/25 % (wt./wt.) PPS/Vectra A950 blends compatibilised with 10 wt.% DCTPPS. The crystallisation temperatures (T_c) are those corresponding to the exothermic peak maxima, corrected as described by Elder and Wlochowicz.¹⁹ The

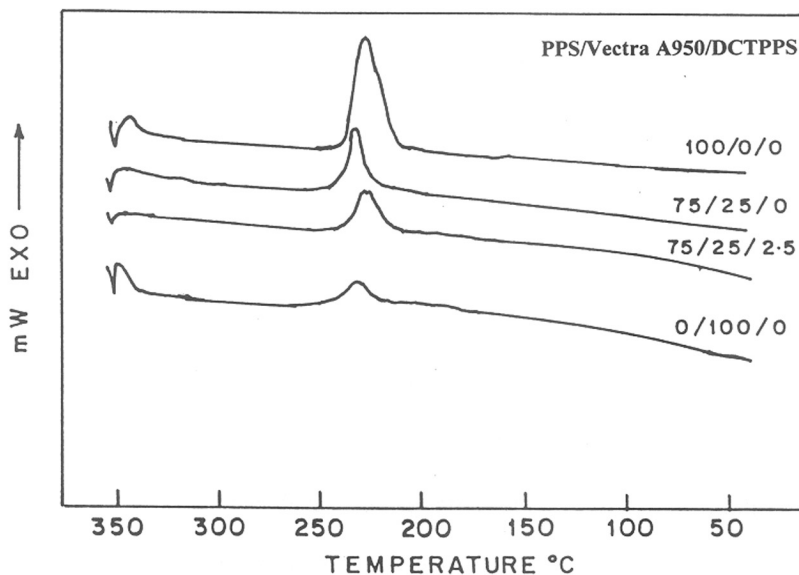


Figure 5.4 DSC curves corresponding to second cooling scans of PPS, Vectra A950, uncompatibilised 75/25 % (wt./wt.) PPS/Vectra A950 blend and 75/25 % (wt./wt.) PPS/Vectra A950 blend compatibilised with 10 wt.% DCTPPS with respect to Vectra A950.

crystallisation temperature (T_c) and heat of crystallisation (ΔH_c) of PPS phase decrease on compatibilisation, as seen in *Table 5.3*, indicating that compatibilisation retards crystallisation process of PPS. The crystallisation peak of PPS phase in the 75/25 wt./wt.% PPS/Vectra A950 compatibilised by 10 wt.% DCTPPS was at 232 °C while in the uncompatibilised blend it was at 238 °C. The temperature range over which PPS crystallises also broadened and its intensity decreased marginally in the compatibilised blend. This indicates that compatibilisation marginally slows down the crystallisation rate of the PPS phase. This leads to an increase in the degree of supercooling ($T_m - T_c = \Delta T$) of PPS phase in compatibilised PPS/Vectra A950 blends. Similar effect of compatibilisation on crystallisation rate of blend components have been reported in the earlier studies.²⁰⁻²⁶ Chang and coworkers^{20,21} reported that the crystallisation behaviour of components of Noryl [blends of poly(phenylene oxide) and polystyrene]/Vectra A950 blends is seriously affected on *in situ* compatibilisation by the addition of reactive components such as styrene-glycidyl methacrylate (SG). Ahn and coworkers²⁴⁻²⁶ recently investigated the compatibilising efficiency of polyacrylate (PAr)-b-polyamide-6 (PA-6) copolymer for PAr/PA-6 blends. They observed a depression in the crystallisation temperature and degree of crystallinity on compatibilisation.

5.3.2.3 Degree of crystallinity

The degree of crystallinity (α) of the PPS phase in both uncompatibilised and compatibilised blends were tabulated in *Table 5.3*. The ΔH_m of Vectra A950 recorded is

rather small (1.8 J/m) as compared to that of PPS (36.0 J/m). Therefore, the degree of crystallinity (α) has been calculated from the enthalpy of fusion normalised to the PPS content assuming that the contribution of the Vectra A950 phase is negligible.²⁷ A value of 146.2 J/g was estimated by Maemura et al²⁸ for enthalpy of fusion of 100% crystalline PPS. The heats of melting and hence the crystallinity of the compatibilised blends are decreased significantly as compared to the uncompatibilised blend of similar composition as seen in *Table 5.3*. *In situ* compatibilisation of immiscible blends results in favourable interaction between the blend components. This interaction leads to a negative contribution to the enthalpy of mixing and this affects crystallisation of blend components. The formation and presence of PPS-Vectra A950 block copolymer is expected to alter the PPS crystallisation, especially in the vicinity of the interface. This observation is in accordance with previous studies on the crystallinity of compatibilised blends.^{20-26, 29-33} As described in **Sections 4.4.3 and 4.4.4**, the crystallisation temperature (T_c) and degree of crystallinity (α) of PPS phase in PPS/PET-OB blends are decreased on addition of copolymer consists of PPS blocks and PET/OB blocks. Chang and coworkers^{21,22} observed a reduction in the degree of crystallinity of polypropylene (PP) in PP/Vectra A950 blends in presence of ethylene-glycidyl methacrylate copolymer (EGMA). They concluded that the EGMA undergoes interchange reactions with Vectra A950 resulting in EGMA-g-Vectra A950 block copolymer which interferes the crystallisation of PP. As indicated earlier, Ahn and coworkers²⁴⁻²⁶ reported a reduction in the crystallinity of PA/PA-6 blends in presence of Par-bPA-6 copolymer. An effective compatibiliser increases the mutual solubilities of the various components, which causes

a reduction in the crystallinity of thermoplastic matrix in thermoplastics (TP)/thermotropic liquid crystalline polymer (TLCP) blends. The DSC results led us to conclude that the increased interactions between the phases modified the crystallisation behaviour of the blend components.

5.3.3 Mechanical properties

There are conflicting reports on the mechanical properties and morphological features of PPS/Vectra A950 blend systems. Previous studies indicate that the mechanical properties of PPS does not show great improvement on blending with Vectra A950. Ramanathan et al.^{34,35} observed that the chemical reaction between the PPS and Vectra A950 during blending results in porous structure which leads to poor mechanical properties. Here we studied the same blend system over a wide range of compositions and have not observed any chemical reaction between the PPS and Vectra A950. A fibril morphology and mechanical reinforcement was observed for PPS/Vectra A950 blends. The tensile strength of neat PPS (82 Mpa) improves on blending with Vectra A950 (PPS containing 25 wt.% Vectra A950 shows 87 Mpa) as seen in *Table 5.4*. However, this improvement in mechanical properties is only marginal on account of phase separation and lack of adhesion between the blend components. This observation agrees with that of Heino et al.^{4,5} who studied the same blend and concluded that there is no chemical reaction between the PPS and Vectra A950.

Tensile bars of uncompatibilised PPS/Vectra A950 blends show brittle fracture whereas compatibilised blends show ductile fracture. This is presumed to be due to the crack preferentially occurring under stress at defects such as voids existing at the

interface between the PPS and Vectra A950 phases in uncompatibilised PPS/Vectra A950 blends.

Table 5.4: Mechanical properties of PPS/Vectra A950 blends

PPS/Vectra A950/DCTPPS (wt./wt.%)	Uncompatibilised			Compatibilised (10 % (w/w) of Vectra A950 content)		
	Toughness J/m	Tensile modulus (MPa)	Break Stress (MPa)	Toughness J/m	Tensile modulus (MPa)	Break Stress (MPa)
100/0	-	3697	82	-	-	-
90/10	-	3987	84	970.3	3649	89
75/25	-	4803	87	810.1	6632	98
50/50	-	5584	96	798.2	9345	108
0/100	-	6447	115	-	-	-

* *Toughness of uncompatibilised blend could not be measured*

The compatibilised blend showed ductile fracture with improved toughness (elongation at break) as a direct consequence of miscibility and improved stress transfer between the two phases. Tensile properties and impact strength were improved on compatibilisation of PPS/Vectra A950 blends. The tensile strength of the uncompatibilised 75/25 PPS/Vectra A950 blend is 86 MPa whereas that of compatibilised 75/25/2.5 is 98 Mpa as shown in *Table 5.4*.

In uncompatibilised blends voids exist across or in between the interfaces causing poor stress transfer between the phases and results in the inferior mechanical properties.

The enhancement in the tensile modulus of the *in situ* compatibilised PPS/Vectra A950 blends suggests improved interfacial adhesion.

The impact strength of the blend is greatly dependent upon the capacity of the dissipating impact energy through the matrix and the delivery of the internal stress of the continuous phase to the dispersed phase. The interface between the phases is important. The impact strength of a blend is very sensitive to changes in interfacial adhesion.³¹ Thus, the impact strength was measured for both notched and unnotched specimen. Most of the compatibilised blends did not fail in the unnotched impact test. The notched impact specimen yielded greater information on the behaviour of the material. The impact strength of the *in situ* compatibilised blends was significantly improved as shown in *Table 5.5*.

Table 5.5: Impact Strength of PPS/Vectra A950 Blends

PPS/ Vectra A950/DCTPPS (wt.%)	uncompatibilised		Compatibilised (10 % (wt./wt.) of Vectra A950 content)	
	Unnotched J/m	Notched J/m	Unnotched J/m	Notched J/m
100/0	27.0	-	-	-
90/10	22.1	18.4	36.8	29.6
75/25	24.0	13.6	41.3	31.1
50/50	21.0	16.4	46.4	33.2
0/100	80.0	-	-	-

The Izod unnotched impact strength of uncompatibilised 75/25 % (wt./wt.) PPS/Vectra A950 blend was 13.4 J/m whereas for the compatibilised blend of the same composition it was 39.1 J/m due to enhanced adhesion at the interface on compatibilisation.

5.3.5 Rheological properties

The rheological behaviour of polymer blend is closely related to the deformation of the droplets in the continuous phase. The dispersed phase is usually not uniform in size and shape, with the average size depending on the blending conditions such as mixing equipments, time of mixing and factors such as volume ratio of each component, the viscosity ratio and the elasticity ratio. The deformation and the orientation angle of the droplets are expressed as a function of the viscosity ratio of the droplet and the suspending medium, the droplet radius, the interfacial tension and the rate of deformation.

Figure 5.5 gives the apparent viscosity vs. shear rate plots for PPS, PPS/Vectra A950, uncompatibilised 50/50 % wt./wt. PPS/Vectra A950 blend and compatibilised 50/50 % wt./wt. PPS/Vectra A950 blend. The uncompatibilised blend has a lower viscosity than both pure components. The compatibilised blend has substantially higher viscosity than the corresponding uncompatibilised blend because of the strong chemical interaction between PPS phase and Vectra A950 phase on reactive compatibilisation. On compatibilisation the deformability of Vectra A950 phase under shear force decreases as a result of improved interfacial adhesion between the PPS and the Vectra A950 phases.

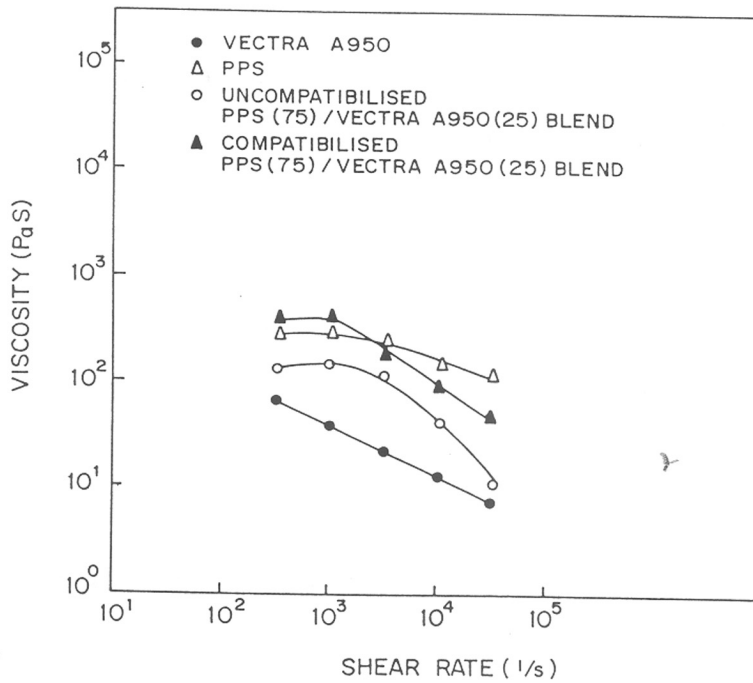


Figure 5.5 Plot of apparent viscosity vs. shear rate showing rheological properties of the uncompatibilised and compatibilised 50/50 % wt./wt. PPS/Vectra A950 blend.

The Vectra A950 phase in the compatibilised blend at lower shear region resists deformation whereas at higher shear region it deforms more easily, due to the improved adhesion between PPS phase and Vectra A950 phase on compatibilisation. This observation is further supported by the polarised light optical microscopy (PLOM) and scanning electron microscopy studies of PPS/Vectra A950 blends.

5.3.6 Polarised light optical microscopy (PLOM)

The hot stage PLOM photograph of strings of uncompatibilised and compatibilised 50/50 wt./wt.% PPS/Vectra A950 blend (containing 10% DCTPPS proportional to Vectra A950) obtained from the capillary rheometrical measurements at different shear rates are presented in *Figure 5.6*. From a comparison of PLOM photographs of uncompatibilised [*Figures 5.6 (a) and (c)*] and compatibilised blends [*Figures 5.6 (b) and (d)*], it is clear that compatibilisation enhances the formation of a greater number of finer Vectra A950 fibrils under high shear rate. At lower shear rate the compatibilised blends exists as droplets whereas at higher shear rate, it exists as fine fibrils as seen in *Figure 5.6*. These fibrils are primarily responsible for the observed improvement in the mechanical properties of the blend on compatibilisation.

5.3.7 Scanning electron microscopy (SEM)

The fractured surface morphologies of the injection moulded specimen were inspected on the planes perpendicular and parallel to the injection flow directions in both the core and near-skin regions. *Figure 5.7* shows scanning electron micrograph of the

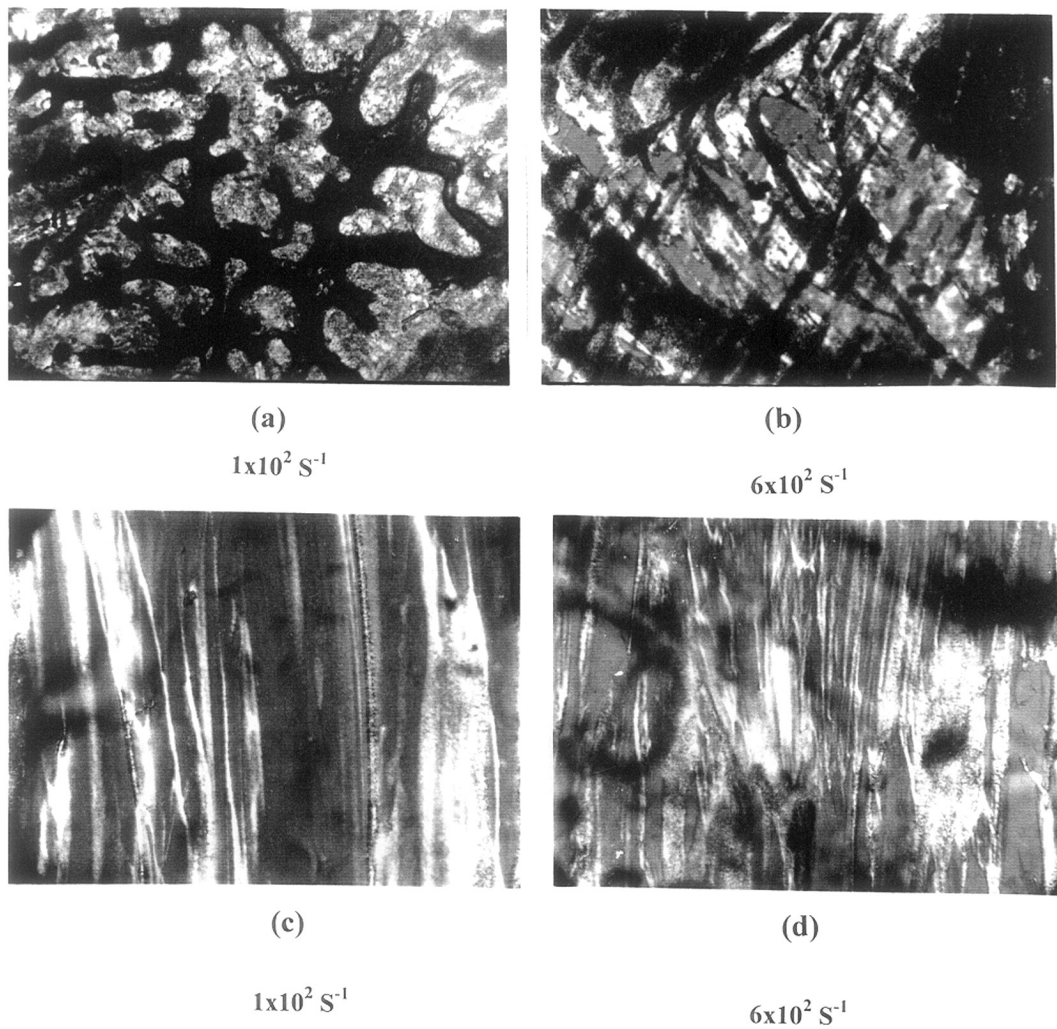
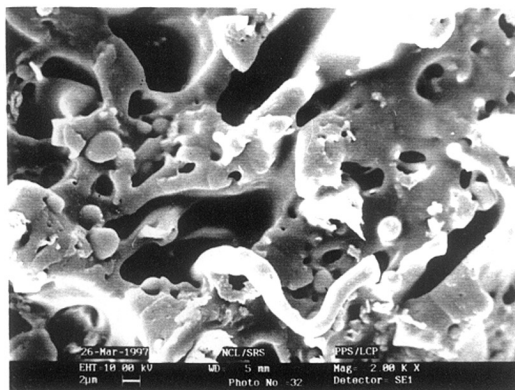


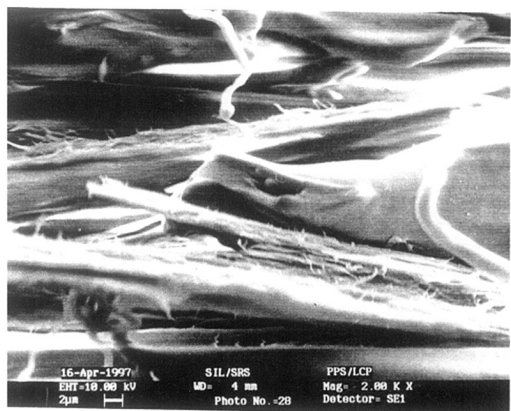
Figure 5.6 Polarised light optical microscope photograph showing molten morphology of uncompatibilised (a, b) and *in situ* compatibilised (c, d) PPS/Vectra A950 blends at different shear rates.



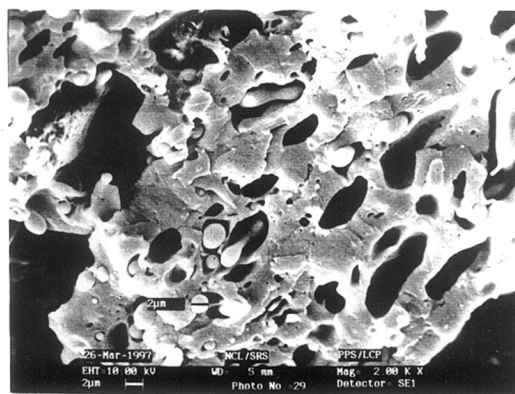
(a)



(b)

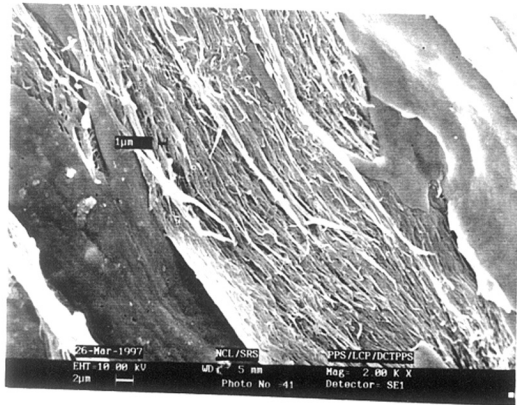


(c)

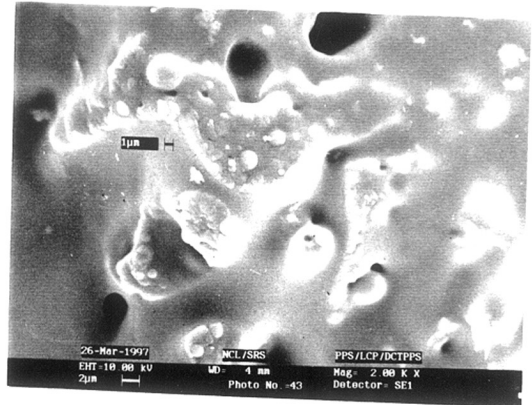


(d)

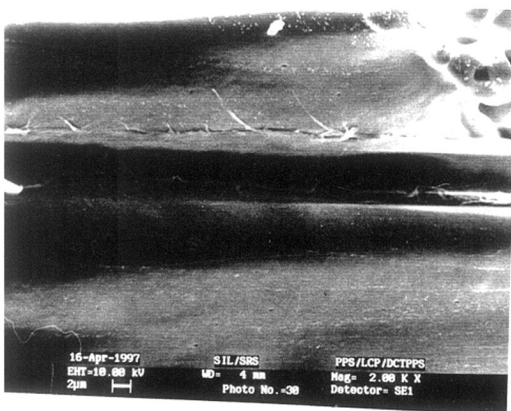
Figure 5.7 SEM micrograph showing skin morphology of uncompatibilised PPS/Vectra A950 blends: (a) Perpendicular to injection flow direction, skin region; (b) core region of the same specimen; (c) Parallel to injection moulded direction, skin region; (d) Core region of the same specimen.



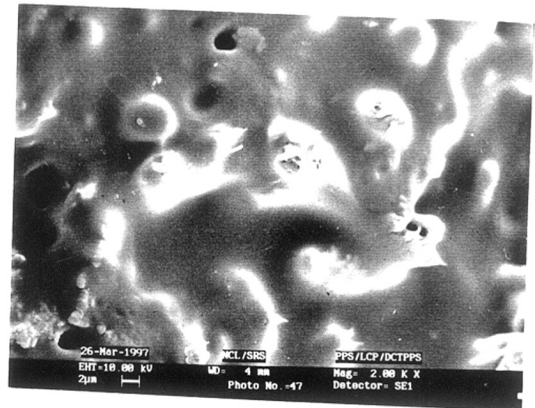
(a)



(b)



(c)



(d)

Figure 5.8 SEM micrograph showing skin morphology of compatibilised PPS/Vectra A950 blends: (a) Perpendicular to injection flow direction, skin region; (b) core region of the same specimen; (c) Parallel to injection moulded direction, skin region; (d) Core region of the same specimen.

uncompatibilised 75/25 wt./wt. % PPS/Vectra A950 blend. *Figure 5.7 (a)* was taken from the plane perpendicular to the injection flow direction, at the skin region, where the Vectra A950 fibrils are fairly long (high aspect ratio). It shows most of them being pulled out from the PPS matrix, which is an indication of poor interfacial adhesion.^{4,5,34,35} *Figure 5.7 (b)* shows the morphology at the core region for the same specimen as *Figure 5.7 (a)*, where the Vectra A950 phase exists as large spherical particles. *Figure 5.7 (c)* shows the micrograph obtained on the plane parallel to the flow direction near the skin region, and displays the presence of larger number of long Vectra A950 fibrils. *Figure 5.7 (d)* shows voids at the interface between PPS matrix and Vectra A950 fibrils as a result of poor interfacial adhesion which results in the inferior mechanical properties. This kind of skin-core dispersed phase morphology has been observed in many polymer blends as a result of the shear difference and quenching rate difference in a typical injection moulding process. Previous studies^{33,36} on the development of such morphologies in neat Vectra A950 and thermoplastics have also indicated the formation of such morphologies during injection moulding as being due to the freezing of the orientation in the layer in contact with the mould due to the steep temperature gradient. The development of skin-core morphology is observable only at Vectra A950 concentration exceeding 25 wt.%. The increase in the mechanical properties of blends with higher concentration of Vectra A950 can be attributed to the formation of skin-core morphology, with the skin region being capable of carrying a much higher stress than the core region, as in the case of TLCP^{37,38}.

Figure 5.8 shows the morphologies of the compatibilised PPS/Vectra A950 /DCTPPS (75/25/2.5) blend, observed at the same locations (same magnification) as described earlier. It shows most of them being pulled out from the PPS matrix, which is an indication of poor interfacial adhesion^{4,5}. *Figure 5.8 (a)* shows the improved interfacial adhesion of fractured Vectra A950 fibrils with PPS matrix. The long thread-like TLCP fibrils are well aligned in the direction of flow. *Figure 5.8 (b)* shows clearly the interfacial bonding between the PPS matrix and Vectra A950 fibrils. This observation revealed that the compatibilisation results in the formation of larger number of finer and longer Vectra A950 fibrils. This is significant in the technological point of view because these fibrils are essential for the reinforcement of the matrix, and lead to enhanced mechanical properties. This morphological observations are in accordance with the rheological properties of the blend (*Section 5.3.5*). In previous studies^{20-26, 33-36}, compatibilisation were shown to alter the fibril morphology of the Vectra A950 phase resulting in inferior mechanical properties. *Figure 5.8 (c)* shows that the size of the Vectra A950 dispersed droplets are considerably smaller than that of the corresponding uncompatibilised blend [*Figure 5.7 (c)*]. This observation further supports the claim of better compatibilisation. At the core region (*Figure 5.8 (d)*) the size of the Vectra A950 droplets become rather small indicating an improved compatibility between the PPS and Vectra A950. By properly choosing the processing conditions and compatibiliser compositions, the mechanical properties can be improved further.

5.4 CONCLUSION

The effect of *in situ* compatibilisation on thermal properties, mechanical properties and morphology of PPS/Vectra A950 blends were investigated. The decrease in the heat of melting, crystallisation temperature and heat of crystallisation of PPS phase in PPS/Vectra A950 blends on compatibilisation points to the presence of favourable interaction between the blend components. Tensile and impact properties of the compatibilised blends are enhanced indicating an improvement in the interfacial adhesion between the components. Toughness of the blend increased on compatibilisation. *In situ* compatibilisation of PPS/Vectra A950 blends results in the formation larger number of fine Vectra A950 fibrils within the PPS matrix. Both uncompatibilised and compatibilised PPS/Vectra A950 blends exhibit skin-core morphology. The *in situ* compatibilisation of PPS/Vectra A950 blends using DCTPPS as reactive component is an efficient way to produce PPS/Vectra A950 molecular composites with unique properties.

5.5 REFERENCES AND NOTES

- 1 T.G. Gopakumar, S. Ponrathnam, C.R. Rajan and A. Fradet, *Polymer* (communicated).
- 2 T.G. Gopakumar, S. Ponrathnam, C.R. Rajan and A. Fradet, *J. Appl. Polym. Sci.* (communicated).
- 3 M.J. Folkes and P.S. Hope, *Polymer Blends and Alloys*, Chapter 8, Chapman & Hall, London (1993).
- 4 M.T. Heino and J.V. Seppala, *J. Appl. Polym. Sci.*, **44**, 1992, 1051.
- 5 M.T. Heino and J.V. Seppala, *J. Appl. Polym. Sci.*, **44**, 1992, 2185.
- 6 G.O. Shonaike, S. Yamaguchi, M. Ohta, H. Hamada, Z. Maekawa, M. Nakamichi and W. Kosaka, *Eur. Polym. J.*, **30**, 1994, 413.
- 7 P.R. Subramaniam and A.I. Isayev, *Polymer*, **32**, 1991, 1961.
- 8 B.C. Kim, S.M. Hong, S.S. Hwang and K.M. Kim, *Polym. Eng. Sci.*, **36**, 1996, 574.
- 9 T.G. Gopakumar, R.S. Ghadage, S. Ponrathnam, C.R. Rajan and A. Fradet, *Polymer*, **38**, 1997, 2209.
- 10 T.G. Gopakumar, S. Ponrathnam, C.R. Rajan and A. Fradet, *Polym. J.* (in Press).
- 11 T.G. Gopakumar, S. Ponrathnam, C.R. Rajan and A. Fradet, *J. Appl. Polym. Sci.* (communicated).
- 12 T.G. Gopakumar, S. Ponrathnam, C.R. Rajan and A. Fradet, *Polymer* (in Press).
- 13 S.B. Brown, "Reactive extrusion: A survey of chemical reactions of monomers and polymers during extrusion processing" in M. Xanthos, Ed., *Reactive Extrusion: Principles and Practice*, Chapter 8, Hanser Publishers, New York, 1992.
- 14 V.N. Ignatov, C. Carraro, V. Tartari, R. Pippa, F. Pilati, C. Berti, M. Toselli and M. Fiorini, *Polymer*, **38**, 1997, 195.

- 15 D.Y. Chang and F.C. Chang, *J. Appl. Polym. Sci.*, **56**, 1995, 1015.
- 16 M.J. Folkes and P.S. Hope, *Polymer Blends and Alloys*, Chapter 3, Chapman & Hall, London (1993).
- 17 A.G.C. Machiels, K.F.J. Denys, J.V. Dm and A.P. Boer, *Polym. Eng. Sci.*, **36**, 1996, 2451.
- 18 C. Lacroix, M. Bousmina, P.J. Crreau, M.F. Liauro, R. Petiand and A. Michel, *Polymer*, **37**, 1996, 249.
- 19 M. Elder and A. Wlochowicz, *Polymer*, **24**, 1983, 1593.
- 20 Y.P. Chiou, D.Y. Chang and F.C. Chang, *Polymer*, **37**, 1996, 5655.
- 21 Y.P. Chiou, K.C. Chiou and F.C. Chang, *Polymer*, **37**, 1996, 4099.
- 22 R.S.Porter and L.H. Wang, *Polymer*, **33**, 1992, 2019.
- 23 A. Legros, P.J. Carreau, B.D. Favis and A. Michel, *Polymer*, **35**, 1994, 758.
- 24 T.O. Ahn, S. Lee, H.M. Jeong and S.W. Lee, *Polymer*, **34**, 1993, 4156.
- 25 T.O. Ahn, S. Lee, H.M. Jeong and S.W. Lee, *Polymer*, **37**, 1996, 3559.
- 26 T.O. Ahn, S.C. Hong, H.M. Jeong and J.H. Kim, *Polymer*, **38**, 1997, 214.
- 27 L.T. Minkova, S. De Petris, M. Paci, M. Pracella, and P.L. Magagnini, "Characterisation of blends of poly(phenylene sulphide) and thermotropic liquid crystalline copolyesteramide" in D. Acierno and F.P. Mantia, Eds., *Processing and Properties of Liquid Crystalline Polymers and LCP Based Blends*, Chem Tec Publishing, Ontario, 1993, 153.
- 28 E. Maemura, M. Cakmak and L.J. White, *Intern. Polym. Proc.*, **3**, 1990, 79.
- 29 L.I. Long, R.A. Shanks and Z.H. Stachurski, *Prog. Polym. Sci.*, **20**, 1995, 651.
- 30 Y.J. Sun, G.H. Hu, M. Lambla and H.K. Kotler, *Polymer*, **37**, 1996, 4119.
- 31 J.L. Rodriguez, J.I. Eguiazabal and J. Nazabal, *Polym. J.*, **28**, 1996, 501.
- 32 P.C. Lee, W.F. Kuo and F.C. Chang, *Polymer*, **35**, 1994, 5641.
- 33 M.M. Miller, J.M.G. Cowie, J.G. Tait, D.L. Brydon and R.R. Mather, *Polymer*, **36**, 1995, 3107.

- 34 R. Ramanathan, K.G. Blizard and D.G. Baird, *SPE ANTEC*, **46**, 1987, 1123.
- 35 P.R. Subramaniam and A.I. Isayev, *Polymer*, **32**, 1991, 1961.
- 36 S. Lee, S.M. Hong, Y. Seo, T.S. Park, S.S. Hwang and K.U. Kim, *Polymer*, **35**, 1994, 519.
- 37 K.H. Wei and K.F. Su, *J. Appl. Polym. Sci.*, **59**, 1996, 787.
- 38 D. Dutta, R.A. Weiss and J. He, *Polymer*, **37**, 1996, 435.

CHAPTER 6

SCOPE
FOR FUTURE WORK

6.1 SCOPE FOR FUTURE WORK

One of the disadvantages of PPS is its poor impact properties. It is too brittle and therefore often cracks develop during processing, especially during molding. The presence of small amount of elastomer will improve the toughness of PPS. Blending TPE with PPS can balance all desirable properties such as tensile properties and impact strength. The presence of elastomer phase within the PPS matrix would improve the toughness by the enhanced crazing or shear yielding mechanisms. The interfacial adhesion between TPE and PPS matrix can be improved by the addition of reactive components such as dicarboxyl terminated PPS. The carboxyl groups can undergo interchange reactions with ester linkages of TPE (such as Hytrel for example) which would lead to the formation of block copolymer comprising of PPS blocks and thermoplastic elastomer blocks. This block copolymer can act as compatibiliser for PPS/TPE blend system. The mechanical properties, rheological behaviour and impact strength of the PPS are strongly affected by the blending. The interfacial adhesion between the PPS matrix and elastomer phase is necessary for improved stress transfer to prevent premature crack development from the crazes. The efficiency of toughening depends on the extent of stress transfer between the PPS matrix and the elastomeric particles.

The scope for future work would involve the following:

- (i) To develop binary and ternary blends of poly(phenylene sulphide), wholly aromatic thermotropic liquid crystalline polymer and TPE, (such as HYTREL based on copolyester of poly(butylene terephthalate-oxybutylene);
- (ii) To study the thermal and crystallisation behaviour of above blends;
- (iii) To compatibilise above blends in the presence of dicarboxyl terminated PPS by reactive extrusion;

- (iv) To study the effect of various parameters such as compatibiliser composition, reactive time, temperature etc. on the blend properties;
- (v) To compare the properties of compatibilised blends generated by step-wise and *in situ* reactive blending;
- (vi) To evaluate the effect of compatibilisation on mechanical properties such as tensile behaviour, impact properties and rheological properties of the blends;
- (vii) To study the correlation between structure, phase behaviour, morphology and properties of the uncompatibilised and compatibilised blends;
- (ix) To investigate the effect of processing condition on the properties of the blends.

LIST OF PUBLICATIONS

- (1) Poly(phenylene sulphide)/Thermotropic liquid crystalline polymer blends: Non-isothermal Crystalline kinetics,

T.G. Gopakumar, R.S. Ghadage, S. Ponrathnam, C.R. Rajan and A. Fradet; *Polymer*, **38**, 1997, 2209.
- (2) Poly(phenylene sulphide)/Thermotropic liquid crystalline polymer blends: Melting, Crystallisation and Phase behaviour,

T.G. Gopakumar, S. Ponrathnam, C.R. Rajan and A. Fradet; *Polym. J.* **29**, (No.11), (1997).
- (3) Poly(phenylene sulphide)/Thermotropic liquid crystalline polymer blends: A comparative study of thermal properties, Morphology and Phase behaviour of blends produced different blending techniques,

T.G. Gopakumar, S. Ponrathnam, C.R. Rajan and A. Fradet; *Polymer* (in Press).
- (4) Poly(phenylene sulphide)/Thermotropic liquid crystalline polymer blends: Thermal properties, Morphology and Phase behaviour,

T.G. Gopakumar, S. Ponrathnam, C.R. Rajan and A. Fradet; (Communicated).
- (5) Block copolymer of telechelic terminated poly(phenylene sulphide) oligomer and semi-aromatic thermotropic liquid crystalline polymer,

T.G. Gopakumar, S. Ponrathnam, C.R. Rajan and A. Fradet; *J. Polym. Sci. Part A: Polymer Chemistry*, Communicated.
- (6) Poly(phenylene Sulphide)/semi-aromatic Thermotropic liquid crystalline polymer blends: Effect of compatibilisation on thermal properties, morphology and phase behaviour,

T.G. Gopakumar, S. Ponrathnam, C.R. Rajan and A. Fradet; *Polymer* (Communicated).
- (7) *In situ* compatibilisation of Poly(phenylene sulphide)/wholly aromatic Thermotropic liquid crystalline polymer blends by reactive extrusion: Morphology, Mechanical properties and thermal properties,

T.G. Gopakumar, S. Ponrathnam, C.R. Rajan, G. Sainkar and A. Fradet; *Polymer*, (in Press).

- (8) *In situ* compatibilisation of poly(phenylene sulphide)/wholly aromatic Thermotropic liquid crystalline polymer blends by reactive extrusion: Morphology and Rheological properties,

T.G. Gopakumar, S. Ponrathnam, C.R. Rajan, and A. Fradet, *Polymer*, Communicated.

- (9) Reactive compatibilisation of poly(phenylene sulphide)/Vectra A950 blends,

T.G. Gopakumar, S. Ponrathnam, C.R. Rajan, and A. Fradet; Accepted for international Symposium **Macro '98** on "Advances in Polymer Science and Technology" to be held in Madras, India.

- (10) Thermal behaviour and crystallisation kinetics of poly(phenylene sulphide),

T.G. Gopakumar, R.S. Ghadage, C.R. Rajan, S. Ponrathnam and P. Sini, *Advances in Polymer technology*, Eds. D. Joseph Francis, K.E. George and Sunil K. Narayanan Kutty, Allied Publishers limited, New Delhi, pp.151 (1996).

Patents filed (Indian)

- (i) A process for the preparation of compatibiliser for the poly(phenylene sulphide)/semi-aromatic thermotropic liquid crystalline polymer blends.

T.G. Gopakumar, S. Ponrathnam, C.R. Rajan, and A. Fradet

- (ii) An improved process for the preparation of compatibilised poly(phenylene sulphide)/semi-aromatic thermotropic liquid crystalline polymer blends.

T.G. Gopakumar, S. Ponrathnam, C.R. Rajan, and A. Fradet

- (iii) A process for the preparation of compatibiliser for the poly(phenylene sulphide)/wholly aromatic thermotropic liquid crystalline polymer blends.

T.G. Gopakumar, S. Ponrathnam, C.R. Rajan, and A. Fradet

- (iv) An improved process for the preparation of compatibilised poly(phenylene sulphide)/wholly aromatic thermotropic liquid crystalline polymer blends.

T.G. Gopakumar, S. Ponrathnam, C.R. Rajan, and A. Fradet